FUNCTIONAL INTERPLAY OF INFLUENZA A VIRUS NS1 AND PA-X PROTEINS MEDIATES HOST SHUTOFF

by

Eileigh C. Kadijk

Submitted in partial fulfillment of the requirements
for the degree of Master of Science

at

Dalhousie University
Halifax, Nova Scotia
October 2022

For Dad and his spirit of perseverance

TABLE OF CONTENTS

LIST OF TABLES

LIST OF FIGURES

ABSTRACT

Host shutoff is a mechanism to inhibit gene expression and limit the innate immune response. IAV produces two host shutoff proteins: PA-X and NS1. PA-X is an endonuclease that targets and cleaves host mRNAs. NS1 limits host pre-mRNA 3'-end processing, nuclear export, translation, and the innate immune response. PA-X and NS1 have important independent roles in host shutoff, but their functional relationship remains elusive. PA-X activity depletes cytoplasmic mRNAs, leading to a nuclear accumulation of cytoplasmic PABP. PA-X activity has also been linked to aberrant increases in nuclear poly adenylated (p(A)) RNAs. Recombinant IAV lacking functional NS1 had no nuclear accumulation of PABP during infection and there was evidence of decreased downregulation of PA-X targeted transcripts. Meanwhile, accumulation of p(A) RNAs during infection occurred independently of PA-X and NS1. These data suggest PA-X and NS1 have an important functional relationship and NS1 may enhance PA-X's host shutoff activity during infection.

LIST OF ABBREVIATIONS USED

2-5A	2–5-oligoadenylate
A549	adeno lung carcinoma cell line
Akt	AKT Serine/Threonine Kinase
BEAS-2B	human bronchial epithelial cell line
BEBM	bronchial epithelial basal medium
BSA	bovine serum albumin
BSC	biosafety cabinet
C	Celsius
CARD	caspase activation and recruitment domains
IP	immunoprecipitation
CPE	cytopathic effect
CPSF	cleavage and polyadenylation specificity factor
CRM1	chromosomal region maintenance 1
cRNA	complimentary RNA
CTD	C-terminal domain
CTT	C-terminal tail
DMEM	Dulbecco's modified eagles medium
ds	double stranded
eIF	eukaryotic initiation factor
ePAT	extension p(A) test
ER	endoplasmic reticulum
FBS	fetal bovine serum
FFU	focus forming units
FISH	fluorescence *in situ* hybridization
GAPDH	glyceraldehyde-3-phosphate dehydrogenase
HA	hemagglutinin
HEK	human embryonic kidney
HERC5	HECT and RLD domain containing E3 ubiquitin protein ligase 5
HSV-1	herpes simplex virus –1

IAV	influenza A virus
IBV	influenza B virus
IF	immunofluorescence
IFIT1	interferon induced protein with tetratricopeptide repeats 1
IFN β	interferon- β
IFN-L1	interferon- λ1
IFNAR	IFN α/β receptor
IKK	IκB kinase
IL	interleukin
ImmunoFISH	immunofluorescence/fluorescent *in situ* hybridization
IRF	interferon regulatory transcription factor
ISG	IFN stimulated gene
ISG15	ISG15 ubiquitin like modifier
ISR	integrated stress response
ISRE	IFN-stimulated response elements
JAK1	Janus kinase 1
kDa	kilodalton
KO	knock out
KSHV	Kaposi's sarcoma-associated herpes virus
LGP2	laboratory of genetics and physiology processing protein 2
lncRNA	long non-coding RNA
LR	linker region
M1	matrix protein
m7G	methylguanylate
MALAT1	metastasis-associated lung adenocarcinoma transcript 1
MAVS	mitochondrial antiviral signaling protein
MDA5	melanoma differentiation-associated protein 5
MDCK	Madin-Darby canine kidney
MEM	minimal essential media
MeOH	methanol
MOI	multiplicity of infection

mRNA	messenger RNA
MyD88	MYD88 innate immune signal transduction adaptor
NA	neuraminidase
NATB	N-terminal acetyltransferase B
NEP	nuclear export protein
NF-κB	Nuclear factor κ-light-chain-enhancer of activated B cells
NLS	nuclear localization sequence
NP	nucleoprotein
NS1	non-structural protein 1 (influenza viruses)
NSP1	non-structural protein 1 (coronaviruses)
NXF1	nuclear RNA export factor 1
NXT1	nuclear transport factor 2 like export factor 1
OAS	oligoadenylate synthetase
p(A)	polyadenylated
PA	polymerase acidic protein
PA-X	polymerase acidic – X protein
PABP	poly-A binding protein cytoplasmic 1
PABPN	poly-A binding protein nuclear 1
PACT	PKR activating protein
PAM2	PABP interacting motif
PAMP	pathogen associated molecular pattern
PB1	polymerase basic protein 1
PB2	polymerase basic protein 2
PBS	phosphate buffered saline
PFA	paraformaldehyde
PI3K	phosphatidylinositol 3-kinase
PKR	protein kinase R
Pol II	RNA polymerase II
Poly(I:C)	polyinosine-polycytidylic acid
PRR	pathogen recognition receptors
PTM	post translational modification

RBD	RNA binding domain
RdRp	RNA dependent RNA polymerase
RIG-I	retinoic acid-inducible gene I
RLR	retinoic acid-inducible gene-I like receptors
RNA	ribonucleic acid
RNase L	ribonuclease L
RNP	ribonucleoprotein
rNTP	ribonucleoside triphosphate
RRM	RNA recognition motifs
SAEC	small airway epithelial cells
SARS-CoV	severe acute respiratory syndrome coronavirus
smFISH	single molecule fluorescent *in situ* hybridization
ss	single stranded
STAT	signal transducer and activator of transcription
SUMO1	small ubiquitin-like modifier 1
TBK1	TANK binding kinase 1
TIR	Toll/IL-1 receptor
TLR	Toll-like receptors
TPCK	L-1-tosylamido-2-phenylethyl chloromethyl ketone
TRAF	TNF receptor associated factor
TRIF	TIR-domain-containing adapter-inducing interferon-β
TRIM25	tripartite motif containing 25
TYK2	tyrosine kinase 2
UTR	untranslated region
VERO	African green monkey kidney epithelial cells
vhs	virion host shutoff protein
vRNA	viral RNA
X-ORF	PA-X open reading frame

ACKNOWLEDGEMENTS

I consider myself lucky to have been surrounded and supported by so many people throughout my academic career. Words cannot describe my gratitude to each and every one of these people, I wouldn't be who or where I am today without you.

I could not have asked for a better supervisor than Dr. Denys Khaperskyy. His excitement for discovery and learning is infectious and he has been one of the most influential mentors of my life. His constant support through the ups and downs and stressors of research has helped me learn that it's okay to keep asking questions and keep seeking answers, as long as you're willing to put in hard work along the way. Thank you for teaching me that we shouldn't fear failure because it can be just as rewarding as success.

I would also like to deeply thank my co-supervisor, Dr. Craig McCormick. Thank you for your support and guidance during my research. Thank you for creating a warm and welcoming lab space with people who take kindly to questions and pose thought-provoking answers.

Thank you to my committee members, Dr. Jean Marshall and Dr. John Rohde. Your support and encouragement throughout the years, in person and online, has been invaluable to my success and growth as a student and scientist.

Thank you to all the members (past and present) of the Khaperskyy lab. To Dr. Shan Ying and Stacia Dolliver, who have been a constant support from day one. Days on the bench seemed a little less chaotic when we were all working together. Shan, Stacia, Juliette, and Kathleen - thank you for bringing joy into the 10G workspace and for inspiring me to be the best co-worker, peer, and friend.

Thank you to all the collaborators and funding sources for making this research possible: Stephen Whitefield and Brianne Lindsey at CMDI, to Alejandro Cohen in the Proteomics CORE, and to Dr. Patrick Murphy at UPEI for running our LC-MS/MS.

Thank you to the friends who supported me throughout all my highs and lows during this degree – specifically to Taylor (and Marlon), Rhea, Mel, Katie, Aurora, and the Tupper Mixer crew.

Finally, thank you to my family for helping me get to where I am today. To my brothers, Jake and Caleb for always encouraging me to be my best self and for all the laughs we had along the way. To my mom, Linda, who taught me how to seek out adventure and who always listened to me talk science, even if she didn't understand it right away. To my dad, Chris, who never stopped encouraging me to chase my dreams and who taught me to always give it your all, even when it's hard. Lastly, thank you to my husband Noah, for going on this and many more journeys in life with me.

CHAPTER 1: INTRODUCTION

1.1.1 Influenza Virus Biology

Influenza A virus (IAV) is an enveloped, negative sense, segmented, single stranded ribonucleic acid (ssRNA) virus and is a member of the *Orthomyxoviridae* family of viruses. The genome of IAV is composed of eight different RNA segments which each encode unique proteins used by the virus for transmission, infection, and replication (Reviewed in Dou et al., 2018). Segment 1 and 2 of the IAV genome encode for two of the three subunits of the RNA-dependent RNA polymerase (RdRp); segment 1 encodes polymerase basic protein 2 (PB2) and segment 2 encodes polymerase basic protein 1 (PB1). Leaky scanning on segment 2 allows the production of PB1-F2 (Chen et al., 2001). Segment 3 encodes the third subunit of the viral polymerase, called polymerase acidic protein (PA). Ribosomal frameshifting during translation of segment 3 produces the polymerase acidic – X (PA-X) protein (Jagger et al., 2012). The glycoprotein hemagglutinin (HA) is encoded by segment 4, of which there are 18 different subtypes – 1, 2, and 3 are all found on human influenza viruses (Reviewed in Dou et al., 2018). Segment 5 encodes the nucleoprotein (NP). Segment 6 encodes the neuraminidase (NA) protein, which is important in the release of the virus from the host cell, and segment 7 encodes for the matrix (M1) protein. Alternative splicing on this segment produces the M2 proteins (Shih et al.,1995). Finally, segment 8 encodes the non-structural protein 1 (NS1), and alternative splicing on the segment also allows the production of the nuclear export protein (NEP) (Lamb & Lai, 1980).

IAV has been the source of emerging pandemics and seasonal epidemics, often caused by zoonotic transmission into humans. There have been four pandemics in the 20th and 21st century caused by influenza, and specifically by H1N1, the first and most destructive of which was the Spanish Flu of 1918. The 1918 pandemic was followed by three more: 1957, 1977, and the most recent occurring in 2009 (Nakajima et al., 1978; Neumann et al., 2009). The pandemic potential of IAV is extremely high due to the potential reassortment of segmented genomes of two or more strains (i.e genetic shift) and the potential zoonotic transmission of highly pathogenic avian influenza strains H7N9 and H5N1 into humans (Sonnberg et al., 2013; Parry, 2013). IAV can infect both

birds and mammals (Webster et al., 1992). The HA of avian influenza viruses binds to the α-2,3 sialic acid receptor, whereas the HA of human influenza viruses attaches to the α-2,6 sialic acid receptor (Rogers & Paulson, 1983; Matrosovich et al., 2000). While there are influenza viruses that are restricted to birds, there are also strains of influenza that can infect an intermediate reservoir. These intermediate (or mixing) reservoirs for IAV are often swine. The upper airway of pigs have an abundance of both α-2,3 and α -2,6 sialic acid, and as an intermediate reservoir, these animals can be infected by IAV that can attach to either type of sialic acid (Kida et al., 1994). Additionally, this greatly increases the probability of genetic reassortment of the various genomic segments during infection in these intermediate reservoirs. Genetic reassortment is often the source of zoonotic cross-over into humans and can create pandemic potential strains.

1.1.2 IAV Replication Cycle

Viral entry is mediated by the HA glycoprotein attaching to the appropriate sialic acid on the cell surface and being endocytosed by clathrin or caveolae mediated endocytosis (Figure 1.1.1,2) (Nunes-Correia et al., 2004). Once inside the cell, the endosome undergoes acidification which allows for a conformational change to occur on HA, exposing the hydrophobic fusion peptide (Sarkar et al., 1989; Carr & Kim, 1993). During this pH change in the endosome, the viral protein M2 allows for essential acidification to occur within the virion (Ciampor et al., 1992). The hydrophobic fusion peptide in HA mediates fusion of the viral envelope with the wall of the endosome and this allows the influenza genome to be released into the cytoplasm of the cell (Reviewed in Blijleven et al., 2016) (Figure 1.1.3). Each RNA segment of the genome is helically wrapped around a core of oligomerized NP, in addition to the trimeric viral RdRp attached at the 3’ end of the RNA to allow for transcription to occur once the RNA has entered the nucleus. NP has a nuclear localization sequence (NLS) which facilitates the nuclear import of the ribonucleoprotein (RNP) through facilitated transport and interaction with α-importins via the nuclear pore complex (Figure 1.1.4) (Cros et al., 2005; O’Neill et al., 1995; Wu et al., 2007; Pemberton & Paschal, 2005). There is also evidence that Nucleoporin 85 interacts with PB1 and PB2 to aid in the nuclear import of vRNPs (Ling et al., 2022). Once in the nucleus, the transcription of the anti-sense

Figure 1.1

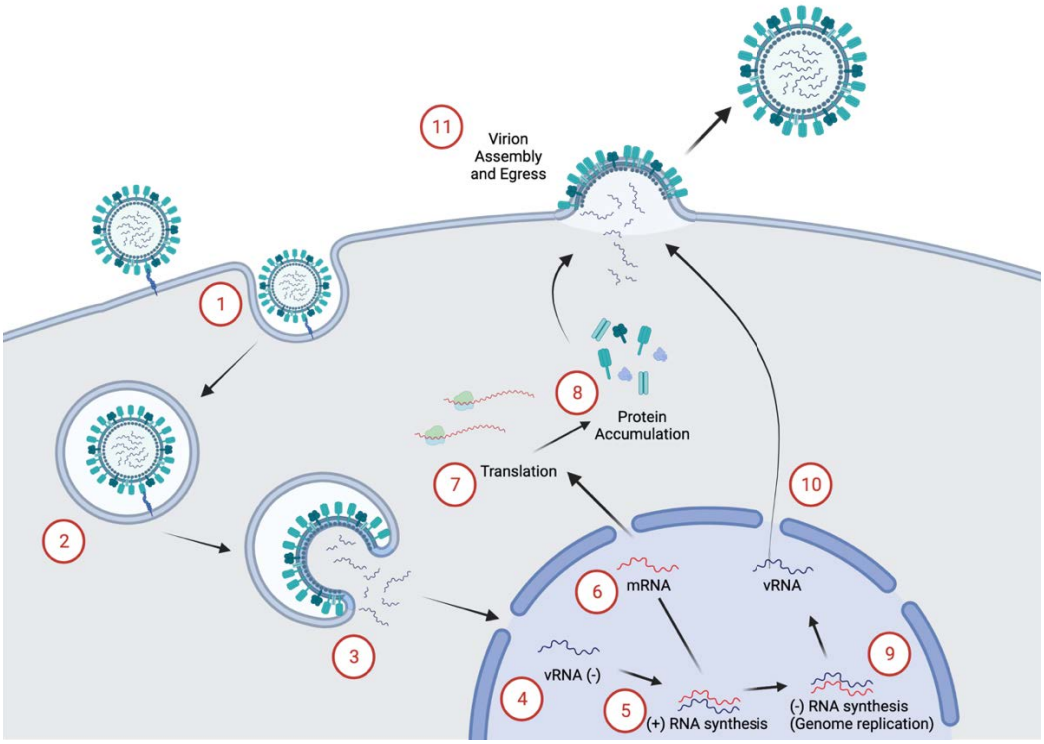

Figure 1.1 Influenza A Virus Life Cycle.

(1) IAV uses the HA glycoprotein to attach to the α-2,3 or the α-2,6 linked sialic acid receptor on the cell surface and is endocytosed by clathrin-mediated endocytosis. (2) Endosomal acidification exposes the hydrophobic fusion peptide on HA. Acidification inside the virion is facilitated by the M2 ion channel. (3) The viral membrane fuses with the endosomal membrane and the vRNP's are released into the cytoplasm of the host. (4) vRNPs traffic into the nucleus of the host cell via the NLS on the NP protein. (5) The RdRp carries out transcription of negative sense vRNA into positive sense mRNA. (6) The mRNA is then transported out of the nucleus (7) where it engages with host translational machinery to produce viral proteins. (8) Viral proteins accumulate, and NP and the viral polymerase proteins are imported into the nucleus which allows (9) genome replication to begin. Positive sense mRNA is transcribed by the RdRp into negative sense vRNA, which associates with NP and is (10) transported out of the nucleus to the cell membrane. (11) Viral proteins and the 8 unique vRNPs assemble at the cell membrane and the virus buds from the host cell. NA facilitates the release of the virus from the sialic acid receptor and the virus is released.

vRNA into positive sense messenger RNA (mRNA) begins (Figure 1.1.5).

Influenza's RdRp is composed of three subunits: PB1, PB2, and PA. Each of these proteins has a vital and unique role in the transcription of the genome. To initiate transcription of the vRNAs, the PB2 subunit of the RdRp binds to the 5' 7-methylguanylate (m7G) caps on cellular pre-mRNAs and the PA subunit uses its endonucleolytic activity to cleave the host pre-mRNA, creating a 10-15 nucleotide-long capped RNA primer (Dias et al., 2009). This process is termed "cap-snatching" and is a method by which the virus can produce a viral RNA with a 5' cap that host proteins can recognize. Following the cap-snatching by PB2 and PA, the PB1 subunit uses the 5'm7G capped primer to begin transcription of the vRNA into mRNA. NP can interact with both PB1 and PB2 and therefore helps keep the vRNA closely associated with the polymerase complex (Biswas et al., 1998). To produce a viral mRNA transcript that will be efficiently exported out of the nucleus, the virus also needs to create a poly-adenylate (p(A)) 3' tail. To produce this p(A) tail, the vRNA contains a 5-7 nucleotide stretch of uridines followed by a double stranded (ds)RNA pan-handle structure (Luo et al., 1991, Zheng et al., 1999). This stretch of uridines causes the polymerase to stutter and subsequently add on additional adenosines to the 3' tail of the new viral mRNA. Once the mRNAs have been transcribed by the RdRp, with their 5' caps and the 3' p(A) tails, they are processed and exported to the cytoplasm through nucleopore complexes with the help of Nucleoporin 93 (Furusawa et al., 2018) (Figure 1.1.6). As the mRNAs enter the cytoplasm they engage in cellular cap-dependent translation (Figure 1.1.7). The 5' m7G caps are bound by host translation factor eukaryotic initiation factor (eIF) 4E, along with eIF4G and the helicase eIF4A, which forms the eIF4F complex (Yángüez & Nieto, 2011). To aid in the preferential translation of viral mRNAs, viral NS1 binds to host eIF4G and allows for increased association of viral mRNA with polysomes (Burgui et al., 2003; de la Luna et al., 1995). The binding of the eIF4F complex to the 5' cap of the viral mRNA allows for the recruitment of the 40S ribosomal complex and translation of the RNA into viral proteins. As the viral proteins begin to accumulate, specifically NP and new subunits of the RdRp complex, the replication of the full-length viral genomic segments starts through the production of complementary (c)RNA (Figure 1.1.8,9). The production of cRNA is through an unprimed process which requires the complementation

of free ribonucleoside triphosphates (rNTPs) with the 3' end of the vRNA (Newcomb et al., 2009, York et al., 2013). Viral NP associates with the newly synthesized cRNA strand as it exits the polymerase (Lee et al., 2017; Williams et al., 2018). Following the production of the cRNP, it is used by the virus as a template to produce more genomic vRNPs, which are also bound by NP in a non-random pattern (Le Sage et al., 2018). As the infection progresses and more viral proteins accumulate, M1 and NEP facilitate the nuclear export of the vRNPs in a chromosomal region maintenance 1 (CRM1) dependent manner (York & Fodor, 2013; Paterson & Fodor, 2012) (Figure 1.1.10). Once the vRNPs are exported into the cytoplasm, they traffic along microtubules to the site of assembly through an association with Rab11A (Eisfeld et al, 2011). Some viral proteins are translated by endoplasmic reticulum (ER) associated ribosomes into the cell membrane (HA, NA), allowing the integration of their transmembrane domain into the ER and the subsequent secretion to the cell surface as transmembrane proteins (Engel et al., 2010; Scheiffele et al., 1997), while M2 traffics independently to the outer region of the cell (Leser & Lamb, 2005). The vRNPs traffic to these regions and each unique segment is assembled into the budding viral particle (Le Sage et al., 2018) (Figure 1.1.11). The actual assembly process of these vRNPs is unknown, but it is theorized that the assembly occurs through precise RNA-RNA interactions between the different vRNPs (Fournier et al., 2012; Gavazzi et al., 2013; Lee et al., 2017; Le Sage et al., 2020). Once all 8 vRNP segments have assembled and the virus has budded, the NA protein functions as a sialidase enzyme and cleaves the sialic acid receptor to facilitate release from the host (Figure 1.1.11).

The lifecycle of influenza, involving primary and secondary transcription events – primary transcription to produce mRNA which increases overall viral protein levels, and secondary transcription, where new vRNAs are transcribed to produce even more mRNAs - means that influenza RNAs need to persist in the host cells for extended periods of time. Additionally, very high levels of protein translation need to occur from those mRNAs to allow for robust viral replication. These factors for productive infection require IAV to evolve strategies to avoid RNA degradation and be preferential translated, and to put a limit on the host immune response. To achieve this, IAV has evolved proteins to be proficient in implementing a pro-viral environment in the host.

1.1.3 Host Shutoff

Host shutoff is an important mechanism that IAV uses during its replication lifecycle to create a pro-viral environment and have a successful infection. Host shutoff is a process by which viruses inhibit the general expression of host genes. This viral process is important not only for promoting cellular factors to favor viral replication, but also aids the virus in evading the host immune response. Many viruses encode specific proteins that carry out host shutoff functions. Alphaherpesviruses like herpes simplex virus –1 (HSV1) encode for virion host shutoff protein (vhs) (Shu et al., 2013; Zenner et al., 2013), gammaherpesviruses like Kaposi's sarcoma-associated herpes virus (KSHV) encode an endonuclease called SOX (Glaunsigner & Ganem, 2004), betacoronaviruses like severe acute respiratory syndrome corona virus (SARS-CoV, SARS-CoV-2) encode non-structural protein 1 (NSP1) **(**Yuan et al., 2021)**,** and orthomyxoviruses' like IAV encode PA-X and NS1. Specifically, for vhs, SOX, NSP1, and PA-X, each of these proteins target host RNAs for cleavage and require the use of host nuclease Xrn1 to degrade the cleaved RNA (Gaglia et al., 2012). For IAV infection, while it utilizes PA-X as a primary host shutoff factor, NS1 also plays a vital role in subverting the host's immune response and aiding in the preferential export and translation of IAV mRNA.

Although IAV is the main cause for seasonal epidemics and emerging pandemics, influenza B virus (IBV) is another member of the *Orthomyxoviridae* family that also contributes to the seasonal epidemics. IBV is similar to IAV in viral structure, genome organization, and replication strategies. While these viruses are quite similar, there are also some fundamental differences in their host range. Unlike IAV, IBV can only infect humans and few other mammals (eg. harbour seals) (Bodewes et al., 2013). As described previously, IAV can undergo both antigenic shift and antigenic drift due to the nature of its host range, whereas IBV has very little potential to undergo antigenic shift, and the antigenic drift of the virus is much more subdued (Bedford et al., 2014). Another important difference between IAV and IBV is that IBV does not encode for host shutoff protein PA-X, and its NS1 has limited sequence similarity to IAV's NS1 with certain functional differences as well. These substantial differences between IAV and IBV's host shutoff proteins have led to many questions about how and if IBV can carry out host shutoff and if not, how does it have successful and productive infection.

1.2 Influenza A Virus Host Shutoff Strategies

1.2.1.1 PA-X

The IAV endonuclease PA-X is produced during translation of PA (Jagger et al., 2012). PA is an RdRp subunit and contains an N-terminal RNA-endonuclease domain that is responsible for aiding in cap-snatching during the transcription of the viral mRNA, as described above (Hara et al., 2006). At a relatively low frequency of 1.3%, during translation of PA there is a ribosomal frameshift into the +1 frame (Jagger et al., 2012). This frameshift occurs at the 191F position and is caused by codon sequence UUU in the P-site and the rare codon CGU in the A-site (Figure 1.2A). The 0-frame codon UUU and the +1-frame codon UUC are decoded by the same phenylalanine tRNA which tends to favor the codon UUC over UUU. Therefore, the confounding factors of favorable P-site repairing to UUC and scarcity of the tRNA with the anticodon for CGU, causes the frameshifting event into the +1 frame (Jagger et al., 2012). Due to the nature of PA-X's production, the protein retains the endonuclease domain of PA, but has a unique C-terminal end termed the "X-ORF" which varies in length from 41- to 61- amino acids (Shi et al., 2012) (Figure 1.2A). This X-ORF is important for PA-X's host shutoff activity, and in particular the N-terminal 15 amino acids in the X-ORF are critical for its ability to suppress host gene expression (Hayashi et al., 2016). Of those 15 important X-ORF domains, the first 9 are imperative for the nuclear localization of PA-X, and the next 6 domains are important to have maximal PA-X function (Hayashi et al., 2016) Additionally, PA-X does not contain the localization domain of PA and therefore does not localize with the other two polymerase subunits of IAV but can still be recruited to the nucleus via specific X-ORF interactions, unlike host shutoff proteins from other viruses (Khaperskyy et al., 2016).

The targeting of PA-X is specific for RNA polymerase II (Pol II) transcripts and requires the activity of host 5' to 3' exonuclease Xrn1 (Khaperskyy et al., 2016). Viral RNAs are produced via the virally derived RdRp which protects them from the targeting and cleavage of PA-X. More specifically, the host shutoff activity of PA-X preferentially

Figure 1.2

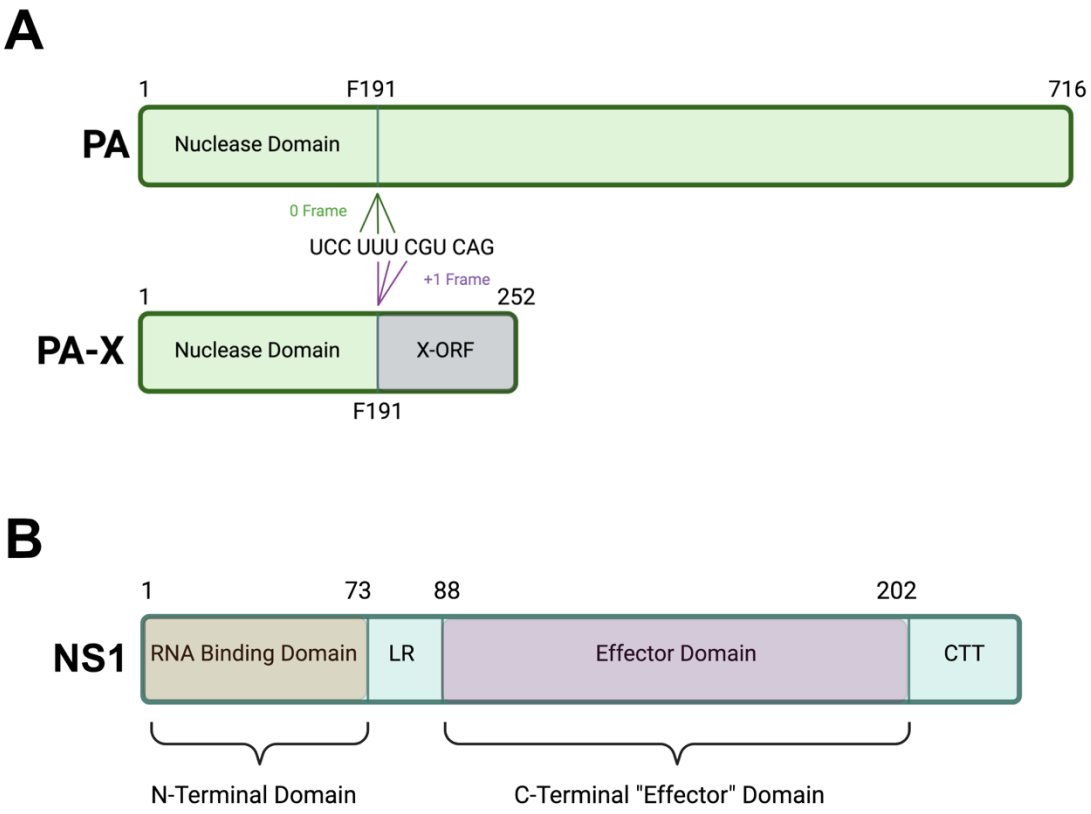

Figure 1.2 Host Shutoff Proteins PA-X and NS1.

(A) The production of PA-X requires a ribosomal frameshift into the +1 frame at position 191 on the PA mRNA during translation. The UUU codon in the 0 frame and the UUC codon in the +1 frame are decoded by the same tRNA, which tends to favor UUC over UUU. This factor in addition to the scarcity of the tRNA with the anticodon for the CGU at position 192 causes the ribosomal frameshift into the +1 frame. This produces a unique C-terminal domain for PA-X, termed the X-ORF, while the N-terminus is consistent with that of PA. **(B)** General overview of the domains of IAV NS1 protein. The N-terminal domain contains the RNA binding domain (specifically amino acids R38 and K41). This is immediately followed by a linker region (LR) to the C-terminal effector domain. The effector domain is important for NS1 dimerization and for facilitating many of NS1's protein interactions. At the very C-terminal region of NS1 is a C-terminal tail (CTT).

targets spliced transcripts in the host (Gaucherand et al., 2019). Furthermore, the X-ORF interacts with proteins involved in mRNA processing, which could dictate the localization of the protein and allow the more specific access to mRNAs that have been processed via splicing (Gaucherand et al., 2019).

PA-X activity during infection drastically decreases the cytoplasmic pool of host RNAs (Khaperskyy et al., 2014). When overexpressed in cells, the presence of PA-X corresponded to cells that had severely decreased cytoplasmic p(A) RNAs and an increase in the amount of endogenously cytoplasmic poly-A binding protein 1 (PABP) in the nucleus (Khaperskyy et al., 2014). The increase of PABP in the nucleus is described, not only as a sign of PA-X function, but other host shutoff nucleases have been shown to create a similar cellular landscape (Lee & Glaunsinger, 2009; Kumar et al., 2011). PABP contains four N-terminal RNA recognition motifs (RRM) which can bind to p(A) tracks, and a C-terminal region important for interacting with proteins that contain a PABP interacting motif (PAM2). In the cytoplasm PABP binds p(A) mRNAs and has been shown to participate in translation initiation, mRNA stabilization, and mRNA decay (Reviewed in Afonina et al., 1998; Caponigro & Parker, 1995). Interestingly, PABP can shuttle in between the cytoplasm and the nucleus through the importin- α/β mechanism, even though it only contains a non-canonical NLS in its RRM (Afonina et al., 1998, Gray et al., 2015). The interaction between the NLS and importins is outcompeted by the binding of the RRM to RNA in the cytoplasm, which means that any PABP bound to RNA will not be imported into the nucleus (Kumar et al., 2011). To aid in translation, PABP interacts with the p(A) tail of the mRNA through its N-terminus, and then also interacts with the eIF4G component of the cap binding complex, which allows the circularization of the mRNAs (Wells et al., 1998; Park et al., 2011). Endogenously nuclear PABP (PABPN) plays an important role in the polyadenylation of pre-mRNAs as it can stimulate the activity of the p(A) polymerase on the 3' end of the RNA in cooperation with the cleavage and polyadenylation specificity factor (CPSF) 30 complex (Wahle, 1991; Kühn et al., 2009). The shuttling into the nucleus of cytoplasmic PABP allows it the opportunity to associate with pre-mRNAs as well, and there has been evidence that PABP in the nucleus can be found near the p(A) polymerase, similarly to PABPN (Hosoda et al., 2006). The accumulation of cytoplasmic PABP in the nucleus has

been shown to induce the hyperadenylation of mRNA transcripts and the nuclear retention of p(A) RNA (Kumar & Glaunsinger, 2010).

PA-X is also known to be important for IAV pathogenicity as its activity targets transcripts that encode host immune factors like interferon-β (INF- β) (Hayashi et al., 2015; Rigby et al., 2019). Interestingly, while PA-X is encoded by all IAV strains, the strength by which it downregulates host transcripts can vary (Hussain et al., 2019). By cleaving host transcripts in both the cytoplasm and in the nucleus, PA-X can limit the number of cellular mRNAs that are shuttled to polysomes for translation. This not only reduces the overall concentration of host transcripts that may be involved in regulating an antiviral immune response, but also frees up the translational machinery for viral transcripts.

1.2.1.2 PA-X Post Translational Modifications

PA-X activity has been shown to be influenced by a post translational modification (PTM) to its N-terminus. The presence of N-terminal acetyltransferase B (NATB) causes an increase in the host shutoff activity of PA-X by causing the acetylation of the second amino acid E2 (Oishi et al., 2018). Interestingly, because PA-X and PA share an N-terminus, it was also discovered that NATB causes the acetylation of PA on the E2 amino acid and when this interaction is inhibited there is lower viral polymerase activity (Oishi et al., 2018). These findings could indicate that acetylation plays an important role in the catalytic function of PA and PA-X during infection.

1.2.2.1 NS1

NS1 is another protein implicated in the host shutoff mechanism of IAV. NS1 has many roles during IAV infection, and its mechanism of action can vary based on the strain of IAV. It is a 26 kilodalton (kDa) protein, is encoded by all IAV strains, and is produced at high concentrations during infection (Krug & Etkind, 1973; Compans, 1973). It plays an important part in aiding viral RNA export, limiting host pre-mRNA processing, and helping viral mRNA association with polysome translational machinery (Reviewed in Hale et al., 2008; Qiu & Krug, 1994). Additionally, NS1 plays a large part in inhibiting the antiviral immune response during infection. NS1 has two main domains: an N-terminal RNA binding domain (residues 1-73), and a C-terminal effector domain (residues 88-202), which are joined together via a linker domain (Kim et al., 2021)

(Figure 1.2B). The remaining residues on the C-terminus are termed the C-terminal tail, which can conformationally change depending on the interactions between NS1 and host proteins (Hale, 2014). In the N-terminal RNA binding domain (RBD), two residues, R38 and K41, are essential for the dsRNA binding activity of NS1 (Chien et al., 2004; Wang et al., 1999). The RBD activity allows IAV to be protected from an antiviral state induced by increased production of IFN β (Chien et al., 2004). NS1 constitutively exists as a homodimer, both the RBD and the effector domain can facilitate dimerization, specifically the W187 domain is vital for effector domain dimerization (Aramini et al., 2011; 2014).

NS1 can function in both the nucleus and the cytoplasm. In the cytoplasm, NS1 aids in the preferential translation of viral mRNAs. Utilizing the N-terminal 113 amino acids, NS1 can bind directly to eIF4G (Aragón et al., 2000). Another important translation factor that NS1 binds to in an RNA independent manner is PABP, through a domain in the N-terminal residues 1-81 (Burgui et al., 2003). The interaction between NS1, eIF4G, and PABP creates a potential heterotrimer which is brought to viral mRNA through NS1's interaction with their 5' untranslated region (UTR) (Burgui et al., 2003). Additionally, NS1 impacts the ability of the host to induce antiviral signaling, which will be introduced in section 1.3.2.

In the nucleus, NS1 prevents the splicing, maturation, and polyadenylation of host RNAs. NS1 associates with spliceosomal factors and U6 snRNA to limit the splicing of pre-mRNA (Lu et al., 1994; Reviewed in Dubois et al., 2014). Pre-mRNA that are not matured through splicing will not be transported out of the nucleus, thereby NS1 effectively diminishes the pool of pre-mRNAs that are matured, exported, and translated. Certain strains of IAV also produce NS1 proteins that can interact with the CPSF30 complex through their C-terminal effector domain (Nemeroff et al., 1998). This interaction prevents further 3' end processing of host pre-mRNAs. Additionally, PABPN is an endogenously nuclear p(A) binding protein that is required for the 3' end cleavage and export of host mRNAs. NS1 proteins can form complexes with CPSF30 and PABPN, which prevents their interactions with host RNAs (Chen et al., 1999). NS1 is also able to interact with the nuclear RNA export factor 1 (NXF1) component of the NXF1- nuclear transport factor 2 like export factor 1 (NXT1) nuclear export complex. The NXF1-NXT1

complex is the main receptor that allows for the translocation of mRNAs through the nuclear pore complex (Kim et al., 2018; Stewart, 2010; Zhang et al., 2019). The interaction between NS1 and the NXF1-NXT1 complex allows the virus to limit the export of host mRNAs, and therefore limits the amount of transcripts associated with antiviral immune-modulation that are exported and translated (Zhang et al., 2019).

1.2.2.2 NS1 Post Translational Modifications

Post-translational modifications of NS1 have been shown to impact the function and the stability of the protein. ISGylation is a type of ubiquitination done by ISG15 ubiquitin like modifier (ISG15) that has been associated with important innate immune responses against viruses and is stimulated by an IFN response (Reviewed in Zhang et al., 2021b). ISGylated NS1 is unable to dimerize and therefore is severely limited in its ability to inhibit the antiviral immune response (Tang et al., 2010). Interestingly, different strains of IAV NS1 have varying ISGylation moieties, indicating there are variable levels of impact depending on the strain of IAV, for example, ISGylation on K41 limits NS1's ability to bind with importin-α (Tang et al., 2010; Zhao et al., 2010). Another post-translational modification that can impact NS1 is SUMOylation (Reviewed in Lamotte & Tafforeau, 2021). During infection IAV increases the global rates of SUMOylation which suggests that this post translational modification is beneficial for the virus (Pal et al., 2011). The conjugation of small ubiquitin-like modifier 1 (SUMO1) to NS1 enhances the proteins stability and increases NS1's half-life, and therefore can have a large impact on the replication efficiency of the virus (Xu et al., 2011; Santos et al., 2013). NS1 also has six sites that can be phosphorylated. Recently, T49 was discovered to be an important phosphorylation site at late time points during infection (Kathum et al., 2016). The phosphorylation of the T49 residue reduced NS1's ability to bind to dsRNA, Tripartite Motif Containing 25 (TRIM25) and retinoic acid-inducible gene I (RIG-I) (Kathum et al., 2016). Finally, acetylation of NS1 also occurs as a post-translational modification. Acetylation on residue K108 is important for the proteins ability to inhibit the Type I IFN response during infection (Ma et al., 2020).

1.3 Influenza A Virus Interaction with Host Cell Immune Response

1.3.1 Innate Immune Response During Infection

As previously described, NS1 is involved in a multitude of ways to inhibit the processing, maturation, export, and translation of cellular mRNAs during infection. This is one set of mechanisms that the virus uses to subvert the host immune response. Many of the cellular RNAs being inhibited during infection are involved in immune signaling or immune modulation (Das et al., 2008). In addition to preventing the expression of those antiviral immune proteins, NS1 also can impact the signaling of various immune modulatory systems in the host cell during infection.

Due to the partial complementarity of the 3' and 5' ends of the viral RNA, it can form small 5' triphosphate dsRNA structures (Pflug et al., 2014). The cell has many different pathogen recognition receptors (PRR) that can identify this structure as a pathogen associated molecular pattern (PAMP). There are two main PRR's that identify the IAV PAMPS: Toll-like receptors (TLR's) and Retinoic acid-inducible gene-I like receptors (RLR's) (Talon et al., 2000). TLR3, located on the surface of respiratory epithelial cells, alveolar macrophages, and dendritic cells, can recognize dsRNA and has a main function to induce pro-inflammatory cytokines and INF in response to IAV infection (Le Goffic et al., 2007; Guillot et al., 2005). When TLR3 is activated, it causes the recruitment of TIR-domain-containing adapter-inducing interferon-β (TRIF) through a Toll/interleukin (IL)-1 receptor (TIR) domain (Yamamoto et al., 2003). TRIF then binds TNF Receptor Associated Factor (TRAF)3/6 (Häcker et al., 2006), which then cause the activation of TANK Binding Kinase 1 (TBK1)/ IκB Kinase (IKK)-ϵ and IKK/IKK-β (Chau et al., 2008). TBK1/IKK-ϵ and IKK/IKK-β play important roles in contributing to the phosphorylation cascade that causes the activation of interferon regulatory transcription factor (IRF) 3 and Nuclear factor κ-light-chain-enhancer of activated B cells (NF-κB) (Fitzgerald et al., 2003). Once activated, IRF3 and NF-κB translocate into the nucleus and act as transcription factors for Type I IFN (IFNβ). TLR7 also functions to identify viral dsRNAs. Once activated by the PRR, TLR7 will interact with MYD88 Innate Immune Signal Transduction Adaptor (MyD88) to activate IRF7, and subsequently cause the translocation of NF-κB and IRF7 into the nucleus to act as

transcription factors for Type I IFN's (Lund et al., 2004). TLR7 is localized to the endosomes of most lung epithelial cells, and therefore can recognize viral RNA early upon entry into the host (Reviewed in Mifsud et al., 2021). The interaction with MyD88 and the activation of NF-κB and IRF7 by TLR7 occurs independently of signaling through the mitochondrial antiviral signaling protein (MAVS) (Reviewed in Mifsud et al., 2021).

In the cytoplasm, RLR's RIG-I, and melanoma differentiation-associated protein 5 (MDA5) both act to respond to IAV infection through interacting with and activating MAVS (Loo et al., 2008). The third class of RLR's - laboratory of genetics and physiology processing protein 2 (LGP2) have been shown to be involved in regulating the signaling of RIG-I and MDA5 as they lack the necessary caspase activation and recruitment domains (CARD) domains to induce signaling through MAVS on their own (Rehwinkel & Gack, 2020; Satoh et al., 2010). MDA5 specifically recognizes the synthetic dsRNA analog polyinosine-polycytidylic acid (poly(I:C)) and plays a vital role in recognizing picornavirus infection (Kato et al., 2006), whereas RIG-I is essential for producing an interferon response during many other RNA virus infections, and specifically for this body of work, IAV (Kato et al., 2006; Rehwinkel & Gack, 2020). RIG-I is composed of N-terminal CARDs, a DEx(D/H) box helicase, and a C-terminal domain (CTD) (Kowalinski et al., 2011). The CTD has a 5'triphosphate binding pocket which allows the base pairs of the RNA to interact with the DEx(D/H) helicase domain (Jiang et al., 2011; Yoneyama et al., 2004). This stable RNA-RIG-I interaction causes the CARD domains to be displaced from their interactions with specific sections of the helicase domain (Kowalinski et al., 2011). The CARD domains oligomerize and are modified via E3 ubiquitin ligase TRIM25, RNF125 or Riplet (Oshiumi et al., 2010, 2013, Gack et al., 2007) and can then interact with the cytoplasmic CARD domain on MAVS (Wu & Hur, 2015).

MAVS is composed of a CARD domain, a long (approximately 400 amino acids) linker domain, and then a transmembrane domain which maintains MAVS localization to the mitochondria (Wu & Hur, 2015). Within the linker domain there is a proline-rich region which binds to the TRAF molecules (Liu et al., 2013). The activation and interaction between MAVS and TRAF2/3/5/6 cause the activation of the TBK1 complex,

composed of TBK1, IKKϵ, and NEMO, whereas interaction between MAVS and TRAF2/5/6 causes activation of the IKK complex, composed of IKKα/β and NEMO (Fang et al., 2017, Reviewed in Ren et al., 2020, Seth et al., 2005). Once activated, the TBK1 complex causes the phosphorylation, homodimerization, and nuclear translocation of IRF3 and/or IRF7 where they bind to IFN-stimulated response elements (ISRE) and induce the transcription of Type I IFN genes. In the same way, activated IKK complexes cause the release of NF-κB and its subsequent translocation into the nucleus where it acts as a transcription factor for proinflammatory cytokines (reviewed in Ren et al., 2020).

Once IFN's are produced in the host cell, they are secreted and bind to IFN α/β receptors (IFNAR)'s on the cell surface. IFNARs are associated with tyrosine kinase 2 (TYK2) and Janus kinase 1 (JAK1), and upon binding to IFN, the IFNAR dimerizes and causes canonical tyrosine autophosphorylation of JAK1 (Reviewed in Mazewski et al., 2020). This autophosphorylation induces the phosphorylation of signal transducer and activator of transcription (STAT) 1 and STAT2 proteins. The STAT1/2 heterodimer forms a complex with IRF9, and this heterotrimeric complex translocates into the nucleus and can bind to ISRE's and induce the transcription of IFN stimulated genes (ISG's) (Platanias, 2005). These ISGs include 2′5′-oligoadenylate synthetase (OAS) and ribonuclease L (RNaseL), IFN-inducible dsRNA-dependent protein kinase R (PKR), RIG-I, and TRIM proteins (Reviewed in Bowie & Unterholzner, 2008).

1.3.2 NS1 Inhibits Innate Immune Signaling

NS1 interacts with many of these innate immune-signaling players and interferes in the progression of signaling cascades to limit the hosts antiviral immune response. Importantly, NS1 is essential for the efficient replication of IAV in host cells that have functional IFN signaling pathways - mutant IAV viruses that are lacking in the NS1 protein are not able to replicate in IFN-competent systems but are able to have successful replication in cells deficient in IFN (Bergmann et al., 2000; Egorov et al., 1998; García-Sastre et al., 1998).

To begin, NS1 can interrupt the early stages of RIG-I signaling through interacting with the two E3 ubiquitin ligases, TRIM25 and Riplet, that are responsible for ubiquitinating RIG-I to allow the signaling cascade to occur (Gack et al., 2009; Rajsbaum et al., 2012). NS1 inhibits the oligomerization of TRIM25, mediated through NS1

residues E96/E97 (Gack et al., 2009). NS1 also directly binds to Riplet through the R38/K41 amino acid residues (Rajsbaum et al., 2012). By interacting with TRIM25 and Riplet, NS1 limits their ability to ubiquitinate the CARD on RIG-I and therefore prevents RIG-I from interacting with the CARD domain on MAVS and inhibits the downstream immune signaling cascade (Gack et al., 2009; Hou et al., 2011). Additionally, NS1 sequesters RNA away from RIG-I to prevent its direct activation as well by using its RNA binding domains. Downstream in the RIG-I signaling cascade, NF-κB is released and translocates to the nucleus where it acts as a transcription factor to promote the transcription of IFN genes. Recently NS1 has been shown to co-localize with NF-κB in the nucleus at the IFN gene promoters and this interaction decreased the enrichment of RNA polymerase II to the transcriptional start sites (Lee et al., 2022).

The ISG PKR is activated by a confirmational change that can occur through binding dsRNA or PKR-activating protein (PACT) (Li et al., 2006; Patel & Sen, 1998; Williams, 1999). PKR activation results in autophosphorylation and then subsequent phosphorylation of eIF2α, which leads to an interruption of translation in the cell (Gale & Katze, 1998; Dey et al., 2005). Because IAV relies on host machinery to translate proteins, this effectively stops viral protein translation. NS1 can bind directly to both ssRNA and dsRNA in infected cells (Hatada & Fukuda, 1992) and the binding of viral RNA allows NS1 to sequester it away from PKR to prevent its activation. Another ISG that is activated by the presence of dsRNA is 2’5' OAS/RNase L. In the presence of dsRNA, 2’5’OAS synthesizes 2–5-oligoadenylate (2–5A) from adenosine triphosphate (ATP), which then goes on to bind to RNase L, causing its dimerization and activation, allowing the endonuclease to cleave a broad spectrum of host and viral RNAs (Dong et al., 1994; Karasik et al., 2021; Li et al., 2016). This endonucleolytic activity is not only bad for the virus, but it also can create new PAMPs for recognition by RIG-I, facilitating further signaling through the RIG-I/MAVS pathway (Reviewed in Chakrabarti et al., 2011).

NS1 has also been shown to play a role in activating the phosphatidylinositol 3-kinase (PI3K)/ AKT Serine/Threonine kinase (Akt) pathway (Ehrhardt et al., 2007). The activated PI3K/Akt pathway is involved in many different cellular functions, most of which are involved in maintaining cell survival, protein synthesis, and preventing

apoptosis (Hemmings & Restuccia, 2012). NS1 binds directly to the p85B subunit of PI3K, which causes its activation and subsequent activation of Akt, therefore contributing to increased cell survival and continued protein synthesis during infection (Ehrhardt et al., 2007, Li et al., 2012).

1.4 Current Model of Host Shutoff

The current model of host shutoff during IAV infection is shown in Figure 1.3. PA cleaves host pre-mRNAs in the nucleus for the process of cap-snatching, diminishing the pool of host pre-mRNAs to be matured. On the 3' end of those pre-mRNAs, NS1 interacts with CPSF30 and PABPN (or PABII) to prevent the 3' cleavage and polyadenylation of the host transcripts. This renders these transcripts unfit and subsequently causes their degradation. NS1 plays many roles (as previously described) to aid in the preferential export of vRNAs to the cytoplasm and their translation. At later times post infection, during the export of vRNPs from the nucleus to be packaged at the cellular membrane, NS1 limits their detection from innate host immune sensors. Additionally, the production and activity of PA-X causes host transcript cleavage in the cytoplasm. This cleavage specifically targets transcripts that have been transcribed by RNA Pol II and have been processed through splicing. The PA-X mediated cleavage causes a depletion of host RNA transcripts in the cytoplasm. The depletion of those transcripts has been associated with increased shuttling of endogenously cytoplasmic PABP into the nucleus. This has been regarded as a hallmark phenotype of PA-X function during infection. The increase of PABP in the nucleus is also classically associated with an increase of p(A) RNA signals in the nucleus as well.

According to this model, PA-X and NS1 activities independently complement each other in mediating efficient host shutoff by IAV. There is currently limited understanding if there is a functional relationship between NS1 and PA-X and if there is interplay between the two host shutoff proteins IAV produces.

Figure 1.3

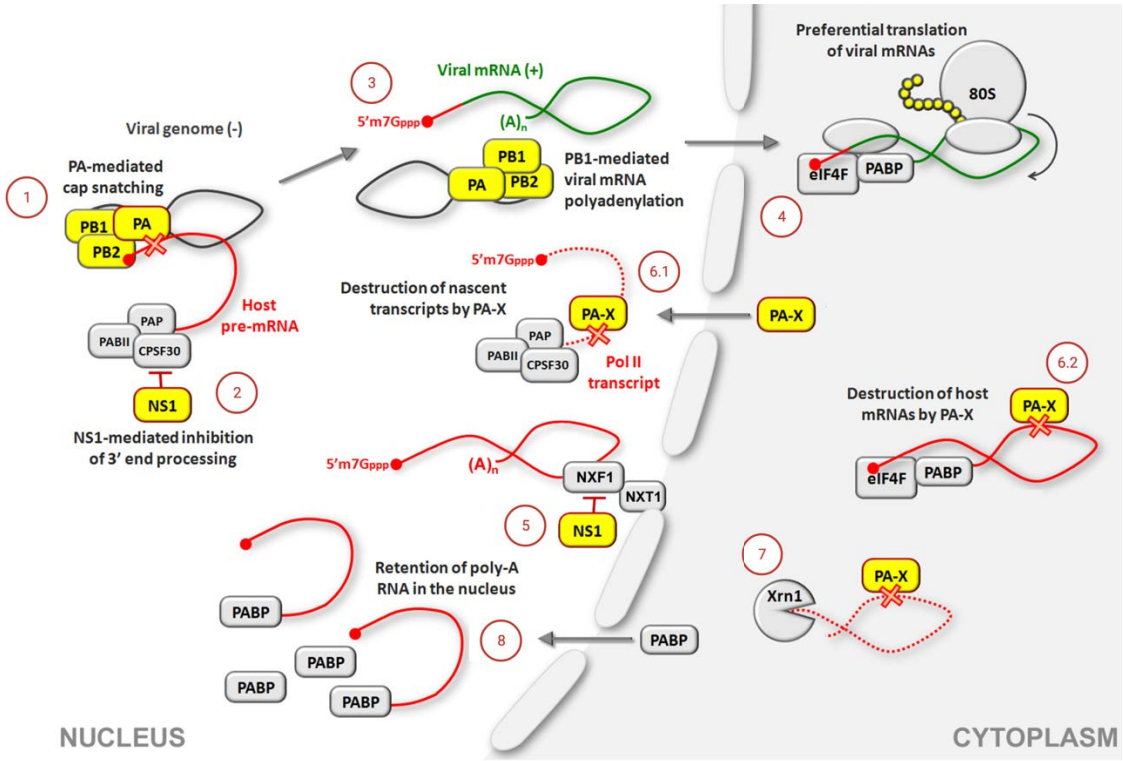

Figure 1.3 Current Model of IAV Host Shutoff.

(1) PA mediates cap-snatching in the nucleus to prime viral transcription and limit host pre-mRNA pool. **(2)** NS1 interacts with CPSF30 to limit the 3' end processing of host pre-mRNAs in the nucleus. **(3)** Viral mRNAs have a host derived 5' cap and a virally derived 3' p(A) tail to allow for efficient export and **(4)** once in the cytoplasm the viral mRNAs will compete for and interact with host machinery for translation of viral proteins. **(5)** NS1 limits the export of host mRNAs by interacting with the NXF1 subunit of the NXF1-NXT1 nuclear export complex. **(6)** PA-X cleaves host transcripts that have been transcribed by host RNA polymerase II in both the **(6.1)** nucleus and the **(6.2)** cytoplasm. **(7)** Host transcripts that are cleaved by PA-X are targeted for degradation by host exonuclease XRN1. **(8)** The depletion of the cytoplasmic pool of mRNAs causes the shuttling of cytoplasmic PABP into the nucleus which causes the retention of p(A) RNAs.

1.5 Question, Rationale, Objectives

This thesis sought to answer the question of if there is specific interplay or a functional relationship between NS1 and PA-X. Additionally, I wanted to understand how that functional relationship may impact IAV host shutoff. To do this I aimed to characterize the impact of NS1 and PA-X on the abundance, presence, and localization of host transcripts during IAV infection. Additionally, I utilized recombinant IAV viruses, NS1 and PA-X mutants, to try to dissect the interplay between the two proteins and how they each had an impact on general IAV host shutoff. Each of these proteins has been shown to have important host shutoff phenotypes independently, during infections or during over-expression analysis, but their impacts together during infection may not simply be additive; instead, they may have a synergistic functional relationship. Ultimately, I hypothesized that NS1 can augment the levels of PA-X during infection to promote increased host shutoff through PA-X mediated cleavage of host transcripts.

To investigate these questions, I used an infection model in A549-Wild Type (WT) and A549-MAVS knock out (KO) cell lines. I infected these cells with a variety of WT and mutant IAV, using the strain H1N1 A/Puerto Rico/8/1934 (PR8). These infection experiments were analyzed via western blotting, RNA isolation, RT-qPCR, immunofluorescence (IF), fluorescent *in situ* hybridization (FISH), and single molecule FISH (smFISH). I also used HEK 293T and 293A transfection models to attempt to isolate PA-X from whole cell samples.

CHAPTER 2: MATERIALS AND METHODS

2.1 Cell Culture

All cell culture work was carried out in a biosafety cabinet (BSC) following the appropriate biosafe protocols. Adenocarcinoma lung cancer (A549) cells, A549-MAVSKO cells (Rahim et al., 2020), Madin-Darby Canine Kidney (MDCK) cells, Human embryonic kidney (HEK) 293A and 293T cells, and African green monkey kidney epithelial cells (VERO) cells were all cultured in Dulbecco's modified Eagles medium (DMEM) supplemented with 10% fetal bovine serum (FBS) and 2mM L-glutamine (All purchased from Thermo Fisher Scientific ((Thermo), Waltham, MA, USA). Transformed human bronchial epithelial (BEAS-2B) cells were a kind gift from Dr. Jean Marshall (Dalhousie University) and were cultured in complete Bronchial Epithelial Basal Medium (BEBM, Lonza, Kingston, ON, Canada) supplemented with the BEGM SingleQuots kit (Lonza). All cells were cultured at 37° Celsius (C) in 5% CO2 and atmospheric oxygen. Dishes used to grow BEAS-2B cells were coated with coating media (0.01 mg/mL fibronectin, 0.03 mg/mL bovine collagen type I and 0.01 mg/mL bovine serum albumin (BSA, Sigma-Aldrich, St. Louis, MO, USA) dissolved in BEBM) overnight before seeding the cells. All cell lines were split when they reached 85% confluency using 0.05% Trypsin-EDTA (Thermo).

2.2 Viruses, Virus Production, Infections

All virus stocks were grown in VERO or MDCK cell lines. A monolayer of cells was infected with virus stock at an multiplicity of infection (MOI) of 0.1 or 1. Infections were done in infection media (DMEM with 0.5% BSA and 1% L-glutamine). Infection media was supplemented with either 1 μg/mL (MDCK) or 2.5 μg/mL (VERO) of L-1-tosylamido-2-phenylethyl chloromethyl ketone (TPCK) trypsin. Supernatants were collected following clearance of the monolayer and clarified, titered via plaque assay or focus forming units (FFU) and stored at –80°C.

Plaque assays were completed in 100% confluent monolayers of MDCK cells. Each titre of the virus was measured in duplicate. The viruses were thawed rapidly at 37° C and then diluted using 10-fold serial dilutions in 0.5% BSA in DMEM. Following a phosphate buffered saline (PBS, Thermo) wash on the MDCK monolayer, the serially diluted virus was added onto the cells and was incubated for 1 hour at 37°C in 5% CO2

and atmospheric oxygen. Every 10 minutes the cells with inoculum were shaken to prevent drying and to allow for effective adsorption. The overlay was prepared using 9 volumes of 2X Minimum Essential Media (MEM, Thermo) to 1 volume 5% BSA in DMEM, supplemented with 2 µg/mL TPCK-trypsin and then kept at 37°C. Equal volumes of the 2XMEM/Trypsin and melted 37°C 2% agarose in water was combined and added to the infected monolayer of cells following a PBS wash. The plates were kept steady at room temperature for 5 minutes to allow the agar to solidify and then incubated at 37°C with 5% CO2 and atmospheric oxygen for 48-72 hours. Following incubation, an equal volume of 10% formaldehyde in PBS was overlayed on the agar and incubated for 1 hour. The formaldehyde was removed and the softened agarose was gently removed from each well. The wells were then covered again with 10% formaldehyde in PBS for 15 more minutes to allow for complete fixation. The wells were then washed gently with PBS twice and stained with crystal violet for 5 minutes. The wells were then washed with tap water and plaques were counted once the wells were dry.

The main strain of IAV used for this project was A/PuertoRico/8/1934(H1N1) and the strain of IBV used was B/Brisbane/60/2008. A variety of different IAV mutants were developed and used for this body of work. I used a NS1 mutant virus that had previously been developed and used in Khaperskyy et al. (2014) called N80. Additionally, NS1 mutants R38A, K41A (38,41A), E96A, E97A (96,97A), I123A, M124A (123,124A), 88A, Y89A, 90A (88-90A), and W187R were used. These mutants were produced using the reverse genetics procedure described later in this section. In addition to these NS1 mutants, I also utilized IAV PA mutants in these investigations. PA(fs) was previously developed and published (Khaperskyy et al., 2014) and does not produce PA-X during infection. Finally, PR8 mutant N80(fs) was made by utilizing the reverse genetics system to produce a PR8 virus that contained both the N80 NS1 mutation as well as the PA(fs) mutation.

Reverse genetics was used to produce new stocks of IAV, as well as to generate new mutants to screen. A co-culture of MDCK and 293T cells were grown to approximately 90% confluency. The replicon pHW-plasmids were each prepared in equal amounts – PA, PB1, PB2, HA, NP, NA, M, NS – to a total of 6 µg DNA/well for a 6-well dish. For mutant virus preparation, the appropriate plasmid was created using site

directed mutagenesis (2.10) or sourced from the plasmid library available in the laboratory and then substituted into the collection of replicon plasmids used for virus generation. The DNA mix was combined with Opti-MEM-I (Reduced serum media, Thermo) to make 250 µL DNA/Opti-MEM-I mix per well. A 12 µL volume of TransIT-LT1 reagent (Mirus, Madison, WI, USA) was then added to the DNA mix and incubated at room temperature to allow the transfection complexes to form. The co-culture was washed with Opti-MEM-I and 0.75 mL of Opti-MEM-I was added to the Opti-MEM-I/DNA/TransIT-LT1 mixture to bring the volume to 1 mL/well. This mixture was added dropwise onto the cells. These were incubated at 37°C and 5% CO2 for 5 hours and then the transfection media was removed and replaced by fresh Opti-MEM-I. The cells were then incubated overnight and checked for transfection efficiency using the replicon control (replaced NA plasmid with the pPolI-WNA-GFP reporter). Once the virus had begun infecting the MDCK's (approximately 2-3 days), the virus was collected, clarified, and transferred onto a new plate of MDCK's supplemented with 1 µg/mL TPCK-trypsin. After evidence of cytopathic effect (CPE) on the new monolayer of MDCK's, the virus was collected, clarified, and stored at –80°C.

2.3 Immunofluorescence, FISH, and smFISH

IF was completed with A549-WT, A549-MAVSKO, MDCK, and 293A cells. Cells were seeded onto coverslips (18mm round, No. 1 or No. 2, VWR) in a 12-well plate (20 mm wells) and incubated overnight. To collect the samples, the media was aspirated from the cells and they were washed once gently with PBS. Following the wash, 1 mL of room temperature 4% paraformaldehyde (PFA, Electron Microscopy Sciences, #15710) in PBS was added to each well and incubated for 15 minutes at room temperature on the shaker to fix the cells to the coverslips. The PFA was aspirated and 0.5 mL of –20°C Methanol (MeOH) was added to each well and incubated with shaking for 10 minutes for permeabilization. The coverslips were then washed 3 times for 5 minutes with PBS while shaking. Coverslips were then placed in 0.5 mL of blocking buffer (4% BSA in PBS) and incubated at room temperature with shaking for 1 hour. Primary antibody mix was prepared in blocking buffer (4% BSA in PBS) using the appropriate antibodies from Table 2.1. The coverslips were inverted onto 100 µL of primary antibody mix and incubated overnight at 4°C. The following day the coverslips were washed in PBS and a

secondary antibody mix was prepared in blocking buffer (4% BSA in PBS) with the fluorescently labelled antibodies in Table 2.1. The coverslips were inverted onto 100 µL of the secondary antibody mix and incubated at room temperature for 1 hour in the dark. To prepare for mounting, the coverslips were washed 3 times for 5 minutes with PBS in the dark and inverted onto a drop of Prolong Gold Anti-fade Mountant (Thermo) on a microscope slide. The samples were left to set in the dark overnight at room temperature and imaged at the Dalhousie University CORES facility on the Zeiss Axio Imager Z2.

smFISH was completed in A549-WT and A549-MAVSKO cells. The probes used were sourced from Stellaris, Biosearch Technologies. The following protocol is adapted from the Stellaris smFISH protocol for adherent cells. The cells were seeded onto No. 1, 18mm round coverslips in a 12-well (20 mm) dish and incubated overnight at 37°C and 5% CO2. To collect the samples, the media was aspirated, the coverslips were washed with PBS, and 1 mL of fixation buffer (4% PFA in PBS) was added to each well. The samples were incubated at room temperature for 10 minutes with shaking and then washed with shaking twice for 5 minutes with PBS. To permeabilize the cells, 1 mL 70% ethanol was added to each well for at least 1 hour at 4°C. After permeabilization, the ethanol was aspirated and 1 mL Wash Buffer A (10% formamide in Wash Buffer A - Biosearch Technologies Cat# SMF-WA1-60) was added to each sample and incubated at room temperature for 5 minutes. A humidification chamber was assembled using a large tissue culture plate. The bottom was lined with a water-saturated paper towel and a piece of parafilm was placed on top of the paper towel. The samples were then inverted onto 100 µL of hybridization buffer (10% formamide in Hybridization Buffer - Biosearch Technologies Cat# SMF-HB1-10) and smFISH probe mix on the parafilm. Probes used were: human GAPDH with Quasar 670 Dye (# SMF-2019-1), human MALAT1 with Quasar 570 Dye (SMF-2035-1), IAV – M vRNA with FAM Fluorescein Dye (Custom made probe, sequence: tcagcatagagctggagtaa gatgctgacgatggtcattt gaaaggaacagcagagtgct ggagtgccaaagtctatgag gaaaggagggccttctacgg accgtcgctttaaatacgga cttgcacttgatattgtgga ttgccgcaaatatcattggg gaaacgaatgggggtgcaga tcttgaaaatttgcaggcct tccagtgctggtctgaaaaa aaccattgggactcatccta aggcaaatggtgcaagcgat catggaggttgctagtcagg cgagtgagcaagcagcagag gctatggagcaaatggctgg tttagccagcactacagcta caaccaacccactaatcaga ggtctcataggcaaatggtg gtatgtgcaacctgtgaaca tgaccactgaagtggcattt atatacaacaggatgggggc gtgcacttgccagttgtatg

atctcactcagttattctgc ttaggatttgtgttcacgct gtcacctctgactaagggga ggctaaagacaagaccaatc gatcttgaggttctcatgga tgaagatgtctttgcaggga acgtacgttctctctatcat). The humidification chamber was sealed with parafilm and then incubated overnight in the dark at 37°C. The samples were kept in the dark as much as possible after the hybridization step was complete. The coverslips were placed cell side up into 1 mL of Wash Buffer A in a new 12-well dish. The samples were incubated in the dark for 30 minutes at 37°C. Wash Buffer A was aspirated and replaced with 1 mL of nuclear stain (Wash Buffer A and 5 ng/mL Hoechst). The samples were incubated again for 30 minutes at 37°C, and then the nuclear staining buffer was removed and replaced with 1 mL of Wash Buffer B (Biosearch Technologies Cat# SMF-WB1-20) and incubated for 5 minutes with shaking at room temperature. The samples were inverted onto a small drop of Prolong Gold Anti-fade Moutant and left to solidify for at least 1 hour. The samples were imaged at the Dalhousie University CORES facility on either the Zeiss Axio Imager Z2 or the Leica TCS SP8 Confocal.

2.4 ImmunoFISH

This procedure was used to combine IF and FISH and was adapted from Kumar & Glaunsinger (2010). Cells were seeded onto No. 1, 18 mm round coverslips in a 12-well dish (20 mm wells). For collection, the samples were washed in PBS and fixed in 4% PFA in PBS for 15 minutes at room temperature with shaking. The samples were washed twice in PBS and permeabilized with 70% ethanol for at least 2 hours at room temperature. The samples were then rehydrated in wash buffer (10% formamide and 2X SCC) for 5 minutes. A hybridization buffer was prepared with 10% dextran sulfate, 0.02% RNAse free BSA, 20 µg yeast tRNA, 2X SCC, 10% formamide, and 35 ng of Alexa-Fluor-555-labeled oligo-dT RNA probe (to detect p(A) RNAs). The coverslips were inverted on 50 µL of the hybridization buffer and incubated overnight at 37°C. To complete the normal FISH protocol, the following day the samples were washed twice for 30 minutes with wash buffer (10% formamide and 2X SCC). Hoechst was added to the wash buffer for the second wash to stain the nuclei, and this was followed by mounting the coverslips on a droplet of Prolong Gold Anti-fade mountant and imaging. To adapt this protocol for ImmunoFISH instead, the following day the samples were washed with wash buffer (10% formamide and 2X SCC) for 15 minutes at 37°C and then with PBS for

5 minutes at room temperature. After the wash, blocking buffer (4% BSA in PBS) was added to each sample and incubated at room temperature for 30 minutes with shaking. The primary antibody mix was prepared using the appropriate antibodies (Table 2.1) in blocking buffer (4% BSA in PBS). Each sample was inverted onto 100 µL droplet of primary antibody mix and incubated overnight at 4°C in the dark. The following day, the samples were washed 3 times with PBS and placed onto a 100 µL droplet of secondary antibody mix containing the appropriate fluorescently tagged antibodies (Table 2.1) and Hoechst in blocking buffer (4% BSA in PBS). The samples were incubated for 1 hour at room temperature in the dark and then washed again with PBS. The coverslips were mounted onto microscope slides using Prolong Gold Anti-fade Mountant and left to set for at least 1 hour. Imaging was done at the Dalhousie University CORES facility on the Zeiss Axio Imager Z2.

2.5 Western Blotting

Samples were collected in 1X Laemelli buffer with DTT and homogenized with a 21-guage needle. The samples were spun down and boiled for 4 minutes at 95°C. The 1-mm SDS PAGE gels were prepared at 10% or 12% for the Bio-Rad Protean system (Bio-Rad, CA, USA). Samples were loaded into the gels, along with a protein standard ladder (New England Biolabs, #P7719S). The gels were run following the Bio-Rad Protean system protocol at 140V until the bromophenol blue reached the bottom of the gel. The PVDF membrane was placed into methanol for 5 minutes and then into 1X Transfer Buffer (BioRad). Two stacks of transfer pads were also placed into 1X Transfer Buffer to saturate. Once the gel finished running, the transfer stack was prepared in the BioRad transfer cassette and the transfer was completed using the TransBlot Turbo Transfer system (BioRad) for 7 minutes with the mixed weight turbo program. Following the transfer, the membrane was washed twice in 1X TBS-T and then placed in 6 mL of blocking buffer (4% BSA in 1X TBS-T). This was incubated for 1 hour on the rocker at room temperature and then washed twice with 1X TBS-T for 5 minutes on the rocker. Following the last wash, primary antibody (Table 2.1) prepared in 4% BSA in TBS-T was added to the membrane and then the membrane was incubated overnight at 4°C on the rocker. The next day the membrane was washed three times with 1X TBS-T and then placed in secondary antibody (the appropriate HRP-linked antibody (Table 2.1) diluted in

4% BSA in TBS-T). The membrane was incubated for 1 hour at room temperature with rocking and then washed three more times in 1X TBS-T. All TBS-T was then removed from the membrane and the dish, and the membrane was incubated in Clarity Max ECL (BioRad) substrate for 2 minutes on each side. Membranes were then imaged on a ChemiDoc (BioRad) and analyzed via ImageLab.

2.6 RNA Analysis

RNA extraction was completed using the Qiagen RNeasy Mini Kit. Cells were washed with PBS briefly and then 350 µL of RLT+ buffer with 2M DTT was added to each well and incubated at room temperature with shaking for 5 minutes. Following lysis, the samples were collected into microcentrifuge tubes, kept on ice, and homogenized using 21-guage needles. The homogenized lysates were transferred to the gDNA Eliminator column in a 2 mL collection tube. They were centrifuged for 30 seconds at >10,000 rpm and the flow-through was saved. One volume of 70% ethanol was added to the flowthrough and then mixed well. The 700 µL sample was then transferred to the RNeasy spin column in a 2 mL collection tube and centrifuged at >10,000 rpm for 30 seconds. The flowthrough was discarded, 700 µL of Buffer RW1 was added, and the samples were centrifuged at >10,000 rpm for 30 seconds. The flowthrough was discarded and 500 µL of Buffer RPE was added to the column and the samples were spun at 10,000 rpm for 30 seconds. The flowthrough was discarded, 500 µL of Buffer RPE was added to the column, and the samples were spun at >10,000 rpm for 2 minutes. The flowthrough was discarded, and the samples were centrifuged at max speed for 1 minute to eliminate any potential buffer carry-over. The RNeasy columns were placed into 1.5 mL collection tubes and 50 µL of RNase free water was added. The samples were centrifuged at >10,000 rpm for 1 minute and the column was discarded. The concentrations of the RNA samples were determined using a NanoDrop and the samples were stored at –20°C for short term storage and –80°C for long term storage.

RNA analysis was predominantly done through RT-qPCR. A 400 ng concentration of RNA was used to prepare the cDNA using qSCRIPT cDNA Supermix (QuantaBio) for first-strand synthesis following the manufacturers protocol. RT-qPCR master mixes were prepared using the appropriate forward and reverse primers in Table 2.2 and Sybr Green (QuantaBio). The RT-qPCR data was normalized to 18S.

2.7 ePAT

To analyze the lengths of the p(A) RNA tails on RNA transcripts during infection, I attempted to adapt the protocol from Jänicke et al. (2012) to carry out an extension p(A) test (ePAT). RNA was extracted and isolated as described in section 2.6. The concentration of RNA used for the ePAT was 750 ng. An 8 µL reaction was prepared with the 750 ng RNA sample and 1 µl of the ePAT-anchor primer (Table 2.2, ePAT-RT). This reaction was incubated at 80°C for 5 minutes and then cooled to room temperature. Next, the Klenow reaction was prepared by adding the Klenow polymerase at 1U/µg of RNA, 1mM DTT, 1mM dNTP, 1X reaction buffer (tested both Maxima H Minus Buffer (Thermo) and NEB Reaction Buffer (New England BioLabs)), and RNase/DNase Free H2O to a total reaction volume of 20 µL. The Klenow reaction was incubated at 20°C for either 1 hour or 15 minutes, the reaction was stopped by incubating it at 70°C for 20 minutes, and then the temperature was placed at 55°C. Maxima H Minus Reverse Transcriptase (Thermo) was added to each reaction at a concentration of 200U and the reaction was incubated at 55°C for 1 hour (Figure 2.1). The mixes were heated to 85°C for 5 minutes to stop the reaction and the samples were stored at 4°C. The samples were diluted 1:6 and then PCR was done using either Phusion High-Fidelity DNA Polymerase (New England BioLabs) or repliQa HiFi ToughMix (QuantaBio). The forward primers used were either β-actin or NEP, and the reverse primers were either the corresponding reverse primer or the ePAT PCR primer (Table 2.2). The PCR was run in a thermocycler: 1 cycle at 98°C for 30 seconds, 30 cycles of 98°C for 10 seconds, 63°C for 30 seconds, and 72°C for 3 minutes, followed by 1 cycle of 72°C for 10 minutes and then finally the reactions were held at 4°C. The samples were then run on 2% agarose gels with 100V for approximately 30 minutes and imaged on a ChemiDoc.

Figure 2.1

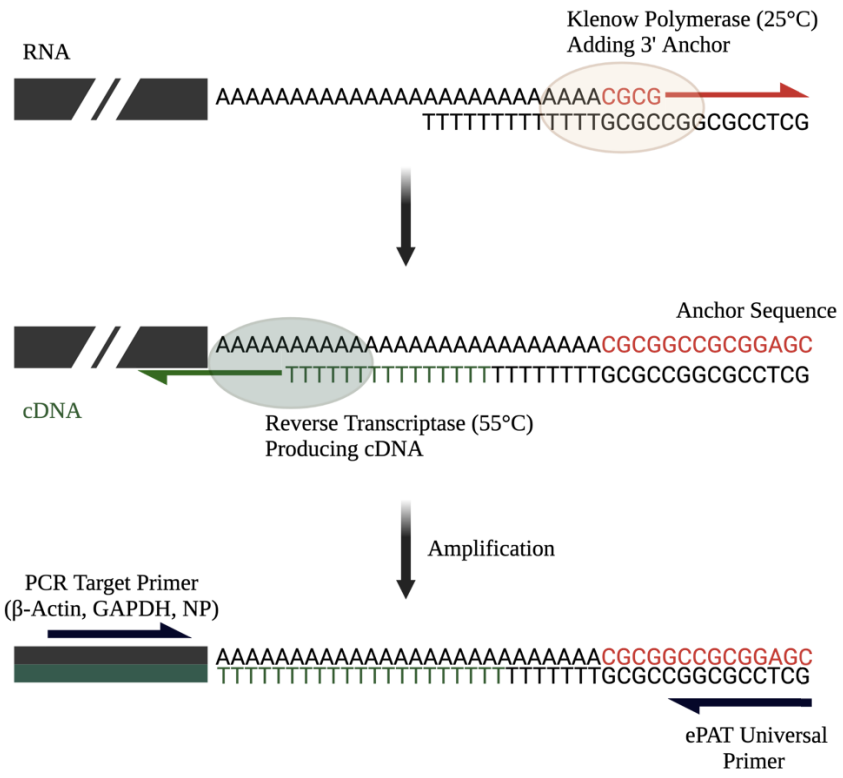

Figure 2.1 ePAT Methodology.

Figure adapted from Jänicke et al., 2012. RNA samples are incubated with a Klenow Polymerase and the ePAT anchor primer. The oligo(T) sequence of the ePAT anchor primer anneals to the end of the 3' p(A) tail of the RNA, and the polymerase adds a specific anchor to the most 3' end of the RNAs. Reverse transcription allows for extension in the 5' direction off the oligo(T) to produce the cDNA transcript with the ePAT anchor on the 3' end of the p(A) tail. Finally, PCR amplification using the ePAT universal primer, which anneals to the anchor and amplifies the p(A) tail, and a PCR primer specific for the target transcript. This allows for the analysis of each target transcripts p(A) tail length.

2.8 Immunoprecipitation

An immunoprecipitation (IP) assay was completed to attempt to pull down HA-tagged PA-X from transfected 293A cells. First 10 cm dishes of 293A cells were reverse transfected (as described in 2.10) with 6 ug DNA per dish. The positive control for this experiment was a SARS-CoV-2 NSP1 construct with an HA tag, and the negative control was empty vector (PUC-19) transfected cells. First, the media was aspirated from the plates and the dishes were placed on ice and washed twice with pre-chilled, ice-cold PBS. Then the samples were lysed in ice-cold RIPA lysis buffer supplemented with 0.5% Igepal and 1X protease inhibitor for 5 minutes and then scraped and transferred into a microcentrifuge tube. The samples were incubated at 4°C for 10 minutes with rotation and then the cell debris was separated out of the sample by centrifugation at 10,000 g for 5 minutes at 4°C. A 200 µL volume was removed and set aside as input control and the remaining clarified supernatant was transferred to a fresh microcentrifuge tube. Each sample had 1 µg of anti-HA antibody added to it and the samples were incubated overnight at 4 °C with rotation.

To prepare the Protein G magnetic beads for pull down they were resuspended in RIPA buffer. A 75 µL volume of the prepared beads was added to each sample and then gently vortexed. The samples were incubated with the beads at 4°C for 1 hour with rotation. The samples were briefly centrifuged, and magnets were applied to the samples with a magnetic rack for 1 minute. A 200 µL volume was removed from the supernatant as a flow through control and the remaining volume was discarded. The beads were then washed with ice cold RIPA buffer and the magnets were applied again for 1 minute. A 200 µL volume was removed as a wash control and the remaining volume was discarded. This wash procedure was repeated twice more. Finally, 150 µL of Laemelli lysis buffer was used to resuspend the beads and the samples were incubated at 75°C for 5 minutes to elute the bound proteins and antibodies. The magnetic beads were removed from the sample and all samples were stored at –20°C before running the western blots as previously described using the appropriate secondary HRP-linked antibody and visualized on the ChemiDoc.

2.9 LC-MS/MS

To determine if PA-X can be detected by LC-MS/MS I prepared a preliminary trial run for investigation. 293A cells were grown in 10 cm dishes and transfected (as described in 2.10) with 6 µg DNA of either empty vector (PUC_19), PA, or PA-X. The samples were lysed at 24 hours post transfection in ice-cold RIPA buffer with 0.5% Igepal and 1X protease inhibitor. The samples were incubated for 1 hour at 4°C with rotation. They were then clarified by centrifugation for 20 minutes at 4°C at a speed of 20,000 g. The samples were stored at –80°C until further processing. The samples were precipitated with chloroform and methanol. A 400 µL volume of methanol was added to 100 µg of each sample. This was vortexed immediately followed by the addition of 100 µL of chloroform and 300 µL of H2O. After vortexing, the samples were centrifuged for 1 minute at 14,000 g. The top (aqueous) layer was removed carefully as to not disrupt the protein layer. A 400 µL volume of methanol was added and the samples were vortexed and then centrifuged for 2 minutes at 14,000 g. The methanol was removed from the sample without disturbing the pellet and the pellet was dried using a SpeedVac. Once the sample was dry, they were stored at –80°C. Protein levels following drying were checked using a stain free gel to continue with the procedure.

The samples were then digested with an In-Solution Trypsin Digestion protocol provided by the Dalhousie Proteomics and Mass Spectrometry Core Facility. The protein samples were resuspended in 200 µL of denature buffer (8M Urea, 0.4M NH4HCO3) and sonicated for 15 minutes. A 10 µL volume of 0.5M DTT was added followed by an incubation at 60°C for 30 minutes and then the samples cooled for 5 minutes at room temperature. A 20 µL volume of 0.7M IAcNH2 was added to each sample, which were then incubated for 30 minutes at room temperature. Next, 1200 µL of H2O was added, followed by 10 µL of 0.1M CaCl2 and 100 µL of 0.02 µg/µL trypsin in 50mM NH4HCO3. The samples were then incubated overnight at 37°C with shaking. The samples had 1 µL of TFA added and were then acidified to a pH <3 using formic acid.

Finally, the samples were de-salted and prepared with Oasis Columns following a protocol provided by the Dalhousie Proteomics and Mass Spectrometry Facility. The columns were conditioned with methanol, followed by a wash with elution buffer 1 (50% ACN-0.1%TFA), and two washes with wash buffer (0.1% TFA). The samples were

loaded onto the columns and then the columns were washed three times with wash buffer. The samples were then eluted with two washes of elution buffer 1 and one wash with elusion buffer II (70% ACN-0.1%TFA). The samples were then dried using the SpeedVac and then stored at –80°C. The LC-MS/MS was run by Dr. Patrick Murphy at University of Prince Edward Island.

2.10 Mutagenesis, Transformations, and Transfections

Site directed mutagenesis was done to produce a PA-myc tagged construct that produced a 2X-HA-tagged PA-X. Forward and reverse primers were designed using BLAST (Table 2.2). The DNA backbone was a PA-myc construct. A standard 20 µL reaction for Phusion PCR was prepared (1X Reaction Buffer, 200 µM dNTPs, 0.5 µM forward and reverse primers, 35 ng backbone, 0.5U of polymerase). This PCR reaction was run in a thermocycler for: 1 cycle, 98°C, 30 seconds; 30 cycles, 98°C for 10 seconds, 62°C for 20 seconds, 72°C for 4 minutes; 1 cycle, 72°C for 7 minutes. Then, 1 µL of Dpn1 was added to each reaction and held at 37°C for 30 minutes. The reactions were then run on a 1% agarose gel and the appropriate bands were cut out and gel extracted. Next, a PNK-T4 Ligase reaction was set up with 5. µL of the PCR reaction, 2.5 µL 10X T4 ligase buffer, nuclease free water to fill to 24 µL. Then 1 µL of PNK was added to each reaction and mixed well by pipetting. The reactions were then incubated at 37°C for 30 minutes. After incubation, T4 ligase was added to the reaction and the reaction was left overnight at 16°C. The next day, the DNA was transformed into E. coli.

To transform DNA, E. coli competent cells were thawed on ice. A 5 ng concentration of DNA was placed in a sterile microcentrifuge tube and 50 µL of competent E. coli cells were added to each prep, which was then incubated on ice for 30 minutes. The DNA/cell suspensions were then heat shocked for 30 seconds at 42°C and promptly placed back on ice for 2 minutes to cool down. A 450 µL volume of LB media with no antibiotics was added to the heat shocked DNA and this was left to incubate at 37°C for 30 minutes to 1 hour. After the incubation, 100 µL was plated onto an LB + carbenicillin plate using sterile glass beads. This was then incubated overnight at 37°C. The next day the plate was checked for colonies and two colonies of each DNA prep were isolated and each placed into 5 mL of LB broth with carbenicillin. This was incubated overnight at 37°C with shaking. The following day the liquid cultures were

prepared using a QIA Spin MiniPrep kit (Qiagen). Samples were sent for confirmation of sequencing to GeneWiz.

Reverse Transfections were done in either 293A or 293T cells. Transfection mixes for transfection of a 12-well plate (20 mm wells) were prepared at 500 ng DNA/well and each mix was prepared in duplicate (a total of 1000 ng DNA/mix). Each construct in the mix was diluted to the appropriate working concentration, and each transfection experiment always had a GFP-transfection control to ensure transfection was successful and to quantify the transfection efficiency. A 100 µL volume of Opti-MEM-I was added to each DNA transfection mix and left to incubate at room temperature for 5 minutes. Next, 1.5 µL/reaction of PEI was added to 50 µL/reaction of Opti-MEM-I and this was also left to incubate at room temperature for 5 minutes. An 100 µL volume of PEI/Opti-MEM-I mixture was added to each 100 µL DNA/Opti-MEM-I mix. This was mixed gently and left to incubate at room temperature for 15 minutes. During this incubation the 293 cells were split and counted to prepare for seeding on top of the DNA mixtures. After the 15-minute incubation, 100 µL of the DNA reaction was added to the well and the 1mL of cell suspension in regular growth media were seeded on top of the transfection mix. The cells were mixed gently side to side and then placed at 37°C with 5% CO2 for 24 hours.

2.11 Dual Luciferase Assay

Cells were transfected as described in 2.10. Each transfection mix also had a CMV promoted firefly luciferase reporter that had an intronic sequence added to the luciferase gene (as described in Gaucherand et al., 2019) and a Renilla luciferase reporter. After 24 hours, the transfections were washed with PBS and lysed using passive lysis buffer (PLB, Promega, Dual-Luciferase Reporter Assay) for 15 minutes with shaking. The lysate was transferred to a microcentrifuge tube. Luciferase Assay Reagent II (LARII, Promega), Stop and Glow Buffer and Stop and Glow Substrate (Promega) were thawed. Stop and Glow substrate was added to the Stop and Glow buffer for a final concentration of 1X. The reactions were read on a luminometer following the manufacturers protocol.

2.12 Statistics and Programs

All statistical analysis were completed using PRISM GraphPad software. Figure production was completed in Affinity Designer, ImageJ, BioRender and ImageLab.

Table 2.1 - Table of Antibodies

Antibody	Species	kDa	WB	IF	Source	ID #
PABP	Rabbit	73	N/A	1:1000	Abcam	ab21060
IBV – NP	Mouse	64	1:1000	1:200	Santa Cruz	sc-57885
IAV	Goat	58, 29	1:2000	1:400	Abcam	Ab20841
IAV – NP	Mouse	56	1:2000	1:1000	Santa Cruz	sc-101352
MAVS	Rabbit	52, 75	1:1000	N/A	Cell Signaling	24930
Phospho-eIF2a	Rabbit	38	1:1000	N/A	Cell Signaling	9721s
Total eIF2a	Rabbit	38	1:1000	N/A	Cell Signaling	5324
NS1	Mouse	26 kDa	1:1000		**	
HRP β-Actin	Mouse	45	1:2000	N/A	Santa Cruz	sc-47778
IAV – M1	Mouse	28	1:1000	N/A	Serotech/Biorad	MCA401
IAV – PA	Rabbit	83	1:1000	N/A	GeneTex	GTX125932
Myc	Rabbit	N/A	1:1000	1:200	Cell Signaling	2278
ISG15	Mouse	15	1:1000	N/A	Santa Cruz	sc-166755
IFIT1	Rabbit	56	1:1000	N/A	Cell Signaling	14769
GFP	Rabbit	27	1:1000	N/A	Cell Signaling	2555
HA-tag	Mouse	N/A	1:1000	N/A	Cell Signaling	2367
Alexa Fluor 488	Mouse	N/A	N/A	1:1000	Invitrogen	A21202
Alexa Fluor 488	Rabbit	N/A	N/A	1:1000	Invitrogen	A21206
Alexa Fluor 555	Rabbit	N/A	N/A	1:1000	Invitrogen	A31572

Table 2.1 - Table of Antibodies Cont.

Antibody	Species	kDa	WB	IF	Source	ID #
Alexa Fluor 555	Mouse	N/A	N/A	1:1000	Invitrogen	A31570
Alexa Fluor 647	Goat	N/A	N/A	1:1000	Invitrogen	A21244
Alexa Fluor 647	Mouse	N/A	N/A	1:1000	Invitrogen	A21463
HRP	Rabbit	N/A	1:4000	N/A	Cell Signaling	7074
HRP	Mouse	N/A	1:4000	N/A	Cell Signaling	7076
HRP	β-Actin	N/A	1:2000	N/A	Santa Cruz	sc-47778
HRP	Rabbit – Native IgG only	N/A	1:2000	N/A	Cell Signaling	#5127

**The mouse anti-NS1 antibody was a kind gift from Dr. Kevin Coombs from the University of Manitoba (Rahim et al., 2013).

Table 2.2 - Table of Primers

Name	Forward Sequence	Reverse Sequence
β-Actin	CATCCGCAAAGACCTGTACG	CCTGCTTGCTGATCCACATC
ePAT – RT	GCGAGCTCCGCGGCCGCGTTTTTTTTTTTT	N/A
ePAT – PCR	GCGAGCTCCGCGGCCGCG	N/A
ePAT - GAPDH	GGCCTCCAAGGAGTAAGACC	TGGTACATGACAAGGTGCGG
ePAT - β-Actin	CACACAGGGGAGGTGATAGC	CAGTGTACAGGTAAGCCCTGG
ePAT – IAV NP	TGCAGCGGAATCTCCCTTTT	GGGTTCGTTGCCTTTTCGTC
ePAT – IBV NP	GCTAAGAAAACCAGTGGAAATGCT	GCTGTGTCCCTCCCAAAGAAG
IAV – NP	CCCAGGATGTGCTCTCTGAT	TTCGTCCATTCTCACCCCTC
IAV – NEP	CTGTGTCAAGCTTTCAGGACA	TTGTTCCCGCCATTTCTC
GAPDH	GAGTCAACGGATTTGGTCGT	TTGATTTTGGAGGGATCTCG
18S	CGTTCTTAGTTGGTGGAGCG	CCGGACATCTAAGGGCATCA
ISG15	TGTCGGTGTCAGAGCTGAAG	GCCCTTGTTATTCCTCACCA
IFIT1	AGCCTCCTTGGGTTCGTCTA	TGGCTGATATCTGGGTGCCT
IFN-β	GCCTCAAGGACAGGATGAAC	AGCCAGGAGGTTCTCAACAA
IFN-λ1	AAAAAGGAGTCCGCTGGCTG	CTCAGGGTGGGTTGACGTTC
POLR2A	GAAACGGTGGACGTGCTTAT	TGCTGAACCAAAGAACATGC
G6PD	TGAGGACCAGATCTACCGCA	AAGGTGAGGATAACGCAGGC
IBV- NP	GCAATTCTGCTGCATTTGAAGAT	GCCCAGTATCTGCTTCTCAGTTC

CHAPTER 3: RESULTS

3.1 Methods Development and Optimization: Imagining Techniques

3.1.1 ImmunoFISH: p(A) RNA and Protein

The relationship between localization of p(A) RNA molecules during infection and that of various cellular and viral proteins was a key interest to further investigate the impact and mechanism of IAV host shutoff. IF was the most optimized method in the laboratory to visualize the subcellular distribution of viral and host proteins during infection. Additionally, I had access to an optimized protocol for FISH and previously published probes for p(A) RNAs (Khaperskyy et al., 2014). It became key for my research that I needed to identify cells that had been infected with IAV, how their PABP protein was distributed subcellularly, and the levels of p(A) RNA within the nucleus. The COVID-19 pandemic had caused severe delays on the IAV FISH probes we had designed, which prevented us from utilizing the FISH technique alone. Furthermore, attempts to make custom probes using the ULYSIS Nucleic Acid Labeling Kits (Life Technologies) were unsuccessful. Due to the availability of the appropriate IF antibodies and the necessary p(A) RNA probe, I investigated the literature for other techniques that could utilize the resources we had. Kumar & Glaunsinger (2010) report using an experimental procedure where they processed their samples for FISH and then immediately processed the same samples for IF. To adapt their protocol, I utilized a similar method (as described in 2.4) where I collected samples and completed the optimized FISH protocol, but before adding the nuclear staining and mounting, I instead started the IF procedure at the blocking phase. These methods produced the results needed to confirm viral infection, PABP localization, and p(A) RNA concentrations, but the incubation times and the specifics of the protocol still needed to be optimized (Optimized protocol described in 2.4). In addition to protocol optimization, the optimization of the microscopy imaging also needed to be completed, and imaging was the highest quality when done within one- or two-days following sample mounting.

3.1.2 smFISH: Stellaris Cellular and Viral Probes

PA-X targets transcripts at the RNA level to inhibit protein expression as a mechanism to create a pro-viral environment in the host cell. To investigate the impact of PA-X and NS1 on host RNAs, I chose two host transcripts that are known to be targeted

during IAV infection for investigation via smFISH. Metastasis-associated lung adenocarcinoma transcript 1 (MALAT1) is a long non-coding RNA (lncRNA) that is located exclusively in the nucleus (reviewed in Zhang et al., 2017) and lacks a 3' poly(A) tail (Wilusz et al., 2008**)**. By choosing a transcript like MALAT1, that lacks a conventional p(A) tail, I could observe the potential that increasing levels of p(A) RNA in the nucleus during infection are due to increasing levels of conventionally polyadenylated RNAs, or if the increase is due to a retention of transcripts which normally don't have 3' p(A) tails, and their potential hyperadenylation. Additionally, MALAT1 has been previously shown to be targeted through a PA-X independent mechanism (Khaperskyy et al., 2016) - during infection with PR8-WT or PR8-PA(fs) there was no significant changes in the downregulation of MALAT1. The other host transcript I chose to investigate through smFISH was glyceraldehyde-3-phosphate dehydrogenase (GAPDH). While MALAT1 is exclusively nuclear and provides a way to determine if nuclear transcripts can be faithfully detected, GAPDH is predominantly and abundantly cytoplasmic (Tristan et al., 2011) and is a known target of PA-X mediated downregulation during IAV infection (Khaperskyy et al., 2016). I chose GAPDH because observing any changes in the subcellular distribution of this transcript could suggest that GAPDH may contribute to the observed accumulation of p(A) RNA in the nucleus during infection. Using GAPDH as a primary investigative probe could reveal potential impacts host shutoff has on the nuclear-cytoplasmic shuttling of RNAs.

Finally, we also designed a custom probe for IAV, created to hybridize to the viral M vRNA. It was imperative we had access to a viral probe to use for smFISH to allow us to identify the infected cells. Additionally, I chose to use the M segment of the viral genome because the M segment is highly conserved between IAV strains (Hom et al., 2019). The highly conserved nature of this segment allows us to use this probe not only for investigating PR8 through smFISH, but also for investigations of other IAV strains in the future.

The smFISH protocol for adherent cells was developed in the lab initially following the Stellaris protocol provided by the manufacturer. The protocol was then optimized further to enhance the captured microscopy images (as described in 2.3). The Leica TCS SP8 Confocal microscope was used to collect the highest quality images of

the probes, and due to the sensitivity of the GAPDH probe, imaging needed to be completed almost immediately after the mountant had solidified and during image collection the exposure time needed to be monitored and adjusted to maintain visualization of the probe.

3.1.3 ePAT

During my investigations into the PA-X and NS1 mediated host shutoff mechanism, I found that there was manipulation occurring to the amount and/or localization of p(A) RNAs during infection. The p(A) tail length has previously been demonstrated to impact the stability and fate of those RNAs. Shorter tail lengths can lead to rapid RNA decay via exosomal function (LaCava et al., 2005). Longer tail lengths and/or hyperadenylation has been suggested to cause a retention of the transcripts in the nucleus, but the exact cause of this is unknown (Kumar & Glaunsinger, 2010). To try to understand if there was a manipulation of the length of the p(A) tails on the RNAs being retained in the nucleus during IAV infection, I attempted to use a protocol published by Jänicke et al., (2012). ePAT utilizes an anchor primer, which binds to the p(A) tail of mRNAs and then uses an anchor sequence that is added to the RNA via Klenow polymerase activity. The Klenow polymerase is vital in this process as it extends the 3' end of the RNA transcript using dNTPs and the annealed anchor DNA template. Following extension using the Klenow polymerase, reverse transcription can occur to create cDNA from the RNA, which now has the anchor sequence at the end of the p(A) tail. Following reverse transcription, PCR amplification using a transcript specific primer and a universal ePAT primer (which binds to the anchor sequence) would allow for amplification of specific transcripts and subsequent analysis of their tail lengths via agarose gel. Special ePAT primers were designed to optimize the protocol; The forward primer for each transcript was designed to anneal approximately 200 nucleotides from the polyadenylation side and the control reverse primer was designed to anneal just upstream of the polyadenylation site. The transcripts I initially investigated were β-actin, GAPDH, and IAV NP. I began troubleshooting the protocol by replacing the ePAT PCR primer in the final step with the transcripts corresponding reverse primer.

The amplicon length for each transcript tested (β-actin, GAPDH, IAV NP) was approximately 50 nucleotides (Figure 3.1A). The expected control amplicon size for β-

actin was 253 nucleotides, the ePAT amplicon size was 300 nucleotides. Likewise, the control amplicon sizes for GAPDH and NP were 216 and 256, respectively, and their ePAT amplicon sizes were only different by 60 and 50 nucleotides, respectively. Typical p(A) tail lengths are between 250-300 nucleotides long, therefore these results suggested that the ePAT was not working properly, as the amplicon was too small to contain the entire p(A) tail. To further investigate which part of the protocol was not functioning properly, I carried out another control ePAT experiment, investigating only β-actin, where I removed the Klenow polymerase from the reactions, or I removed the reverse transcriptase from the reactions. As expected, when there was no reverse transcriptase, no product was formed (Figure 3.1B). Regardless of whether Klenow polymerase was added into the reaction or not, the ePAT reaction produced an amplicon size that varied approximately 50 base pairs from the control (Figure 3.1B). I examined two different buffers to determine if the buffer composition was important to reaction success, as a reaction buffer was not specified in Jänicke et al (2012). I used the NEB recommended Klenow reaction buffer in one set of ePAT reactions and in the other I used the Maxima H Minus RT Buffer. In the Maxima H Minus RT buffer there were larger additional non-specific bands in the lanes that contained the β-actin forward primer (either alone or with the ePAT universal primer) (Figure 3.1C). In both the buffers, the β-actin ePAT reaction produced two bands of larger, unexpected size (Figure 3.1C). The control β-actin reaction produced a replicon of the expected size (Figure 3.1C). After these trials and various other troubleshooting methods it was determined that this was not the most effective or reliable method to evaluate the p(A) tail lengths and their modifications.

Figure 3.1

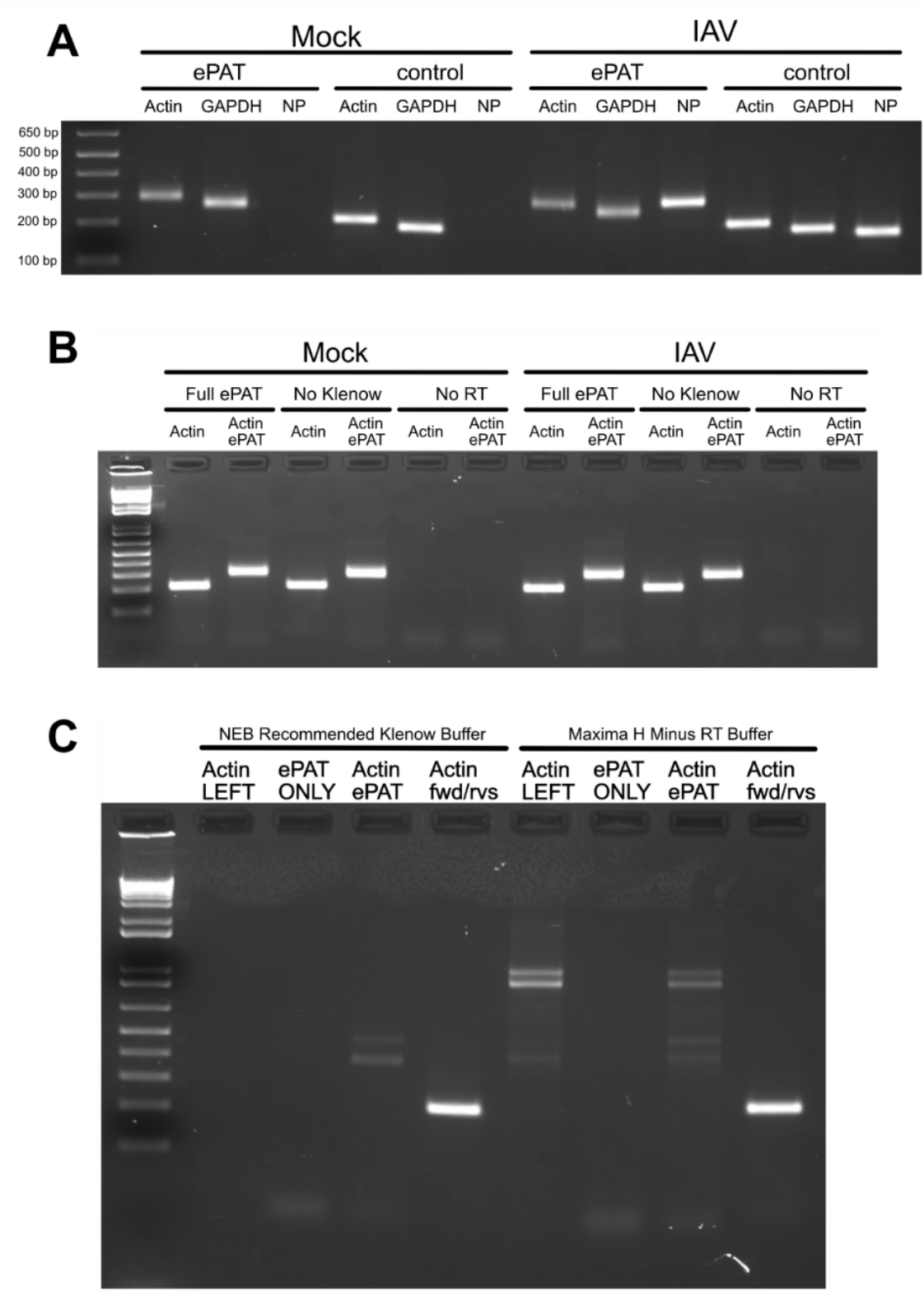
A
Mock
IAV
ePAT
control
ePAT
control
Actin GAPDH NP Actin GAPDH NP Actin GAPDH NP Actin GAPDH NP
650 bp
500 bp
400 bp
300 bp
200 bp
100 bp
B
Mock
IAV
Full ePAT
No Klenow
No RT
Full ePAT
No Klenow
No RT
Actin
Actin ePAT
C
NEB Recommended Klenow Buffer
Maxima H Minus RT Buffer
Actin LEFT
ePAT ONLY
Actin ePAT
Actin fwd/rvs

Figure 3.1 The Extension Polyadenylation Test was Unsuccessful in Determining p(A) Tail Length.

(**A**) Samples were either mock infected or infected with IAV WT at an MOI = 1 and were collected at 20 hpi. ePAT samples were run on 2% UPA agarose gel for 30 minutes at 100V. ePAT samples were created using the target forward primer and the ePAT universal reverse primer, control samples were made using the forward and reverse primers for each target. (**B**) The same infection samples from (A) were used to troubleshoot the ePAT protocol. Full ePAT samples were created using the normal ePAT protocol, No Klenow samples had no Klenow polymerase added, and No RT (reverse transcription) samples had no reverse transcriptase added. Each prep was made with either a β-actin control (using the forward and reverse primer) or an β-actin ePAT (using β-actin forward and ePAT reverse primers). (**C**) The mock infected samples from (A) were used for final trouble shooting of the ePAT procedure. β-actin LEFT lanes had samples that were prepared with only the forward primer for β-actin and no reverse primer. EPAT ONLY lanes were loaded with samples that were prepared with only the ePAT universal anchor primer. β-actin ePAT lanes were loaded with samples that had the β-actin forward primer and the ePAT universal anchor primer. β-actin fwd/rvs lanes were loaded with samples that had both the forward and reverse primer for β-actin.

3.2 Influenza B Virus

3.2.1 PA-X is not Required For p(A) RNA Accumulation During IBV Infection

The ability of IBV to cause host shutoff through RNA manipulation like IAV is unknown. Unlike IAV, IBV does not produce PA-X, and its NS1 is not involved in the same immune modulation functions. To understand if there is any RNA manipulation occurring during IBV infection, I sought to look at the distribution of PABP and subsequently the subcellular localization of p(A) RNAs. The current accepted model of IAV host shutoff suggests that during IAV infection the accumulation of PABP in the nucleus is a result of the depletion of host transcripts in the cytoplasm due to PA-X activity, subsequently causing an increase in unbound cytoplasmic PABP, which is then imported into the nucleus. This is also suggested to be linked directly to a notable increase of nuclear p(A) RNAs and a decrease of those RNAs from the cytoplasm. It has been previously shown that overexpression of PA-X in cells will cause an increase of nuclear p(A) RNAs, as well as a similar increase in the accumulation of PABP (Khaperskyy et al., 2014). Because of these previous findings we expected to see no nuclear accumulation of PABP or p(A) RNA during infection of A549s with IBV. I infected A549 MAVS-KO cells with IBV for 20 hours and processed the samples through ImmunoFISH to look at viral infection, p(A) RNA localization, and PABP subcellular distribution. As expected, there was no nuclear accumulation of PABP in infected cells (Figure 3.2A). Contrary to what I expected, while there was no nuclear accumulation of PABP, there was a change in the distribution of p(A) RNAs during infection (Figure 3.2A). The IBV infected cells showed evidence of increased levels of nuclear p(A) RNAs in the absence of nuclear PABP at 20 hours post infection. This was the first indication that the accumulation of p(A) RNAs may be occurring in a PA-X independent manner, unlike what was previously understood about IAV infection and PA-X activity.

Figure 3.2

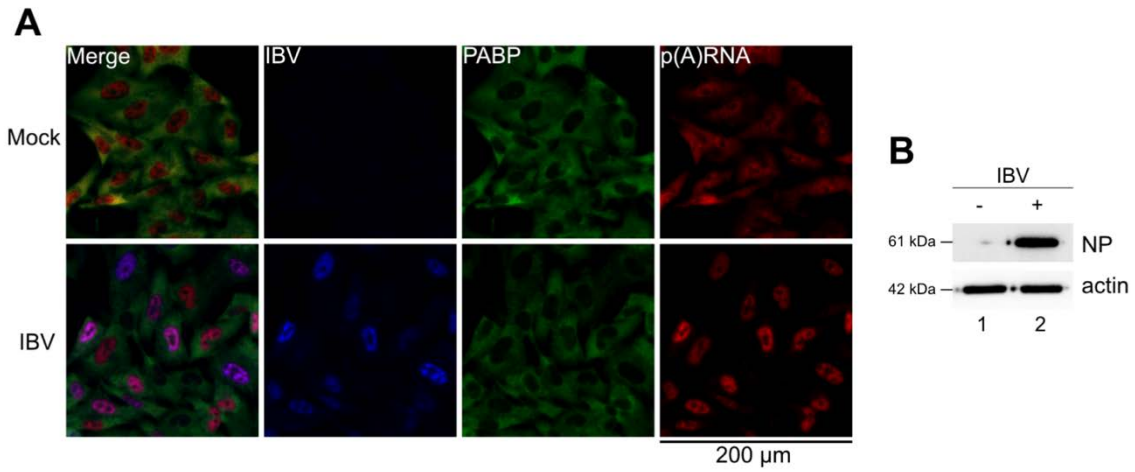

Figure 3.2. Nuclear Accumulation of p(A) RNAs in IBV Infected Cells Independent from Nuclear PABP Accumulation.

(**A**) A540-MAVSKO cells were either mock infected or infected with IBV at an MOI = 1 and collected at 20 hpi. The samples were processed through ImmunoFISH – using anti-IBV NP (blue), and anti-PABP (green) antibodies, and Alexa-Fluor-555-labeled oligo-dT probe to detect p(A) RNA (red). Images were collected on the Zeiss Axio Imager Z2. Images are 200 µm X 200 µm. (**B**) Corresponding samples from (A) were lysed and run on a western blot. Membranes were probed for IBV NP (61 kDa) and the loading control β-actin (42 kDa).

3.2.2 BEAS-2B Cells do not Serve as a Good Secondary Cell Line for IAV or IBV Infection Models

My model cell line for researching IAV and IBV infections was A549s. A549s are lung adenocarcinoma cells, meaning they are a useful starting model for early molecular investigations into host shutoff functions, but it would be beneficial to corroborate the findings into a more relevant cell line. To do this, I chose BEAS-2B cells. I tested if these cells could be successfully infected with both IAV and IBV, and thus be used for a secondary, permissive cell model for our studies. I infected BEAS-2B cells with either IAV or IBV at an MOI = 1 for 20 hours and processed the samples through IF to visualize infected cells and the distribution of PABP during infection (Figure 3.3A). Only about 10% of the BEAS-2B cells were stained positive for either IAV or IBV (Figure 3.3B) indicating that these cells are not as permissible as A549s for influenza infection. This is supported by published literature indicating that while BEAS-2B cells are commonly used for respiratory epithelial cell lines, these cells produce high basal levels of ISG's which can restrict influenza virus infection (Seng et al., 2014). Although there were very low infection rates, and BEAS-2B cells may not be the best infection model for our studies, there was symmetry in the nuclear localization of PABP between A549 and BEAS-2B cells. While both IAV and IBV infected BEAS-2B to the same low levels, approximately 60% of IAV infected cells had nuclear PABP, whereas 0% of the IBV infected cells showed an accumulation of nuclear PABP (Figure 3.3A,B).

Figure 3.3

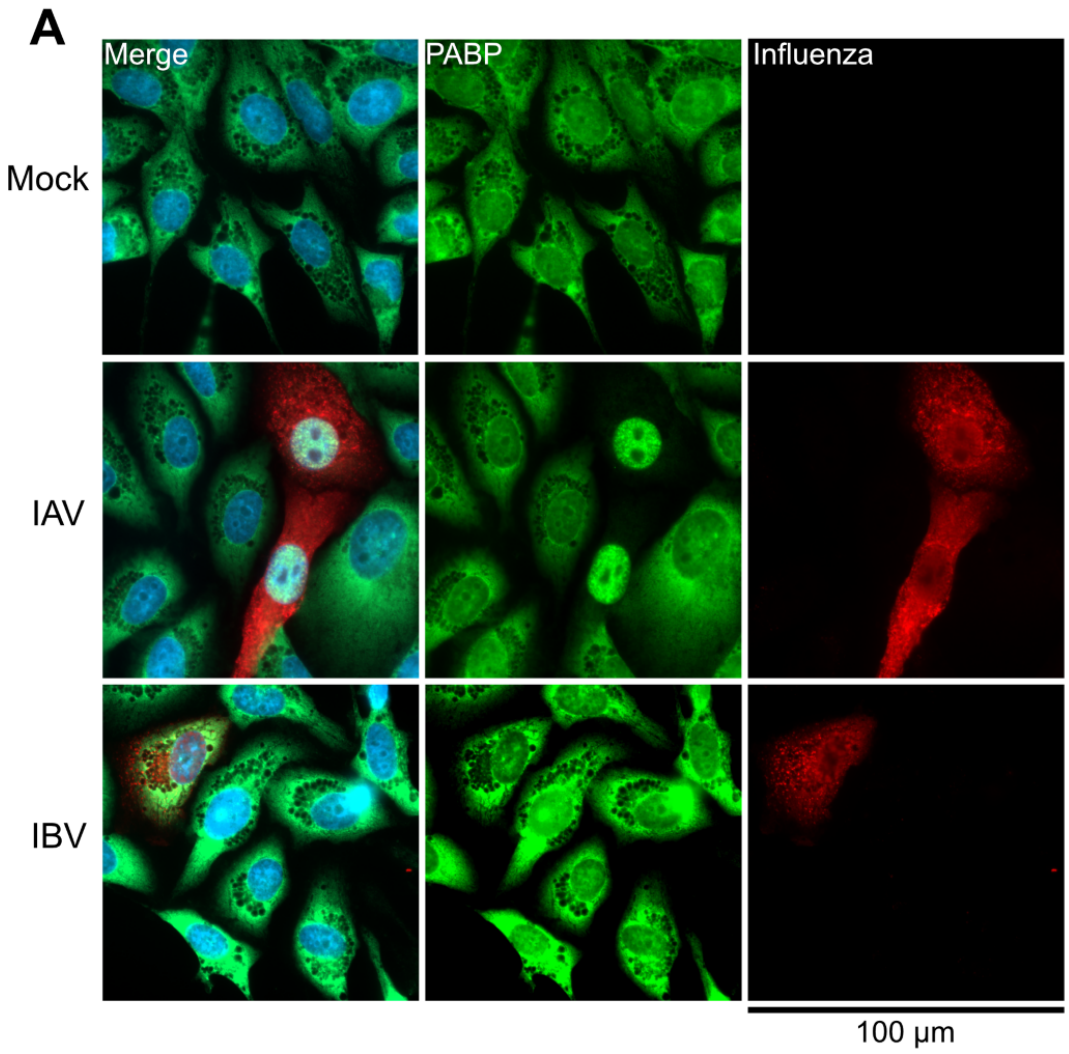
A
Merge
PABP
Influenza
Mock
IAV
IBV
100 µm

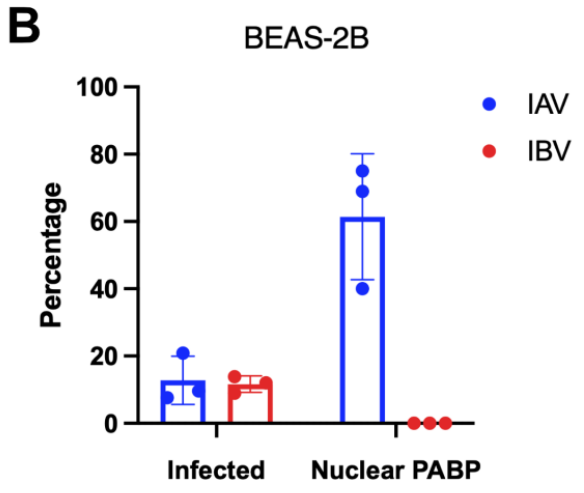
B
BEAS-2B
IAV
IBV
Percentage
100
80
60
40
20
0
Infected
Nuclear PABP

Figure 3.3 BEAS-2B Cells are Non-Permissive to IAV and IBV

(**A**) BEAS-2B cells were mock infected or infected with either IAV or IBV at an MOI = 1. Samples were collected at 20hpi and processed through IF for PABP (green) and either IAV HA, NA, M1 (red) or IBV NP (red). Images were collected on the Zeiss Axio Imager Z2 and are 100 µm X 100 µm. (**B**) Quantification of (A) where percentage of infected cells was approximately 10% and the percentage of those infected cells with nuclear PABP varied between IAV and IBV. Quantifications were done with ImageJ.

3.3 NS1 C-Terminus Influences PABP Subcellular Distribution but not p(A) RNA Accumulation

3.3.1 Nuclear PABP Accumulation Requires NS1 C-Terminus and Nuclear p(A) RNA Accumulation Occurs in the Absence of Nuclear PABP During IAV Infection

Cytoplasmic PABP, under normal cellular conditions, often is associated with actively translating mRNAs on polysomes, and is therefore unavailable to move freely from the cytoplasm to the nucleus (Burgess & Gray, 2012). When PABP is not bound to translating mRNAs it is free to interact with α-importins and can be shuttled into the nucleus. Once in the nucleus, these endogenously cytoplasmic PABP molecules are thought to engage with pre-mRNAs that have a p(A) tail alongside endogenous nuclear PABP (Hosoda et al., 2006). During infection with IAV, the host shutoff protein PA-X targets host transcripts in the cytoplasm for cleavage and degradation. As cytoplasmic RNAs are cleaved and degraded, this causes a depletion of cytoplasmic p(A) mRNAs available for PABP to associate with. The current host shutoff model suggests that this causes an influx of cytoplasmic PABP into the nucleus. Additionally, in cells where PA-X is active, it has been proposed that the influx of PABP into the nucleus causes the accumulation of p(A) RNAs in the nucleus as well. Kumar & Glaunsinger (2010) proposed that this accumulation of the p(A) RNAs was due to the aberrant RNAs hyperadenylation and inefficient export. Additionally, it has been previously published that overexpressing PA-X alone in cells causes an increase of PABP and p(A) RNAs in the nucleus (Khaperskyy et al., 2014). With the new understanding that p(A) RNAs can accumulate in a PABP independent and PA-X independent manner – as during IBV infection – I sought to investigate if in IAV-infected cells nuclear p(A) RNA accumulation required PA-X and/or NS1.

To answer this question, I used the process of ImmunoFISH to allow the visualization of the p(A) RNA, viral infection, and the localization of PABP. I infected A549-WT cells for 20 hours with either the PR8-WT or PR8-N80 mutant virus. As previously observed and expected, PR8-WT infected cells had an increase in nuclear PABP, as well as a significant increase in p(A) RNAs (Figure 3.4 A, C, E). Surprisingly, A549-WT cells that were infected with PR8-N80 mutant virus did not have any nuclear PABP accumulation (Figure 3.4A, E). Although this mutant virus was lacking the

effector domain of NS1, there was no mutation in PA-X or the sequence that produces PA-X which may have limited the ability of PA-X to target and cleave host transcripts. Additionally, while there was no increase in the nuclear accumulation of PABP during infection, there was evidence of significant increases in the amount of p(A) RNAs present in the nucleus (Figure 3.4D). These data suggest that nuclear re-localization of PABP during infection is dependent, not solely on PA-X activity, but also on the C-terminus of NS1. Additionally, the data suggests that p(A) RNA accumulation in the nucleus is not directly linked to the nuclear accumulation of PABP and can occur independently of these phenotypes.

These results were reflected in PR8-WT and PR8-N80 mutant infections in A549-MAVSKO cells as well (Figure 3.4B), indicating that nuclear p(A) RNA accumulation and/or PABP redistribution in infected cells are not resulting from MAVS-mediated antiviral response by the cell (discussed further in 3.3.2).

Figure 3.4

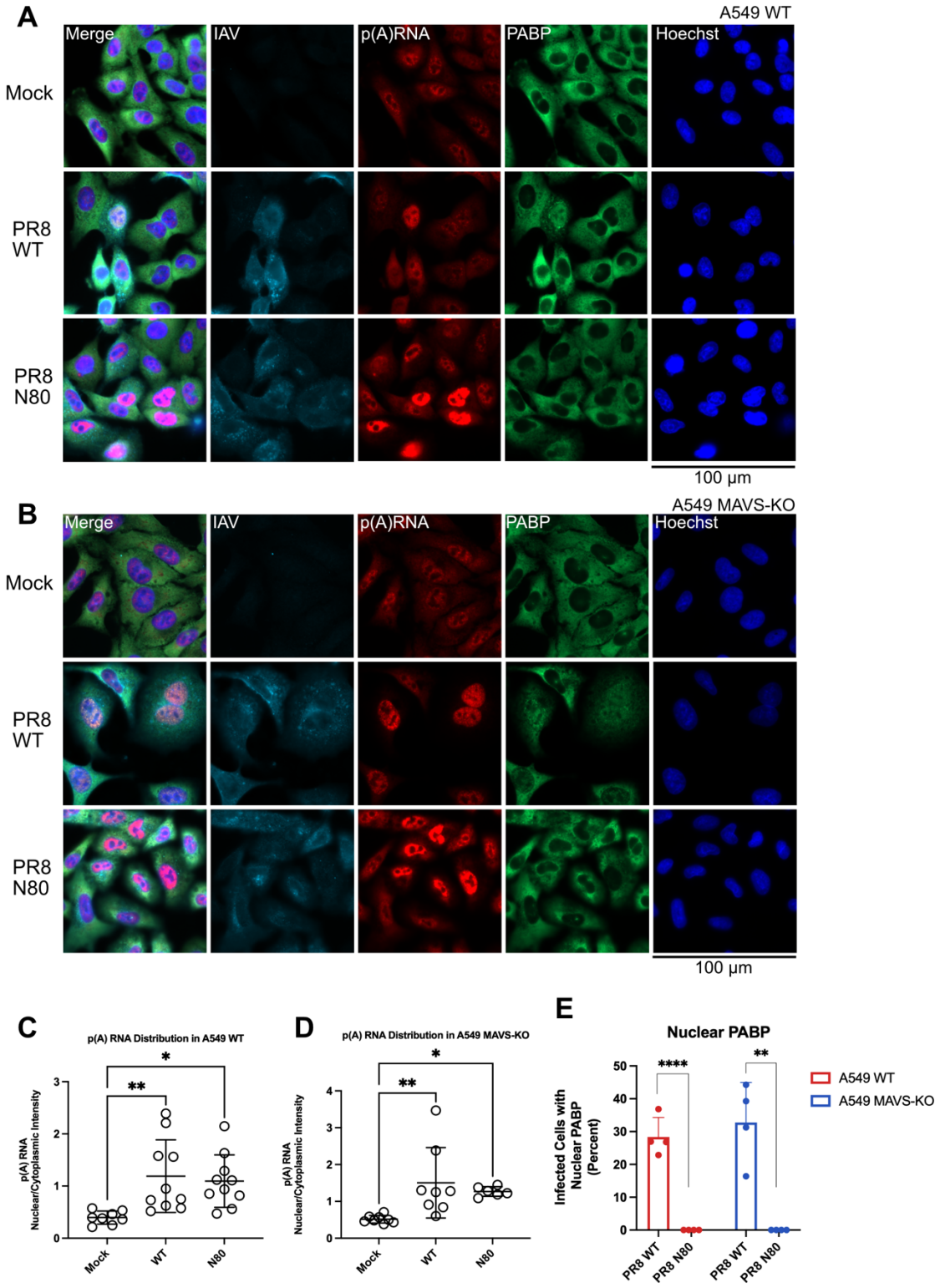
A
A549 WT
Merge
IAV
p(A)RNA
PABP
Hoechst
Mock
PR8 WT
PR8 N80
100 µm
B
A549 MAVS-KO
Merge
IAV
p(A)RNA
PABP
Hoechst
Mock
PR8 WT
PR8 N80
100 µm
C
p(A) RNA Distribution in A549 WT
p(A) RNA Nuclear/Cytoplasmic Intensity
Mock
WT
N80
D
p(A) RNA Distribution in A549 MAVS-KO
p(A) RNA Nuclear/Cytoplasmic Intensity
Mock
WT
N80
E
Nuclear PABP
Infected Cells with Nuclear PABP (Percent)
PR8 WT
PR8 N80
PR8 WT
PR8 N80
A549 WT
A549 MAVS-KO

Figure 3.4 Nuclear Accumulation of PABP Requires C-terminus of NS1 and is not Required for p(A) RNA Nuclear Accumulation.

(**A**) A549-WT cells were mock infected or infected with either PR8-WT or PR8-N80 mutant virus at an MOI = 1. Samples were collected at 20 hpi and processed through ImmunoFISH for IAV (cyan), PABP (green), p(A) RNA (red), and Hoechst (blue). Images were collected on the Zeiss Axio Imager Z2 and are 100 μm X 100 μm. (**B**) A549-MAVSKO cells were mock infected or infected with either PR8-WT or PR8-N80 mutant virus at an MOI = 1. Samples were collected and processed the same as in (A). (**C**) Nuclear to Cytoplasmic Intensity Ratio for p(A) RNA signal for samples in (A). Intensity ratio was calculated using ImageJ/Fiji with the extension "Intensity Ratio Nuclei Cytoplasm Tool, RRID:SCR_018573". N=3 and 2-4 fields of view were quantified per replicate. Significance was determined through a one-way ANOVA followed by a Holm-Sídák multiple comparisons test. *(0.05), **(0.01). (**D**) Nuclear to Cytoplasmic Intensity Ratio for p(A) RNA signal for samples in (B). Intensity ratio was following the sample procedure outlined in (C). Significance was determined through a one-way ANOVA followed by a Holm-Sídák multiple comparisons test. *(0.05), **(0.01). (**E**) Percent of infected cells with nuclear PABP, calculated from samples in (A) and (B). Quantified using ImageJ. Significance was determined with an unpaired T-test. **(0.01), ****(<0.0001).

3.3.2 MAVS-KO Cells are Optimal for IAV NS1 Mutant Virus Infection Due to the Elimination of the MAVS-Mediated Antiviral Immune Response

IAV NS1 activity is imperative for the virus to limit the antiviral immune response. NS1 plays a role in the host shutoff of IAV through inhibiting the mRNA maturation, polyadenylation, and export from the nucleus, in addition to its role in limiting the antiviral immune response during infection (Nacken et al., 2021; Krug, 2015; Gack et al., 2009; Meyerson et al., 2017; Nemeroff et al., 1998). One specific way NS1 works is to limit the RIG-I activated MAVS mediated antiviral response. Because of NS1's important role in preventing antiviral signaling from occurring, utilizing NS1 mutants that lack the ability to interact with immune molecules in A549-WT cells could lead to skewing results for immune function rather than virus induced host shutoff. I had also observed that during infection in A549 WT cells, N80 mutant viruses often replicated to slightly lower levels and there was higher immune signaling, as observed through interferon induced protein with tetratricopeptide repeats 1 (IFIT1) and ISG15, two immune markers that are involved in the MAVS-mediated antiviral immune response (Figure 3.5A). It's important to note that the lack of NS1 in the PR8-N80 lanes is due to the epitope of interaction between the primary antibody used for the western blot (Figure 3.5A, Table 2.2). The NS1 antibody available to use binds to an epitope in the C-terminus of the protein, which is not present in the PR8-N80 mutant virus. I observed high levels of IFN-L1 during infection with PR8-N80 in A549 WT cells, which was completely abolished when infecting A549-MAVSKO cells with the same mutant virus (Figure 3.5B, C *note the scale bar differences). This data suggests that using A549-MAVSKO cells allowed the NS1 mutant virus an optimal environment to replicate and provided us the opportunity to observe impacts on the host that were occurring due to the virus, not because of immune signaling. The phenotypes I had observed in the A549-WT cells infected with PR8-N80 virus was mirrored in the A549-MAVSKO cells, indicating that the p(A) RNA accumulation in the nucleus I observed was not due specifically to MAVS-mediated antiviral signaling (Figure 3.4B).

Figure 3.5

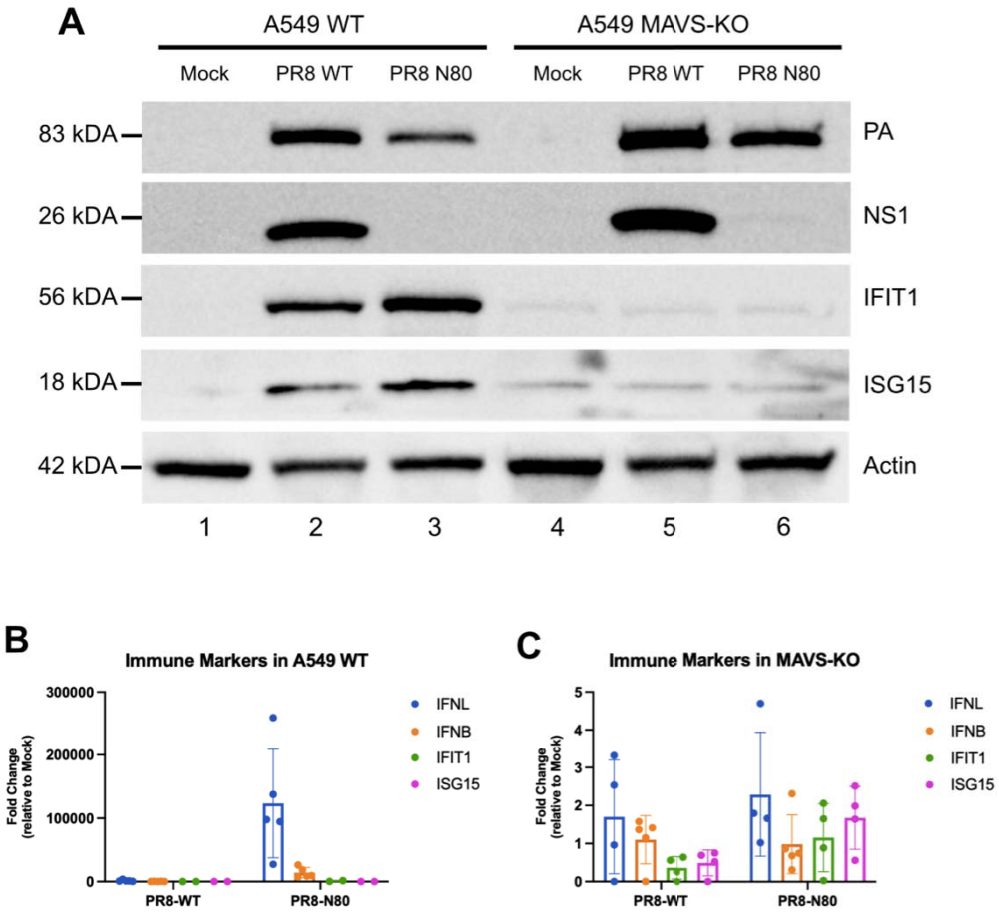

Figure 3.5 A549-MAVSKO Cells Have Limited MAVS-Mediated Antiviral Immune Response During PR8-N80 Infection.

(**A**) A549-WT and A549-MAVSKO cells were mock infected or infected with PR8-WT or PR8-N80. Cells were infected at an MOI = 1 and were collected at 20 hpi. Membranes were probed for IAV PA, NS1 (C-terminal epitope), IFIT1, ISG15, and a loading control β-actin. Membranes were exposed on a ChemiDoc and the images were processed through ImageLab. (**B**) Corresponding RNA samples from the A549-WT infections in (A) were collected and prepared for RT-qPCR looking at targets IFN-L(1), IFNβ, IFIT1, and ISG15. Data was normalized to 18S and is presented as fold change relative to mock infected cells. (**C**) As in (B) but with the A549-MAVSKO samples.

3.4 PA-X Mediated Host Shutoff may be Dependent on the Presence of Functional NS1 During IAV Infection

Both PA-X and NS1 are important host shutoff factors for IAV infection, and my data thus far suggests that NS1 may influence PA-X mediated host shutoff phenotypes. The production of PA-X requires a rare ribosomal frameshifting event to occur into the +1 frame of PA and only occurs about 1.3% of the time during translation (Jagger et al., 2012). The previous understanding of PA-X function suggested that PA-X alone can cause the host shutoff phenotypes of accumulated PABP in the nucleus and the nuclear accumulation of p(A) RNAs. This is evident during infection of PR8-WT virus and is also true in overexpression systems of PA-X (Khaperskyy et al., 2014). The analysis of PA-X in an overexpression system may influence certain host shutoff phenotypes due to the difference in the amount of PA-X in the system compared to a typical infection model. To determine if both PA-X and NS1 play roles in these host shutoff phenotypes, and if there was any impact from NS1 alone on the accumulation of PABP in the nucleus during transfection, I transfected 293A cells with a combination of WT or mutant NS1 and WT or mutant PA. The mutant PA I used was the PA(fs) mutant. This mutant has been previously published and has a codon optimization where the ribosomal frameshift occurs to produce PA-X (Khaperskyy et al., 2014; 2016). By optimizing those codons, the ribosome pausing on that sequence occurs less frequently and there is severely limited production of PA-X. I used the WT and mutant construct of PA instead of a PA-X construct to evaluate if there were any changes in the PABP phenotypes and potentially PA-X activity that could be due to a modulation of PA-X production from PA in the presence of NS1. IF analysis of the transfected cells showed that cells transfected with WT NS1 and PA had evidence of significant nuclear PABP accumulation, compared to cells transfected with N80 and PA, as well as cells transfection with mutant PA (Figure 3.6A). It is important to note that each of these constructs had a -myc tag, which was used for their labeling during IF. While utilizing the -myc tag was useful for protein identification on the western blots, IF analysis is limited because there is no differential staining between the NS1 and the PA construct. Quantification and statistical analysis of these data show that the only condition with a significant increase in PABP in the nucleus

was cells transfected with both NS1 and PA (Figure 3.6B). Additionally, there was a slight increase in the amount of PA protein (both WT and mutant) when it was transfected in combination with wild-type NS1 (Figure 3.6C). These data suggest that the presence of NS1 may enhance the production of PA, and therefore may also increase the amount of PA-X present during transfection. PA-X was not resolved on the western blot and therefore these conclusions would need to be further confirmed through quantifiable analysis of PA-X production levels and how they are impacted in the presence of NS1 WT and mutant constructs. Additionally, this data suggests that both NS1 and PA-X need to be present to create an environment where nuclear PABP accumulates or where PA-X is present at high enough concentrations, or active enough to cleave enough host transcripts in the cytoplasm and cause the subsequent redistribution of PABP into the nucleus.

Figure 3.6

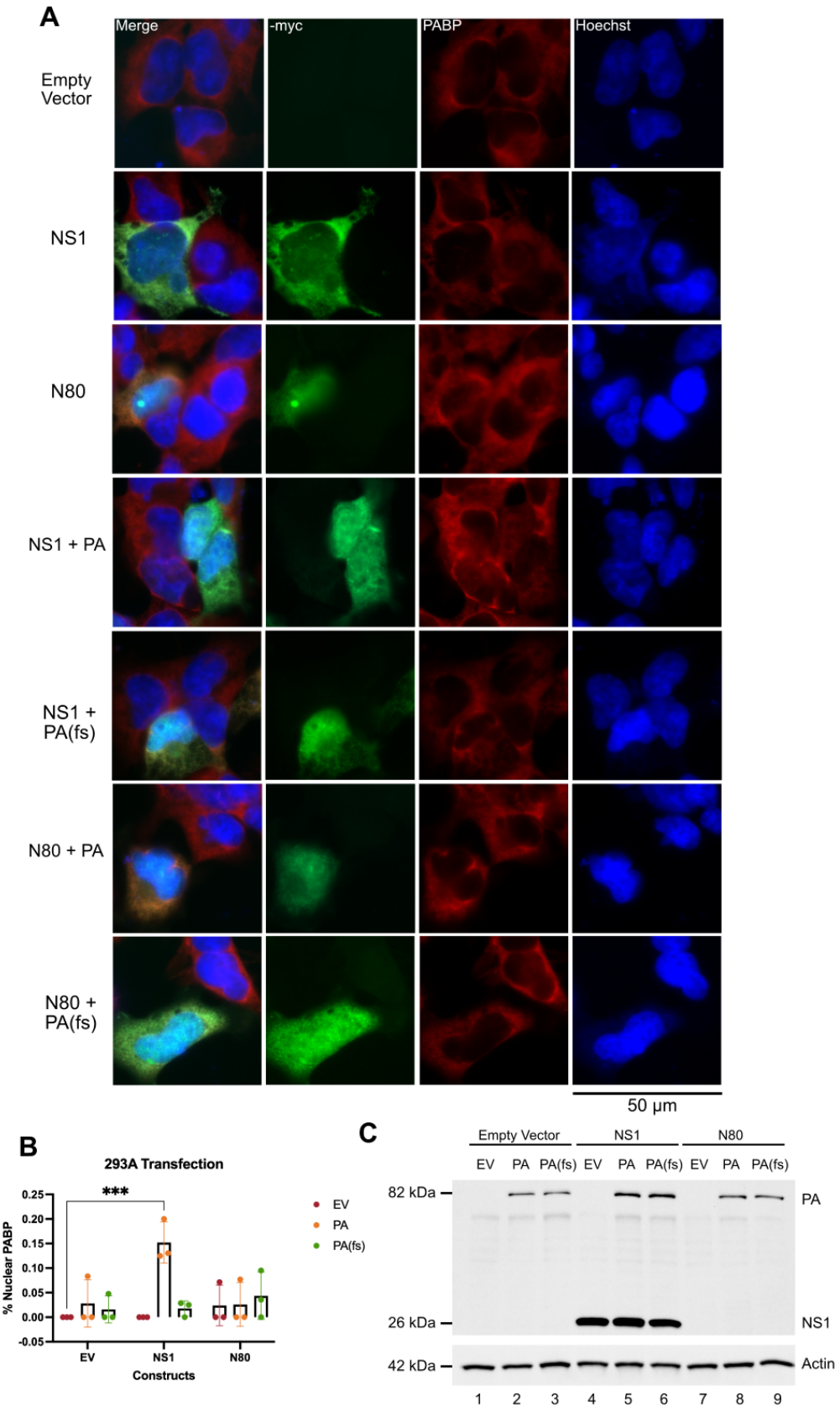
A
Merge
-myc
PABP
Hoechst
Empty Vector
NS1
N80
NS1 + PA
NS1 + PA(fs)
N80 + PA
N80 + PA(fs)
50 µm
B
293A Transfection
***
% Nuclear PABP
0.25
0.20
0.15
0.10
0.05
0.00
-0.05
EV
NS1
N80
Constructs
EV
PA
PA(fs)
C
Empty Vector
NS1
N80
EV PA PA(fs) EV PA PA(fs) EV PA PA(fs)
82 kDa
PA
26 kDa
NS1
42 kDa
Actin
1 2 3 4 5 6 7 8 9

Figure 3.6 NS1 and PA-X are Required for Nuclear PABP Accumulation.
(**A**) 293A cells were reverse transfected with a combination of -myc tagged NS1, N80, PA, and PA(fs) constructs. Samples were collected at 24 hours post transfection and processed for IF for anti-myc (green), PABP (red), and nuclei (blue). Images were taken on the Zeiss Axio Imager Z2 and are 50 μm X 50 μm. (**B**) Quantification of the percentage of transfected cells with nuclear PABP. Significance was determined with a two-way ANOVA followed by a Dunnett's multiple comparisons. ***(0.001). (**C**) Corresponding transfection samples were collected and analyzed via western blot. The membrane was blotted for anti-myc and loading control β-actin. EV = empty vector. The membrane was imaged with a ChemiDoc and the images were manipulated in ImageLab.

3.5 Nuclear p(A) RNA Accumulation was Confirmed to Occur Independently of Nuclear PABP Accumulation and Independently of PA-X and NS1 Activity.

The data thus far suggests that both PA-X and NS1 are needed to cause the nuclear accumulation of PABP and I hypothesized that this was due to NS1 influencing the production of PA-X. To further investigate the influence of PA-X and NS1 on the accumulation of p(A) RNAs in the nucleus during infection, I used two mutant viruses: PA(fs), and a double mutant N80(fs). PR8-N80(fs) has both the truncated N80 NS1 protein and the PA(fs) mutation. This virus is severely limited in its ability to carry out host shutoff, and I wanted to evaluate if there were any changes to the subcellular distribution of PABP, and if the p(A) RNA signal was influenced by the host shutoff factors presence. I infected A549-WT cells with PR8-WT and the panel of mutants (N80, PA(fs), N80(fs)), and collected the infections at 20 hpi. Compared to PR8-WT, each mutant virus had significant decreases in the percent of infected cells with nuclear PABP (Figure 3.7A, B). Remarkably, all the infections had significant increases in the nuclear to cytoplasmic ratio of p(A) RNA in infected cells compared to uninfected (Figure 3.7A, C). This data suggests that while both PA-X and NS1 are important for PABP nuclear accumulation, and therefore host shutoff function, neither are necessary for nuclear p(A) RNA accumulation during infection.

To confirm the phenotypes I was seeing in a cell line without MAVS-mediated antiviral signaling, and in order to evaluate the impact of antiviral signaling on these phenotypes, I investigated PABP nuclear localization and p(A) RNA nuclear intensity in A549-MAVSKO cells infected with the PA(fs) mutant virus. Similarly to the N80 mutant virus (Figure 3.4B) the PA(fs) mutant infection in A549-MAVSKO cells mirrored the phenotypes I was observing in the A549 WT cells (Figure 3.8A). Additionally, there was still a significant decrease in the percent of infected cells with nuclear PABP accumulation (Figure 3.8B), and a significant increase in the nuclear intensity of p(A) RNA's (Figure 3.8C). Together this data suggests that the phenotypes we are seeing in the A549-WT cells infected with mutant viruses are not due to MAVS-mediated antiviral immune signaling and are more likely caused by a viral mechanism during infection.

Figure 3.7

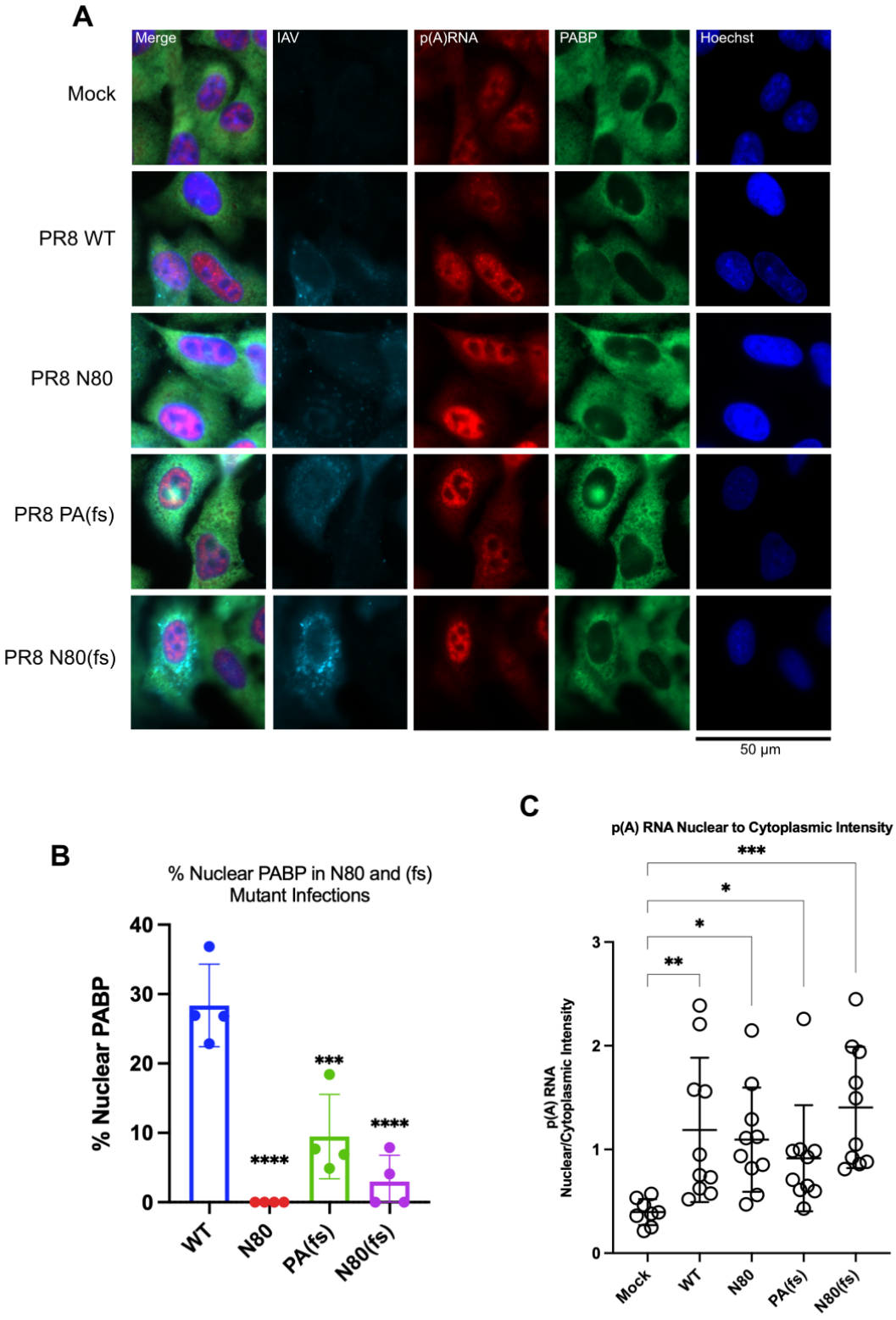
A
Merge
IAV
p(A)RNA
PABP
Hoechst
Mock
PR8 WT
PR8 N80
PR8 PA(fs)
PR8 N80(fs)
50 µm
B
% Nuclear PABP in N80 and (fs) Mutant Infections
% Nuclear PABP
40
30
20
10
0
****
***
****
WT
N80
PA(fs)
N80(fs)
C
p(A) RNA Nuclear to Cytoplasmic Intensity
p(A) RNA Nuclear/Cytoplasmic Intensity
***
*
*
**
3
2
1
0
Mock
WT
N80
PA(fs)
N80(fs)

Figure 3.7 p(A) RNA is Retained in the Nucleus of Mutant PA-X and NS1 Infected Cells.

(**A**) A549-WT cells were mock infected, infected with PR8-WT, or infected with a PR8 mutant virus. The mutant viruses used in this screen were PR8-N80, PR8-PA(fs), and PR8-N80(fs). Cells were infected with an MOI = 1 and collected at 20 hpi. The samples were process for ImF for IAV (cyan), PABP (green), p(A) RNA (red), and Hoechst (blue). Images were collected on the Zeiss Axio Imager Z2 and are 50 μm X 50 μm. (**B**) Quantification of the percentage of infected cells with nuclear PABP for the samples in (A). Statistical significance was determined though a one-way ANOVA followed by a Dunnett's multiple comparisons test. ***(0.001), ****(<0.0001). (**C**) nuclear to cytoplasmic intensity ratio for p(A) RNA signal for samples in (A). Intensity ratio was calculated using ImageJ/Fiji with the extension "Intensity Ratio Nuclei Cytoplasm Tool, RRID:SCR_018573". N=3 and 2-4 fields of view were quantified per replicate. Significance was determined using a one-way ANOVA followed by a Holm-Sídák multiple comparisons test. *(0.05), **(0.01), ***(0.001).

Figure 3.8

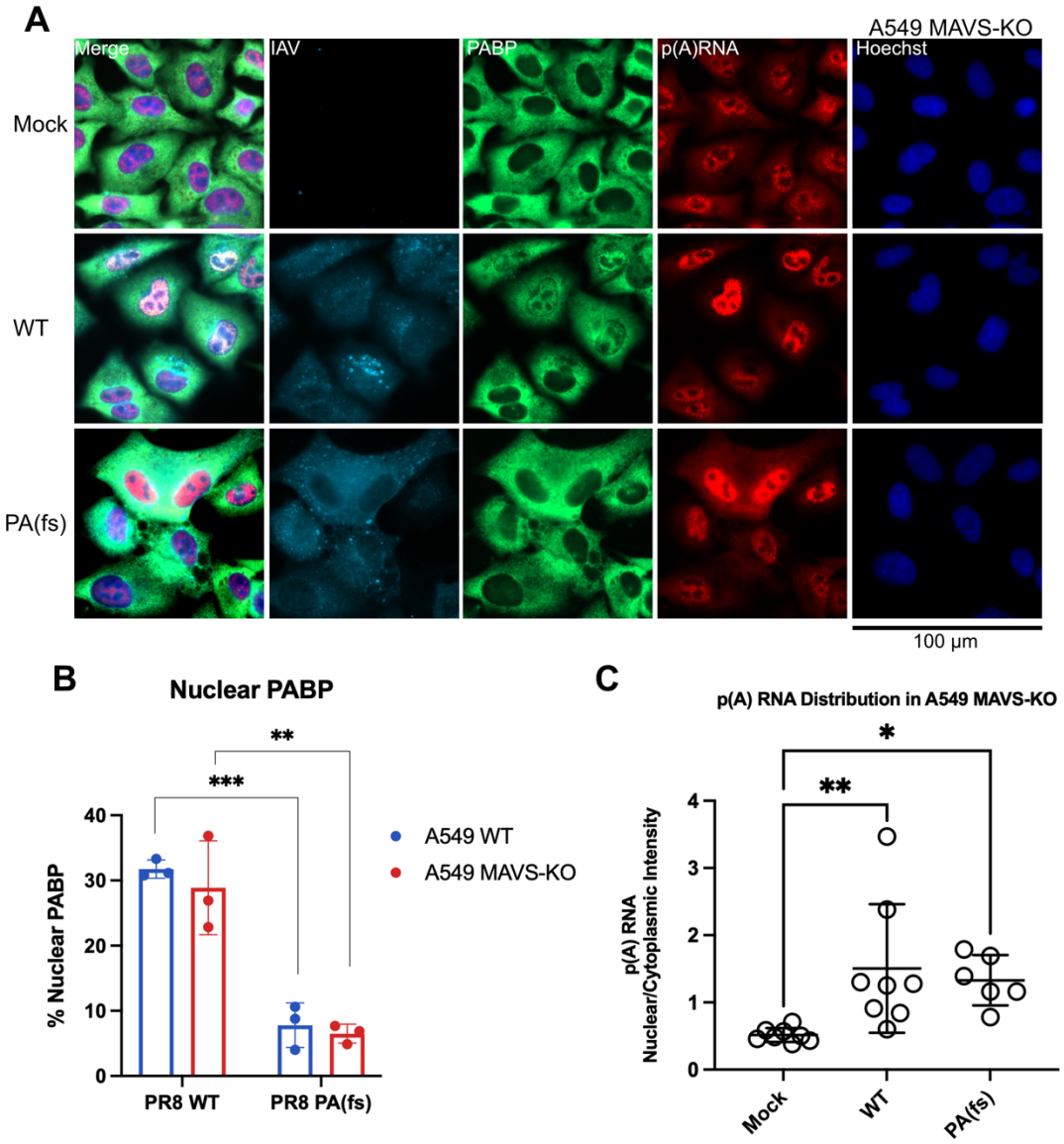
A
A549 MAVS-KO
Merge
IAV
PABP
p(A)RNA
Hoechst
Mock
WT
PA(fs)
100 μm
B
Nuclear PABP
**
***
% Nuclear PABP
40
30
20
10
0
PR8 WT
PR8 PA(fs)
A549 WT
A549 MAVS-KO
C
p(A) RNA Distribution in A549 MAVS-KO
*
**
p(A) RNA
Nuclear/Cytoplasmic Intensity
4
3
2
1
0
Mock
WT
PA(fs)

Figure 3.8 PA(fs) Mutant Virus Causes Increase in p(A) RNA in the Absence of Nuclear Accumulation of PABP in A549-MAVSKO Cells.

(A) A549-MAVSKO cells were mock infected, infected with PR8-WT, or infected with PR8-PA(fs). Cells were infected at an MOI = 1 and the samples were collected at 20 hpi. The infections were processed through ImmunoFISH for IAV (cyan), PABP (green), p(A) RNA (red), and Hoechst (blue). Images were taken on the Zeiss Axio Imager Z2 and are 50 μm X 50 μm. (**B**). Quantification of the percentage of infected cells in (A) with nuclear PABP. Quantifications were done with ImageJ. Significance was determined with an unpaired t test. **(0.01), ***(0.001). (**C**) Nuclear to cytoplasmic intensity ratio for p(A) RNA signal for samples in (A). Intensity ratio was calculated using ImageJ/Fiji with the extension "Intensity Ratio Nuclei Cytoplasm Tool, RRID:SCR_018573". N=3 and 2-4 fields of view were quantified per replicate. Significance was determined using a one-way ANOVA followed by a Holm-Sídák multiple comparisons test. *(0.05), **(0.01).

3.6 Host Shutoff is Reduced During Mutant NS1 IAV Infection

While viral targeting of host transcripts for degradation during infection is most often attributed to PA-X activity, my data suggests that NS1 plays an integral role in these host shutoff phenotypes. To further understand the impact of NS1, I investigated the expression levels of various host targets that are known to be downregulated during IAV infection using a small panel of NS1 mutant viruses. The N80 mutant virus, which does not have the NS1 effector domain, the N80(fs) mutant virus, which is missing the NS1 effector domain and does not produce PA-X, and finally an NS1 point mutant, 123,124A, which is defective in its ability to bind PKR (Min et al., 2007). I wanted to determine if there was any impact on PA-X mediated downregulation of targets based on NS1 mutations. The targets I used were β-actin, G6PD, GAPDH, MALAT1, and POLR2A. All these targets are known to be PA-X targeted transcripts, except for MALAT1 which has been previously shown to be targeted in a PA-X independent manner (Khaperskyy et al., 2016). In PR8-WT infected cells there was strong downregulation of each of the transcripts, and interestingly, there was a significant change in the amount targeted, or downregulation, of each of the targets for all the NS1 mutant viruses compared to WT (Figure 3.9A). This is true except for GAPDH in 123,124A mutant infection. These data only represent two distinct biological repeats and adding a third replicate would most likely add the statistical power to this target as well compared to WT infection. Overall, this suggests that there is a significant change in the ability of the virus to target these transcripts with PA-X when it does not have fully functional NS1 present. The relative levels of PA were also determined to have no significant differences between the different mutant infections, indicating the results I observed were not due to significant changes in MOI (Figure 3.9B).

Figure 3.9

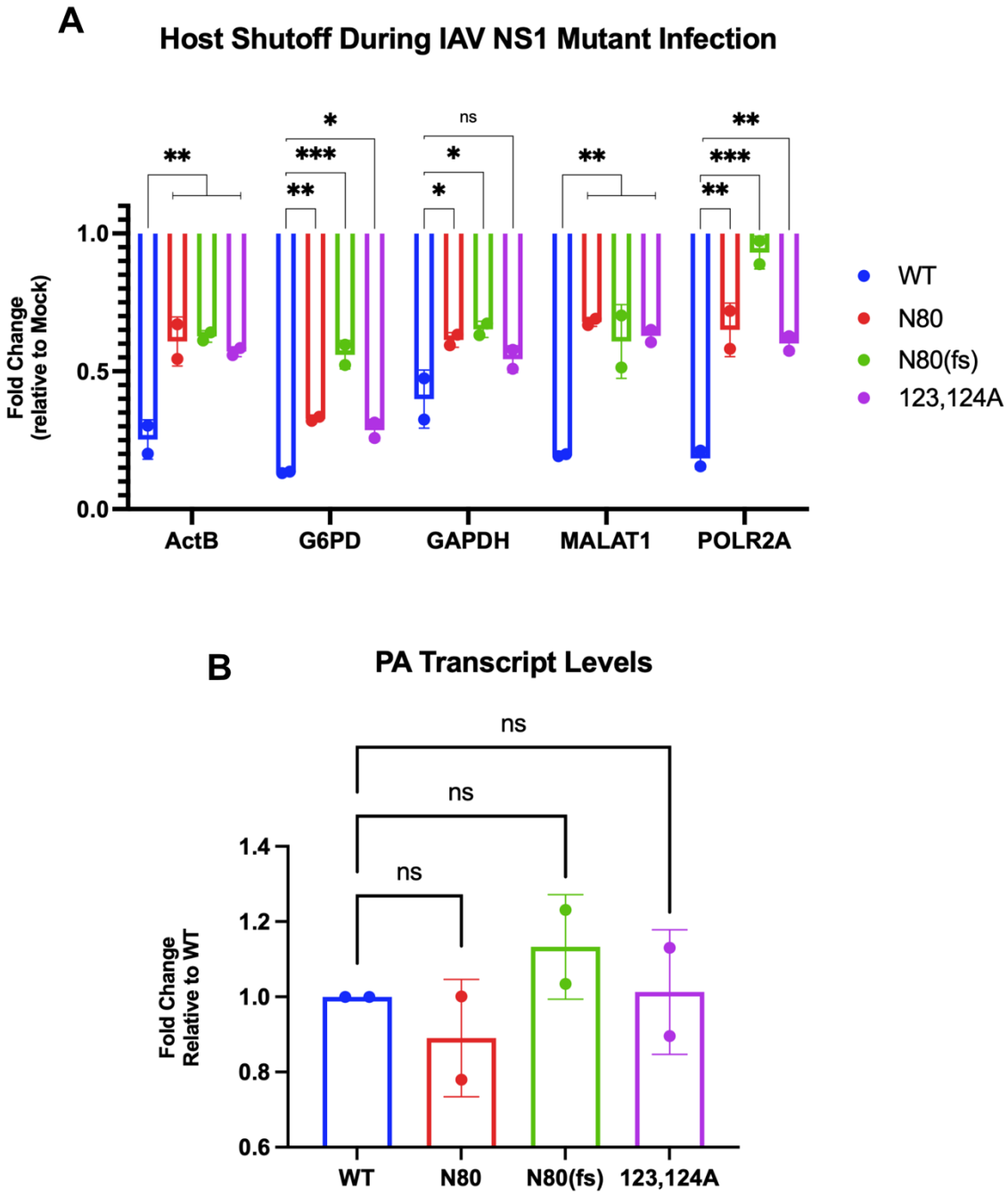
A
Host Shutoff During IAV NS1 Mutant Infection
Fold Change (relative to Mock)
1.0
0.5
0.0
**
*
***
**
ns
*
*
**
**
***
**
ActB
G6PD
GAPDH
MALAT1
POLR2A
WT
N80
N80(fs)
123,124A
B
PA Transcript Levels
Fold Change Relative to WT
1.4
1.2
1.0
0.8
0.6
ns
ns
ns
WT
N80
N80(fs)
123,124A

Figure 3.9 Mutant NS1 Infection Limits the Host Shutoff Function of IAV.
(**A**) A549-WT cells were mock infected, infected with PR8-WT, or infected with PR8 mutant viruses. The mutant viruses used were PR8-N80, PR8-N80(fs), and PR8-123,124A. Cells were infected at an MOI = 1 and RNA was collected at 20 hpi. RT-qPCR was done on the samples for host shutoff targets β-actin (ActB), G6PD, GAPDH, MALAT1, and POLR2A. Data was normalized to 18S and is presented as fold-change relative to mock infected cells. N=2. Significance was determined with a one-way ANOVA followed by a Dunnett's multiple comparisons test. *(0.05), **(0.01), ***(0.001), ns = not significant. (**B**) Samples were processed as in (A). RT-qPCR was done to target the PA mRNA transcript of IAV. Data was normalized to 18S and is shown as a function of Log10. N=2. Significance was determined with a one-way ANOVA followed by a Tukey's multiple comparisons test. ns = not significant (>0.05).

3.7 MALAT1 And GAPDH do not Contribute to Increased Nuclear p(A) RNA During Infection

3.7.1 Host lncRNA MALAT1 Downregulation may be NS1 Dependent.

In Figure 3.9A, the data suggests that PA-X targets and downregulates host transcripts, but the strength of the downregulation is significantly impacted by the presence of NS1. MALAT1 is a lncRNA that is transcribed by RNA polymerase II. As such, it is a potential target for PA-X cleavage and therefore downregulation during infection. In Khaperskyy et al. (2016), they showed that while it is downregulated during PR8-WT infection, it is not downregulated during PR8-PA(fs) infection, indicating that it is not targeted by PA-X, but rather by some other mechanism during infection. Moreover, I have shown that infection with an NS1 mutant virus reduces the magnitude of MALAT1 downregulation, suggesting that rather than being modulated by PA-X, its expression levels are being modulated by NS1. I infected A549 cells with the previously presented panel of mutant NS1 viruses, along with two new point mutants, R38A, K41A (38,41A), and E96A, E97A (96,97A). Mutant 38,41A has a mutation in its N-terminal RNA binding domain and 96,97A has two point mutations that limit its ability to bind to TRIM25. Each of these NS1 mutant viruses were used to infect A549 cells at an MOI of 1 and were collected at 20 hpi. The samples were processed for smFISH using Stellaris probes for hybridization to IAV-M, MALAT1, and GAPDH (justification for targets described in 3.1.2). There was evidence that NS1 was influencing the targeting of MALAT1, and visualization of MALAT1 through smFISH showed that compared to PR8-WT, N80 mutant infection did not have a decrease in the amount of MALAT1 in the nucleus (Figure 3.10). Each point mutant seemed to follow a similar pattern with very limited downregulation of MALAT1 occurring in the nucleus (Figure 3.10). This data suggests that NS1 is required for MALAT1 mediated downregulation during infection. The significance of the difference in the number of MALAT1 transcripts between the PR8-WT and mutant infections could not be determined. SmFISH was a protocol chosen because the number of particles can be quantified from microscopy images. Unfortunately, due to the volume of the particles in the nucleus, and the lack of appropriate programming, the exact quantifications of the particles could not be determined.

Figure 3.10

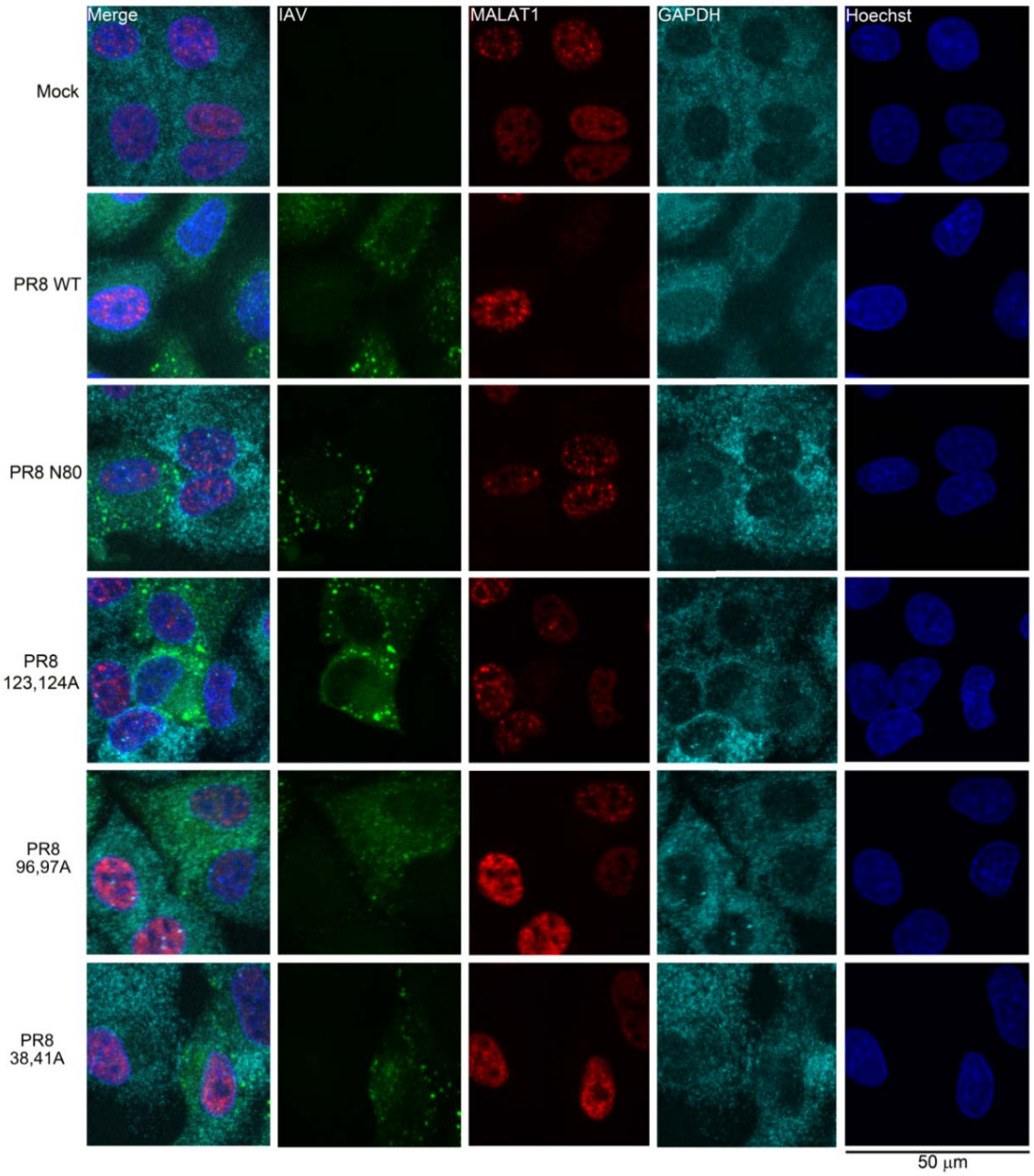
Merge
IAV
MALAT1
GAPDH
Hoechst
Mock
PR8 WT
PR8 N80
PR8 123,124A
PR8 96,97A
PR8 38,41A
50 µm

Figure 3.10 smFISH of NS1 Mutant Virus Infection Suggests MALAT1 Downregulation is NS1 Dependent and GAPDH is not Retained in the Nucleus. A549-WT cells were mock infected or infected with a panel of NS1 mutant viruses (PR8-N80, PR8-123,124A, PR8-96,97A, PR8-38,41A). Cells were infected at MOI = 1 and were collected at 20 hpi. The samples were then processed through smFISH for IAV-M (green), MALAT1 (red), and GAPDH (cyan). Images were collected on the Leica TCS SP8 Confocal and processed using the Imaris Imaging Processer. Representative images are 50 µm X 50 µm.

3.7.2 p(A) RNA Increase During Infection is not due to Retention of p(A) PA-X Targeted Transcripts (e.g GAPDH) in the Nucleus.

To further investigate the nature of the p(A) RNAs that were being retained in the nucleus during IAV infection independent of PA-X and NS1 activity, I investigated the subcellular distribution of GAPDH, an abundant, predominately cytoplasmic transcript. GAPDH is targeted by IAV host shutoff – during infection it is cleaved and degraded by PA-X. The aberrant accumulation of p(A) RNAs during infection could be due to the retention of host transcripts in the nucleus, in association with cleavage of the target RNAs in the cytoplasm. Interestingly, I saw no obvious accumulation of GAPDH in the nucleus of infected cells, PR8-WT or mutant (Figure 3.10). This data suggests that while there is a significant increase in p(A) RNA in the nucleus during infection (Figure 3.7C), this increase is not due to a nuclear retention of GAPDH transcripts (Figure 3.10).

3.8 Mutations in NS1 Disrupt NS1-Mediated Enhancement of PA-X Host Shutoff

My data thus far suggests NS1 is important for PA-X mediated host shutoff and the downregulation of host transcripts during infection. While nuclear accumulation of PABP is an important indicator of PA-X function, NS1 also plays a role - when NS1 loses its effector domain there is limited to no nuclear accumulation of PABP (Figure 3.7). I wanted to determine if there were specific epitopes on NS1 that were important for this impact on host shutoff. We produced two more NS1 mutant viruses to analyze: 88-90A has a mutation that impacts its ability to bind to PI3K and mutant 187R has been shown to be defective in NS1 dimerization (Aramini et al., 2011; Kerry et al., 2011). We sought to investigate if these mutants had any effect on the sub-cellular distribution of PABP during infection. The mutant NS1 virus: 123, 124A; 38,41A; 96,97A; and 88-90A showed limited to no increase in nuclear PABP during infection (Figure 3.11A). The percentage of infected cells with nuclear PABP was significantly lower in each of the mutant virus infections compared to PR8-WT (Figure 3.11B). This data suggests that these epitopes may contribute to NS1's enhancement of PA-X mediated host shutoff or may play a role in PABP intracellular shuttling. One mutant, 187R, did not have any significant change in the percentage of infected cells with nuclear PABP compared to PR8-WT infection (Figure 3.11A, B). This suggests that the 187 epitope may not contribute in the same way to host shutoff or to PABP shuttling as the other mutants.

Figure 3.11

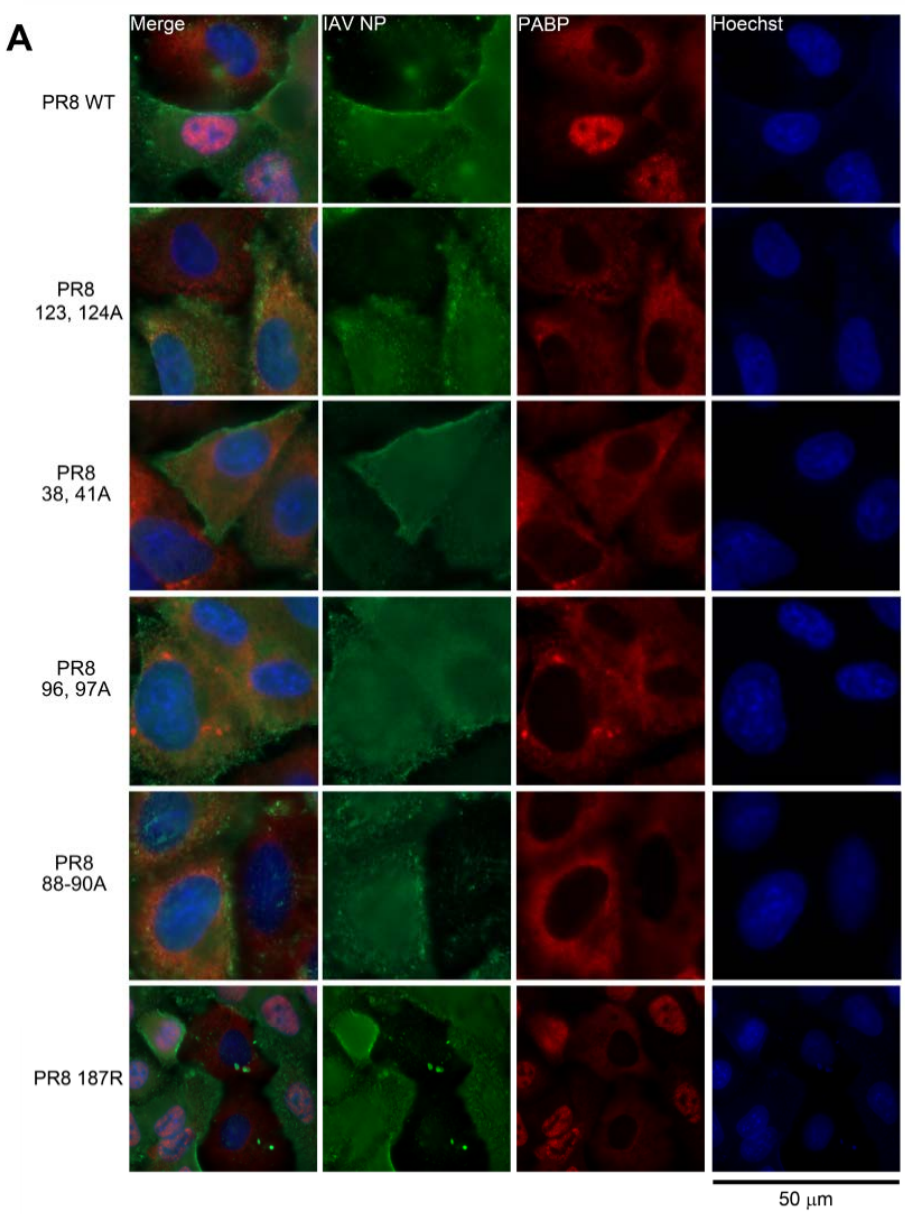
A
Merge
IAV NP
PABP
Hoechst
PR8 WT
PR8
123, 124A
PR8
38, 41A
PR8
96, 97A
PR8
88-90A
PR8 187R
50 μm
B
NS1 Mutant - Nuclear PABP
% Nuclear PABP
150
100
50
0
****
****
ns
Mock
WT
123, 124A
38,41A
96,97A
88,90A
187R

Figure 3.11 NS1 Epitopes may Contribute to Host Shutoff as a Function of Nuclear Accumulation of PABP.

(**A**) A549-MAVSKO cells were mock infected or infected with a panel of mutant NS1 viruses: PR8-123,124A, PR8-38,41A, PR8-96,97A, PR8-88-90A, PR8-187R. Cells were infected at an MOI = 1 and collected at 24hpi. Samples were processed for IF for IAV NP (green), PABP (red), and Hoechst (blue). Images were collected on the Zeiss Axio Imager Z2 and the representative images are 50 μm X 50 μm. (**B**) Quantifications of the percent of infected cells in (A) that have nuclear accumulation of PABP. N=3. Significance was determined through a one-way ANOVA followed by a Dunnett's multiple comparisons test. Ns = not significant (>0.05), ****(<0.0001).

3.9 The Subcellular Localization of NS1 may Impact the Host Shutoff Phenotype of PA-X.

NS1 has many important functions in both the nucleus and the cytoplasm, therefore its subcellular distribution impacts the efficiency of NS1's functions. NS1 has an N-terminal nuclear localization signal (NLS) (amino acids 35, 38, 41). The nuclear export signal (NES) on NS1 is located in the C-terminus of the protein (amino acids 138–147) and is a classic hydrophobic leucine-rich export signal (Tynell et al., 2014). These classic export signals are often bound directly by the CRM1 exportin molecule, which then mediates the transport of NS1 through the nuclear pore complex (NPC) (Reviewed in Sorokin et al., 2007). We considered the importance of the localization of NS1 and wanted to investigate whether the subcellular distribution of PABP corresponded to any changes in NS1 localization, and therefore how this may be an indicator of how the distribution of NS1 impacts its effect on PA-X mediated shutoff. In PR8-WT infected cells, the distribution of NS1 was predominantly cytoplasmic at 24 hpi (Figure 3.12). Interestingly, no other NS1 mutant virus had only cytoplasmic distribution at 24 hpi (Figure 3.12). Mutant 123,124A was retained in the nucleus at 24 hpi (Figure 3.12). Mutants 38,41A and 187R were distributed diffusely through the infected cell (Figure 3.12). Finally, mutants 96,97A and 88-90A were distributed throughout the cell with some accumulation in the nucleus (Figure 3.12). These data suggest that the subcellular localization of NS1 and the distribution of PABP during infection may have a more complicated relationship than previously considered.

Figure 3.12

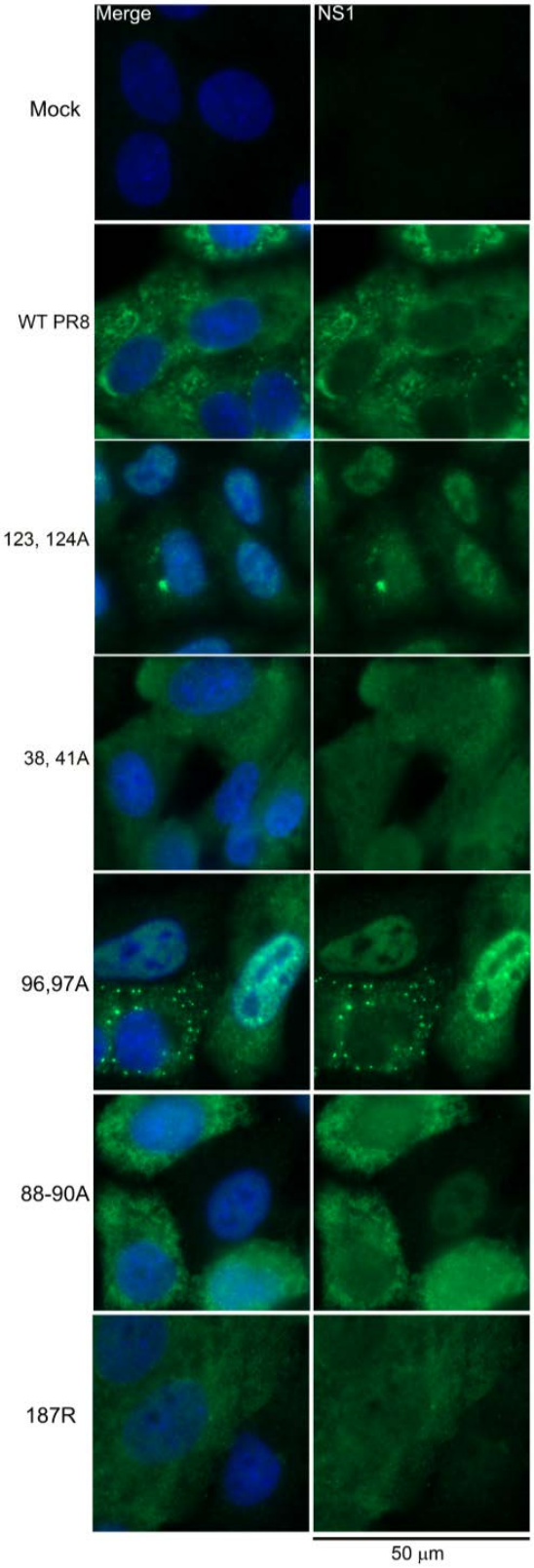

Figure 3.12 The Subcellular Distribution of NS1 is Influenced by Point Mutations. A549-MAVSKO cells were mock infected or infected with a panel of mutant viruses (as described in Figure 3.11). The cells were infected at an MOI = 1 and were collected at 24 hpi. The samples were then processed through IF to visualize the localization of NS1 (green) during infection. N=3. Images were collected on the Zeiss Axio Imager Z2 and the representative images are 50 μm X 50 μm.

3.10 PA-X Remains Elusive from Identification via Western Blotting, Co-Immunoprecipitation, and Mass Spectrometry

NS1 may have an impact on the amount of host shutoff occurring during IAV infection, and this could be measured as a function of the level of PA-X present in the infected cell. PA-X is produced in very low amounts during infection, which makes visualizing or quantifying the amount or changes in its concentration during infection difficult. To attempt to visualize PA-X through western blotting, I infected cells with PR8-WT virus and collected the samples at 20 hpi. These samples were processed for western blotting and run on a 12% gel. The membrane was cut following the transfer to separate the full-length PA (82 kDa) from the smaller and less abundant PA-X (29 kDa). The primary antibody I used was the same for each section of the membrane, as it binds to the shared N-terminal epitope. Unfortunately, PA-X specific bands were not identified in repeated trials of western blotting and infecting at varying MOIs.

Next, I attempted to produce a multifunctional PA/PA-X construct that, when transfected, would produce a PA-myc and a PA-X with a double-HA tag. The 2xHA tag was added in the +1 frame of PA. This recoding introduced 15 amino acid substitutions in the 728 amino acid long PA-myc protein (between amino acids 253 and 272) without impact on full length PA. The construct was transfected into 293T cells in addition to control transfections containing PA-myc, NS1-myc and a control HA-tagged construct (SARS-CoV-2 NSP1) available in the lab and collected 24 hours post transfection. The samples were run on a western blot and visualized using either an anti-myc antibody or an anti-HA antibody. While the NS1-myc and PA-myc was visible in all the appropriate lanes (Figure 3.13A), there was no PA-X-HA present in the lanes transfected with the PA-X-HA construct (Figure 3.13B).

Moving forward I attempted to determine the amount of PA-X activity as a function of luciferase output using a CMV (+) intron luciferase reporter that has previously been published in Gaucherand et al., (2019). Instead of transfection with PA-X, I transfected cells with PA and NS1 to determine if we could detect more endogenous levels of PA-X. Unfortunately, there was no reliable evidence that we could detect PA-X activity output using this luciferase reporter assay.

I carried out an immunoprecipitation assay to attempt to pull-down PA-X using the 2xHA tag. I transfected 293T cells with either the PA-X-HA construct or with a SARS-CoV-2 NSP1-HA construct as a control. I transfected each construct into separate 10 cm dishes and collected the samples at 24 hours post transfection. Unfortunately, the pull down was not successful in identifying the control NSP1-HA construct in the eluant (Figure 3.13C). There is evidence of transfection success as the membrane probed with anti-PA antibody identified a band in the PA-X-HA samples, and there was evidence of NSP1-HA construct in the input sample on the membrane probed with anti-HA, but there was no evidence of PA-X in the PA transfected samples (Figure 13.C). This suggests that PA-X remains very difficult to identify though conventional molecular biology techniques and the quantifiable impact of NS1 on PA-X production or function requires further investigation.

Finally, to attempt to determine the changes in the amount of PA-X present in a sample, I did one preliminary LC-MS/MS experiment. This was done to determine if we could identify any PA-X in transfected samples by mass spectrometry and potentially therefore look at the changes in levels of PA-X during infection of different mutant viruses to see how NS1 impacted the levels of PA-X. Three samples were prepared for untagged LC-MS/MS: empty vector, PA, and PA-X transfected cells. The samples were sent to the laboratory of Dr. Patrick Murphy (University of Prince Edward Island) and there were no PA-X specific peptides present in the PA transfected cells. This indicates that our challenges in detecting PA-X via western blotting are largely due to very low levels of PA-X protein and not the poor anti-PA N-terminus antibody or anti-HA tag antibody specificity or avidity.

Figure 3.13

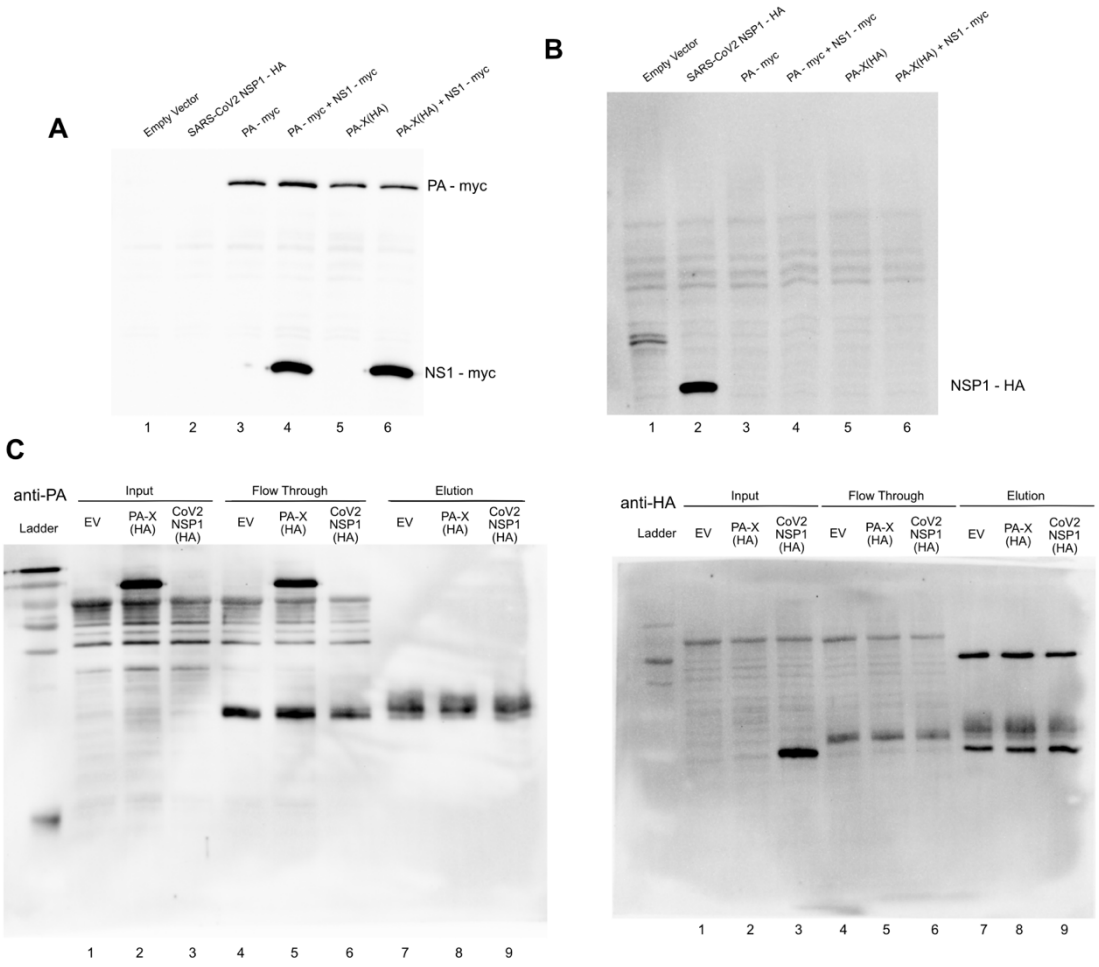

Figure 3.13 PA-X Identification was Unsuccessful in Transfection and IP Pulldowns. (**A**) 293T cells were reverse transfected with a panel of –myc and –HA tagged constructs. Transfections were collected at 24 hours post transfection and the samples were lysed and run on western blots. The membranes were blotted for anti-myc to identify expression levels of the PA-myc and NS1-myc constructs. (**B**) Samples were processed as in (A). Membranes were blotted for anti-HA to identify the expression levels of SARS-CoV-2 NSP1-HA control and PA-X-HA. PA-X-HA was estimated to be around 29 kDa. (**C**) Immunoprecipitation of 293T cells transfected with PA-X-HA or the NSP1-HA control. Samples were run on a western blot and blotted for either PA (82 kDa) or HA tag.

CHAPTER 4: DISCUSSION

4.1 Implications of Breaking the Accepted IAV Host Shutoff Model

Host shutoff is an important mechanism that enables IAV to target and inhibit host gene expression and to limit the antiviral immune response induced during infection. The data presented in this thesis suggests that the current accepted model of IAV host shutoff may not represent the whole story of what occurs during infection. In PA-X overexpression models, there is strong evidence of both the nuclear import of cytoplasmic PABP, as well as an increase in the nuclear signal of p(A) RNAs (Khaperskyy et al., 2016). When PABPs are unable to interact with RNAs in the cytoplasm, they can bind to importin-α and be imported into the nucleus (Kumar et al., 2011). Kumar & Glaunsigner (2010) have also presented a model where the import of PABP into the nucleus causes the hyperadenylation and retention of host mRNAs. These two findings, together suggest that PA-X activity, on its own, causes an increase in unbound PABP, which is imported into the nucleus at an increased frequency, and once in the nucleus causes modifications to the p(A) tails of pre-mRNAs to prevent their subsequent export. In this body of work, I have shown that the nuclear import of PABP is dependent not just on PA-X, but also on a yet to be identified function of the NS1 effector domain. Furthermore, the increase of p(A) RNAs in the nucleus in infected cells is not the direct consequence of import and accumulation of PABP.

Un-linking these two markers associated with IAV host shutoff – nuclear p(A) RNA accumulation and nuclear PABP accumulation - means that the proposed mechanism of host shutoff needs to be re-evaluated. It is also likely the import of PABP is not the only or not the main mechanism for accumulation of p(A) RNAs in the nucleus during IAV infection. Perhaps the mechanistic function of PA-X at endogenously expressed levels is different from that of PA-X expressed at much higher levels (like in overexpression models). Studying the function of PA-X has some challenges, for example: it cannot be transformed into cells to be stably expressed because it becomes cytotoxic. For this reason, Khaperskyy et al. (2016) developed doxycycline inducible transformed cell lines which would induce the overexpression of PA-X upon the addition of doxycycline. Unfortunately, this does not engage research of PA-X's function at the endogenously produced level, like during infection. This could potentially be solved by

transforming cells instead with the PA construct, allowing for more physiological PA-X levels, but it would be very difficult to separate PA and PA-X effects in this model.

4.2 Implications of IAV Utilizing Two Proteins for Host Shutoff

Research from Chaimayo et al., (2018) suggested that there was some type of functional interplay between PA-X and NS1 that impacted the ability of each protein to carry out its functions most effectively and create the most optimal environment for IAV infection. The cleavage of host RNAs in the cytoplasm by PA-X and the subsequent translocation of PABP into the nucleus was dependent on having an NS1 present that had the C-terminal region of the protein. When I infected A549 cells with the N80 mutant virus, there was no evidence of nuclear PABP accumulation, even though those viruses produced PA-X. Additionally, the N80 mutant viruses had significantly reduced downregulation of select host transcripts that are normally targeted by PA-X during infection. This was also replicated when I infected cells with a PA-X mutant virus (PA(fs)), and with a double mutant (N80(fs)). These data together suggest that the C-terminal effector domain of NS1 plays a vital role in the host shutoff activity of PA-X and the subsequent changes in cellular protein distribution. The data also suggests that both NS1 and PA-X are needed in the host cell during infection to produce these host shutoff phenotypes. As both NS1 and PA-X are working towards the same goal in infection – to limit host cell gene expression and the immune response – their potential interactions or functional link would ultimately aid in achieving those impacts in the host.

My hypothesis is that the presence of functional NS1 enhances the production of PA-X to ultimately allow for increased PA-X function and increased viral host shutoff. Although this is my hypothesis, there are other alternatives that could be true: NS1 and PA-X could potentially have direct interactions with each other which may enhance PA-X targeting; or NS1 may cause a cascade of signaling that could influence the efficiency of PA-X cleavage of host RNAs. Interestingly, PA-X is highly conserved between different IAV strains, but the shutoff activity varies substantially – human IAV PA-X tends to have less host shutoff activity compared to avian strains (Desmet et al., 2013). This is also the case for NS1: while all IAV strains produce NS1 not all strains are able to carry out general host shutoff through binding to CPSF30 (Hale et al., 2010; Hayashi et

al., 2016). Due to these changing factors between different IAV strains, the research behind understanding their complimentary relationship is difficult. This thesis focused on the IAV H1N1 strain PR8, which produces an NS1 that is unable to bind to CPSF30. Due to the strain-specific variety and magnitude of NS1 functions, the impact that PR8 NS1 has on PA-X may differ from the NS1 of the H1N1 2009 strain or of H3N2 Udorn IAV and would require more investigation to understand.

4.3 Potential Functional Links for NS1 and PA-X

One of the first conditions that needs to be determined to further understand the relationship between NS1 and PA-X is the nature of their interaction. Overexpression of PA-X shows that it is able to function without NS1 present (Khaperskyy et al., 2014), which means that an interaction that facilitates PA-X basic functions may not be likely. When PA-X is expressed at endogenous levels NS1 may be able to facilitate targeting at a higher capacity than PA-X can on its own (Chiamayo et al., 2018). This potential interaction could be mediated through close interaction of NS1 with translational machinery, which could draw PA-X into proximity to its mRNA targets in the cytoplasm.

NS1 has a functional capacity to enhance the translation of viral mRNAs over cellular mRNAs. The binding of viral mRNAs to NS1's RNA binding domain and then subsequent interaction with the translation initiation factor eIF4G allows viral mRNAs to be preferentially translated and engage with polysomes at a higher concentration than cellular mRNAs (Burgui et al., 2003). To increase the production of PA-X, there needs to be increased translational activity on the viral PA mRNA. NS1 has been shown to play a role in increasing the production of viral mRNAs, so this interaction could be key in ensuring the virus has increased translational activity on the PA segment, which could lead to increased production of PA-X. Not only could NS1 enhance PA segment translation, but it could also play a role in mediating the frame shifting event to allow the production of PA-X.

Using recombinant mutant viruses, I showed that IAV requires NS1 to have its C-terminal effector domain to induce PA-X host shutoff (Figure 3.7, 3.9). Additionally, I suspected that the subcellular localization of NS1 may play a role in the activity of PA-X and have some participation in their functional relationship. The mutants I tested did have

differential distribution during infection, but the data suggests that there was no change on the nuclear accumulation of PABP due to NS1 localization differences. Mutant 38,41A and 187R both had NS1 spread diffusely through the cell during infection, but 38,41A did not have any nuclear accumulation of PABP whereas 187R had the same level of PABP in the nucleus as PR8-WT infection. This indicates that the localization of NS1 may not be a determining factor to its functional relationship with PA-X.

4.4 The Role of the Different Domains of NS1 and the Implications of the Mutants Used on Host Shutoff Phenotypes

I used various NS1 mutant viruses to try to dissect the interplay between NS1 and PA-X and to attempt to determine if there is a specific domain that is involved in enhancing PA-X mediated host shutoff. The NS1 mutants I used in this study were: N80; R38A, K41A; 88-90A; E96A, E97A; 123,124A; 187R.

N80 is a truncated mutant which only retains the N-terminal 80 amino acids of the protein. This greatly limits its capacity for impacting the host during infection and is limited to its RNA binding domain with key amino acid residues R38, and K41. R38 is the essential amino acid for facilitating RNA binding. NS1 also uses its RBD to bind to NXF1 and also to facilitate RIG-I binding (Jureka et al., 2020; Zhang et al., 2019). Residues 88-90 have been suggested to be important for PI3K binding, specifically residue Y89 (Hale et al., 2008; Hrincius et al., 2012). Residues 96 and 97 have been shown to be important for TRIM25 binding and when these residues are mutated there is evidence that there is an increased turnover of NS1 which prevents its accumulation (Gack et al., 2009; Khaperskyy et al., 2012). The 123, 124 residues have an unclear function, but residue 126 is ISGylated by ISG15 (Reviewed in Klemm et al., 2018). Finally, residue W187 is important for NS1 dimerization (Carrillo et al., 2014).

Each of these mutants are responsible for different NS1 impacts on the host, and I wanted to see if they could be implicated in impacting PA-X mediated host shutoff. Every mutant we investigated did not cause the nuclear accumulation of PABP, except for W187R (Figure 3.12). This data suggests that the dimerization of NS1's effector domains is not important for the functional relationship between NS1 and PA-X, but each of the other residues or functions of NS1 may play some role in impacting the accumulation or the functional activity of PA-X, although how they impact PA-X

production or function remains unclear. It is important to note that each of the mutations we examined affected not only the previously reported interaction with host proteins, but also decreased levels of NS1 accumulation in infected cells to various degrees (96,97A the most and 187R the least). As discussed above, these mutations also caused changes in subcellular distribution of NS1. All these combined effects make it hard to pinpoint the exact NS1 function that is required for augmenting PA-X activity. Future investigation will likely involve an even broader panel of NS1 mutants to separate these effects.

4.5 How Timing Impacts Host Shutoff Phenotypes

The accumulation of proteins over time during infection can impact the effects of host shutoff. NS1 is produced early in infection and beings targeting mRNA processing and translation at those early stages. I studied the implications of NS1 and PA-X at later times post infection as PA-X activity is not evident at early times post infection. The mechanism of translation of PA-X means that it is produced slowly and over time it will accumulate to be present at optimal levels for productive host shutoff and the creation of a pro-viral environment for the virus to optimize assembly and egress without triggering the host immune response. At approximately 12 hpi PA-X has accumulated to sufficient volumes to start carrying out host shutoff. At later stages of infection, the two host shutoff proteins work together to limit the immune response of the host through PA-X mediated cleavage of host transcripts and through NS1 inhibiting the dsRNA detection by PKR and RIG-I. At early times during infection, the virus may not need substantial PA-X driven inhibition of the host because of the minimal accumulation of viral mRNAs and the presence of NS1.

4.6 Implications of PABP Redistribution During Infection

PABP has an important role for the host in the cytoplasm of the cell. The interactions between PABP and both eIF4G and the p(A) tail of the host transcripts aid in transcript circularization and the rate of translation on the transcript. PABP redistribution during IAV infection may be influenced by both PA-X and NS1. Both PABP and NS1 bind to eIF4G in the cap-binding translation initiation complex. There is potential that these interactions are competitive and that NS1 can outcompete PABP in binding to eIF4G. This could increase the concentration of unbound PABP, which is more susceptible to transport into the nucleus, as without binding to eIF4G, PABP's non-

canonical importin-α sequence is available for interaction. The loss of cytoplasmic PABP through this mechanism may allow PA-X to function more freely and efficiently to cleave its target transcripts and could be one mechanism through which NS1 aids in PA-X mediated host shutoff.

The secondary implication of PABP being imported into the nucleus has been described by Kumar & Glaunsinger (2010). They found that nuclear accumulation of PABP, and specifically the first two RRM on the protein, were required for the retention of p(A) RNAs in the nucleus. IAV and many other viruses produce host shutoff endonucleases that have shown evidence of the nuclear accumulation of PABP, and the connected increase of p(A) RNAs. What is interesting about this data is that we see an increase in the nuclear p(A) RNA during infection in the absence of nuclear accumulation of PABP when we infect A549 cells with NS1 mutant viruses. What this indicates to us is that although the nuclear accumulation of PABP can contribute to the increase in nuclear p(A) RNAs during infection, it may not be the sole cause of this phenotype.

4.7 Implications of p(A) RNA Accumulation During Infection

Under normal conditions, host cells maintain a relatively even distribution of p(A) RNAs between the nucleus and the cytoplasm. The maturation of pre-mRNAs into mature p(A) mRNAs and their subsequent export is a well-regulated process in the cell. We have shown that there is an increase of p(A) RNA in the nucleus, independent from the nuclear accumulation of PABP during infection with IAV. As these two events had been previously linked through the mechanism that the p(A) RNAs accumulate during IAV infection due to hyperadenylation from increased nuclear PABP, there is further investigation that needs to be done into which p(A) mRNAs are being retained and through what mechanism that retention is occurring through. The data presented has shown that the cause of p(A) RNA increase in the nucleus during IAV infection may not be due to the polyadenylation of RNAs that canonically lack a p(A) tail, like MALAT1. While MALAT1 is not being aberrantly increased in the nucleus, we did observe that its downregulation during infection appears to be NS1 dependent (Figure 3.10). Additionally, abundantly cytoplasmic transcript (like GAPDH) did not seem to accumulate in the nucleus, indicating that it is not all transcripts that are being retained and contributing to the increase of p(A) RNAs.

One alternative mechanism is through an increase in the mis-splicing of mRNAs (reviewed in Wegener & Müller-McNicoll, 2018). There has been evidence that suggests the inhibition of the U4 component of the spliceosome inhibited splicing in cells and caused the un-spliced p(A) transcripts, splicing components, and PABPN to be localized to enlarged nuclear speckles (Hett & West, 2014) Interestingly, in addition to the mRNA retention in the nucleus, specifically in nuclear speckles, there was no evidence of mRNA decay machinery localizing to those speckles (Hett & West, 2014). There has also been evidence of NS1 binding to a region on U6 snRNA and inhibiting the U6-U4 interaction during splicing, which ultimately inhibits the splicing of pre-mRNA (Qiu et al., 1995). Qiu et al. (1995) suggests that these mRNAs are un-spliced, p(A) mRNAs that are not degraded immediately and, from what we have observed, if the virus is able to inhibit splicing through some similar mechanism, this could be contributing to the PABP-independent increase in p(A) RNA occurring during IAV infection.

4.8 Immune Modulatory or Host Effects Outside of RIG-I/MAVS Mediated Immune Signaling that may Impact Mutant Virus Infection

We repeated analysis of our infection models in A549-MAVSKO cell lines to ensure that the phenotypes we were observing were not caused by innate immune signaling in the cell. Using NS1 mutant viruses, there is a much stronger immune response initiated during infection due to the inability of the virus to inhibit the activation of RIG-I and PKR and its inability to interact with other proteins that help modulate the expression of IFN. By using A549-MAVSKO cells, we were able to limit a large portion of the cellular antiviral innate immune response to IAV and determine the nature of the accumulation of p(A) RNAs in the nucleus during infection was not due to an increase in MAVS-mediated immune signaling. Although knocking out MAVS in the host cell is a substantial way to decrease the innate immune response potential in these cells, there are still other potential ways for the virus to initiate an immune response in the absence of MAVS. The immune signaling through TLR3 and TLR7 (as described in 1.3.1) is still active and has the potential to allow for a cellular IFN response to IAV infection. While this is still a vital part of immune signaling for the host against IAV, the overall impact of TLR3 or TLR7 signaling on its own does not show evidence to induce large amounts of IFN (Figure 3.5C).

4.9 Comparable Host Shutoff Strategies

IAV host shutoff strategies involve utilizing both NS1 and PA-X, where PA-X works to cleave host transcripts and one of NS1's functions works to limits host transcript expression by preventing host mRNA nuclear export. IAV is not the only virus that uses this type of strategy: cleaving transcripts and limiting the nuclear export to limit the host. Betacoronaviruses like SARS-CoV and SARS-CoV-2 (the cause for the COVID-19 pandemic) produce NSP1 which acts in a similar way. NSP1 interacts with NXF1 of the NXF1-NXT1 mRNA nuclear export complex to prevent the export of host mRNAs to the cytoplasm (Zhang et al., 2021a). NSP1 also has the capacity to induce mRNA cleavage during infection. While NSP1 itself does not have a nuclease domain, SARS-CoV NSP1 has been shown to recruit host exonucleases, like Xrn1, to degrade the host mRNA (Gaglia et al., 2012). Gammaherpesviruses, like KSHV, also encodes two unique proteins that restrict the host through a similar strategy. SOX is an endonuclease encoded by ORF37 and causes the cleavage of host transcripts which limits their accumulation during infection (Glaunsinger & Ganem, 2004; Glaunsinger et al., 2005). SOX also utilizes the host exonuclease Xrn1 for the complete degradation of host mRNAs (Gaglia et al., 2012). In addition to SOX, the protein produced from ORF10 interacts with Rae1, a nuclear export factor that interacts with Nup98, which prevents the nuclear export of host mRNAs and their subsequent expression (Gong et al., 2016).

Each of these viruses, betacoronaviruses, influenza viruses, and gammaherpesviruses, are unique in their genome organization, replication cycle, and host tropism and yet they engage in similar host shutoff strategies. The redundancy in these strategies suggest the importance on not only limiting the pool of mRNAs during infection in the cell but also limiting the expression of those mRNAs that are not targeted or downregulated by the endonuclease. This further supports the idea that IAV host shutoff, as carried out by PA-X and NS1 together, is an important component to the productive infection of IAV. Each of the viruses described in this section carry out host shutoff through unique proteins but maintain key mechanisms – utilizing a host exonuclease for complete degradation of targeted host RNAs and creating a block in the nuclear export of host mRNAs – suggesting the large role these functions have on the success of the virus during infection.

4.10 Limitations and Future Directions of the Study

It is important to note that while the findings highlighted in this thesis are important to aid in understanding the functional relationship between NS1 and PA-X and how that influences the host shutoff of IAV, there were several limitations to this work that should be considered.

The first limitation I wanted to highlight was the lack of a secondary cell line. I used A549s primarily for the study of the phenotypes I was observing, and while these cells are a good cell model for IAV study, the results should be corroborated into a secondary cell line that is permissive to IAV and represents a relevant biological system. The use of A549-MAVSKO cells was important to expand our understanding of how the MAVS-mediated immune response impacted the host environment during NS1 mutant virus infection. HEK 293 cells were used for their permissibility of transfection, compared to A549 cells. It will be important to expand these results in alternative cell lines, like small airway epithelial cells (SAEC), and further into expanded models like an air-liquid interface model to analyze the functional relationship between NS1 and PA-X in more complex systems.

Secondly, for these investigations I used one strain of IAV – PR8. PR8 is a lab adapted strain of H1N1 that is commonly used to investigate molecular mechanisms during IAV infection. While it is a good representative virus, it does not encapsulate the functions and mechanisms of all IAV, nor of all H1N1 viruses. The results shown in this study are notable and it is important to expand the results to include additional IAV strains, of both human and avian origin. Including the 2009 pandemic H1N1 strain, as well as a strain like H3N2 - Udorn which has an NS1 that is able to bind to CPSF30 (unlike PR8) would increase the reliability of our findings. Highly pathogenic avian influenza's like H7N9 or H5N1 could also be important to dissecting the specifics of the interplay between NS1 and PA-X and how they may contribute to the pathogenicity of the virus.

Another important limitation to note is the lack of quantifications for the smFISH data. While this data does allow some interpretation from qualitative analysis, the results would be more definitive if the appropriate tools had been available to quantify the puncta. SmFISH is an excellent experimental technique that is best analyzed via

quantification as the puncta are representative of a single transcript, compared to IF, where the intensity of the fluorescent signal is measured. Future analysis of this smFISH data and adding in a nuclear membrane marker or a cytoplasm marker may aid in having more precise quantifications and aid in the processing of the images.

Direct analysis of the levels of PA-X were also not completed in this research. Due to the limited production of PA-X in IAV infected cells, the isolation and quantification of the protein was unsuccessful. Additionally, when PA was transfected into cells, PA-X was not visualized through western blotting, IP, or LC-MS/MS. I was surprised that analysis by LC-MS/MS did not work to identify PA-X in these samples, as PA-X has a unique X-ORF and should have had peptides that were clearly identifiable. Having some reliable mechanism for the quantification of PA-X activity and presence is necessary to further understanding the functional relationship between NS1 and PA-X. Potentially utilizing a constitutively expressed reporter in cells that can be infected by IAV may allow for some analysis of the activity of PA-X during infection and therefore some indication of the levels of PA-X present. This method could then be expanded to infection with NS1 mutant viruses and therefore elucidate if there is any enhancement to PA-X activity by NS1.

Moving forward, investigating if there is a structural relationship between PA-X and NS1 or if there is a common interacting partner between the two proteins could allow for a deeper understanding to their relationship and their suggested interconnected functions. The data in this thesis suggests that PA-X requires the presence and activity of NS1 to efficiently carry out host shutoff during infection, and the intricacies of this relationship remain to be discovered.

4.11 Conclusions and Model

The host shutoff activity of IAV is a complex, interconnected mechanism that the virus needs to create an optimal environment for infection. This thesis sought to answer the question of if there is functional interplay between NS1 and PA-X and how that potential functional interplay may impact the magnitude and specificity of IAV host shutoff. I aimed to characterize the impact NS1 had on PA-X's abundance and activity, and on how that relationship impacted the localization of host transcripts during IAV infection. Additionally, I aimed to use mutant IAV viruses to help dissect the relationship

between NS1 and PA-X. The data presented in this thesis suggests that NS1 and PA-X do have a functional relationship which allows PA-X to function at optimal rates.

Initially, I found that p(A) RNA accumulates in a PA-X independent manner in IBV infected cells. Following that discovery, I used infections with PR8-WT, PR8-N80, and PR8-PA(fs) mutant viruses and found that the presence or absence of PA-X and NS1 do not impact the accumulation of nuclear p(A) RNA, and rather this occurs in an independent manner. I then elucidated that nuclear PABP accumulation during infection needs both NS1 and PA-X to occur, contrary to previously understood models. Finally, through smFISH, my data suggests that MALAT1 depletion is dependent on full length NS1, and that GAPDH nuclear accumulation does not contribute to increased p(A) RNA, suggesting that it is not global mRNA retention that is causing the accumulation that we observed. Taken together, this data supports the hypothesis that NS1 enhances PA-X activity or production to allow for functional relevance during infection and to maintain and enhance the pro-viral environment within an infected cell.

The model I propose, in contrast to the previously accepted model, is shown in Figure 4.1 and described as such: PA functions in the nucleus to facilitate cap snatching and remove the 5'm7G caps off the host pre-mRNAs to allow for viral transcription to occur. NS1 interacts with 3' processing proteins, like CPSF30, to inhibit the 3' end processing and maturation of host pre-mRNAs. NS1 also interacts with the NXF1-NXT1 nuclear export complex to inhibit the interaction with mature host mRNAs and prevent their export and subsequent translation. The inhibition of the maturation of host mRNAs and their limited export allows for the preferential export and association of viral mRNA with polysomes in the cytoplasm and for their preferential translation and protein expression. The presence of NS1 impacts the accumulation of PA-X through an undetermined mechanism of either impacting PA-X levels and/or impacting PA-X activity. In either scenario, PA-X can accumulate in the host in the presence of functional NS1 and functions in the cytoplasm and the nucleus to target and cleave host transcripts that have been transcribed by RNA Pol II and have been processed through splicing. Those cleaved transcripts are degraded by host exonuclease Xrn1. During infection, NS1 influences the nuclear import of PABP through an undetermined mechanism which may include PA-X function. Finally, there is an accumulation of p(A) RNAs which can occur

due to the accumulation of PABP in the nucleus but can also occur independent of this mechanism and independent of NS1 and PA-X presence in a host cell.

Elucidating these mechanisms aids in the complex understanding of IAV host shutoff and of cellular processing involving RNA maturation and export. Further understanding how IAV carries out host shutoff is important to contributing to our preparedness for emerging IAV pandemics and could help drug developers and clinicians develop more specific treatments against influenza. Ultimately, elucidating the roles of PA-X and NS1 and their functional interrelationship will highlight new details on the specific lifecycle of IAV and will contribute to our understanding of how the virus functions to have successful infection and cause disease.

Figure 4.1

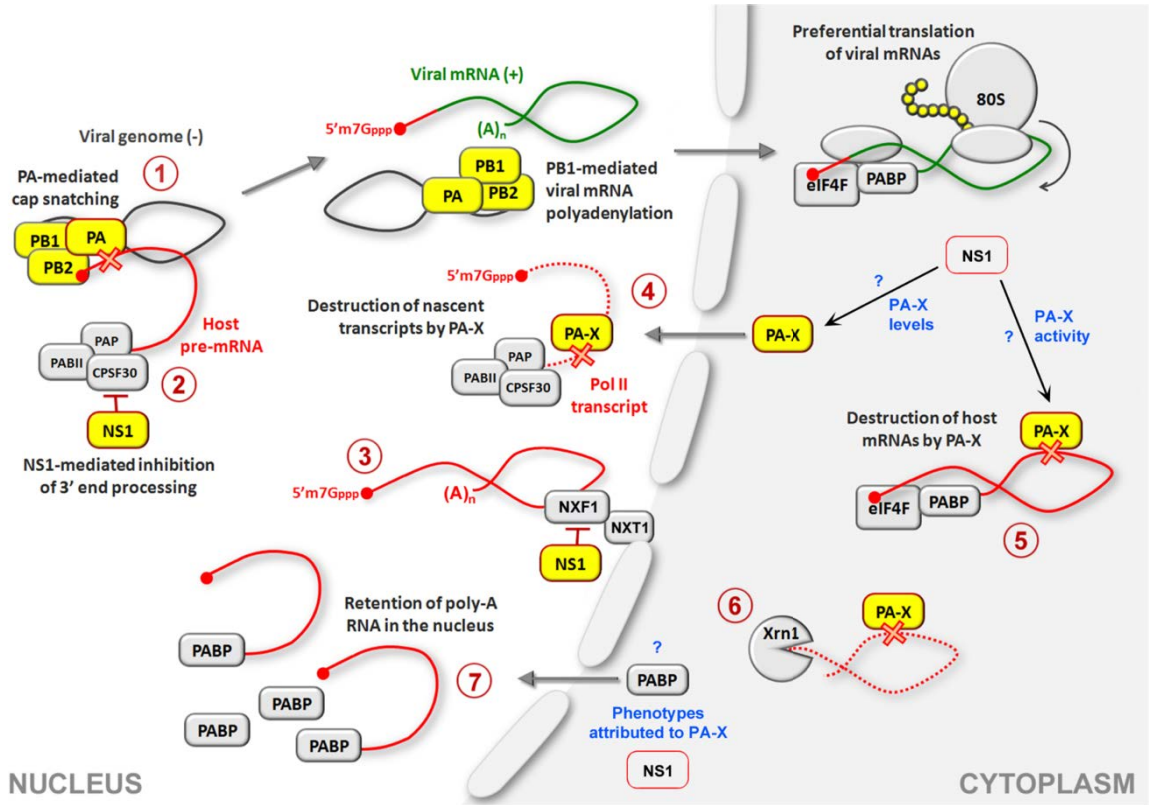

Figure 4.1 Model of Concerted Action of PA-X and NS1.

(1) Cap snatching by viral RNA polymerase destroys host pre-mRNAs to supply capped primers for viral transcription. (2) NS1 inhibits polyadenylation of host transcripts by sequestering CPSF30. (3) NS1 interacts with NXF1/NXT1 and blocks host mRNA export. (4/5) NS1 impacts PA-X production or activity to allow for efficient PA-X-mediated host shutoff. (4) PA-X enters the nucleus where it is recruited to the RNA Pol II transcripts. (5) Cytoplasmic mRNAs are cleaved by PA-X. (6) Host 5' to 3' exonuclease Xrn1 degrades fragments generated by PA-X. (7) IAV host shutoff causes nuclear accumulation of PABP and poly(A) RNA (phenotypes previously attributed to depletion of cytoplasmic mRNAs by PA-X).

REFERENCES

Afonina, E., Stauber, R., & Pavlakis, G. N. (1998). The human poly(A)-binding protein 1 shuttles between the nucleus and the cytoplasm. *Journal of Biological Chemistry*, *273*(21), 13015–13021. https://doi.org/10.1074/jbc.273.21.13015

Aragón, T., de la Luna, S., Novoa, I., Carrasco, L., Ortín, J., & Nieto, A. (2000). Eukaryotic Translation Initiation Factor 4GI Is a cellular target for NS1 protein, a translational activator of influenza virus. *Molecular and Cellular Biology*, *20*(17), 6259–6268.

Aramini, J. M., Hamilton, K., Ma, L.-C., Swapna, G. V. T., Leonard, P. G., Ladbury, J. E., Krug, R. M., & Montelione, G. T. (2014). 19F NMR reveals multiple conformations at the dimer interface of the Non-Structural Protein 1 effector domain from Influenza A Virus. *Structure (London, England : 1993)*, *22*(4), 515–525. https://doi.org/10.1016/j.str.2014.01.010

Aramini, J. M., Ma, L.-C., Zhou, L., Schauder, C. M., Hamilton, K., Amer, B. R., Mack, T. R., Lee, H.-W., Ciccosanti, C. T., Zhao, L., Xiao, R., Krug, R. M., & Montelione, G. T. (2011). Dimer interface of the effector domain of Non-structural Protein 1 from Influenza A Virus. *The Journal of Biological Chemistry*, *286*(29), 26050–26060. https://doi.org/10.1074/jbc.M111.248765

Bedford, T., Suchard, M. A., Lemey, P., Dudas, G., Gregory, V., Hay, A. J., McCauley, J. W., Russell, C. A., Smith, D. J., & Rambaut, A. (2014). Integrating influenza antigenic dynamics with molecular evolution. *ELife*, *3*, e01914. https://doi.org/10.7554/eLife.01914

Bergmann, M., Garcia-Sastre, A., Carnero, E., Pehamberger, H., Wolff, K., Palese, P., & Muster, T. (2000). Influenza Virus NS1 protein counteracts PKR-mediated inhibition of replication. *Journal of Virology*, *74*(13), 6203–6206. https://doi.org/10.1128/JVI.74.13.6203-6206.2000

Biswas, S., Boutz, P., & Natak, D. (1998). Influenza Virus nucleoprotein interacts with influenza virus polymerase proteins. *Journal of Virology, 72*(7), 5493-5501 https://doi.org/10.1128/JVI.72.7.5493-5501.1998

Blijleven, J. S., Boonstra, S., Onck, P. R., van der Giessen, E., & van Oijen, A. M. (2016). Mechanisms of influenza viral membrane fusion. *Seminars in Cell & Developmental Biology*, *60*, 78–88. https://doi.org/10.1016/j.semcdb.2016.07.007'

Bodewes, R., Morick, D., de Mutsert, G., Osinga, N., Bestebroer, T., van der Vliet, S., Smits, S. L., Kuiken, T., Rimmelzwaan, G. F., Fouchier, R. A. M., & Osterhaus, A. D. M. E. (2013). Recurring Influenza B Virus infections in seals. *Emerging Infectious Diseases*, *19*(3), 511–512. https://doi.org/10.3201/eid1903.120965

Bowie, A. G., & Unterholzner, L. (2008). Viral evasion and subversion of pattern-recognition receptor signalling. *Nature Reviews. Immunology*, *8*(12), 911–922. https://doi.org/10.1038/nri2436

Burgess, H. M., & Gray, N. K. (2012). An integrated model for the nucleo-cytoplasmic transport of cytoplasmic poly(A)-binding proteins. *Communicative & Integrative Biology*, *5*(3), 243–247. https://doi.org/10.4161/cib.19347

Burgui, I., Aragón, T., Ortín, J., & Nieto, A. (2003). PABP1 and eIF4GI associate with influenza virus NS1 protein in viral mRNA translation initiation complexes. *The Journal of General Virology*, *84*(Pt 12), 3263–3274. https://doi.org/10.1099/vir.0.19487-0

Caponigro, G., & Parker, R. (1995). Multiple functions for the poly(A)-binding protein in mRNA decapping and deadenylation in yeast. *Genes & Development*, *9*(19), 2421–2432. https://doi.org/10.1101/gad.9.19.2421

Carr, C. M., & Kim, P. S. (1993). A spring-loaded mechanism for the conformational change of influenza hemagglutinin. *Cell*, *73*(4), 823–832. https://doi.org/10.1016/0092-8674(93)90260-w

Carrillo, B., Choi, J.-M., Bornholdt, Z. A., Sankaran, B., Rice, A. P., & Prasad, B. V. V. (2014). The Influenza A Virus protein NS1 displays structural polymorphism. *Journal of Virology*, *88*(8), 4113–4122. https://doi.org/10.1128/JVI.03692-13

Chaimayo, C., Dunagan, M., Hayashi, T., Santoso, N., & Takimoto, T. (2018). Specificity and functional interplay between influenza virus PA-X and NS1 shutoff activity. *PLOS Pathogens*, *14*(11), e1007465. https://doi.org/10.1371/journal.ppat.1007465

Chakrabarti, A., Jha, B. K., & Silverman, R. H. (2011). New insights into the role of RNase L in innate immunity. *Journal of Interferon & Cytokine Research*, *31*(1), 49–57. https://doi.org/10.1089/jir.2010.0120

Chau, T.-L., Gioia, R., Gatot, J.-S., Patrascu, F., Carpentier, I., Chapelle, J.-P., O'Neill, L., Beyaert, R., Piette, J., & Chariot, A. (2008). Are the IKKs and IKK-related kinases TBK1 and IKK-ε similarly activated? *Trends in Biochemical Sciences*, *33*(4), 171–180. https://doi.org/10.1016/j.tibs.2008.01.002

Chen, W., Calvo, P. A., Malide, D., Gibbs, J., Schubert, U., Bacik, I., Basta, S., O'Neill, R., Schickli, J., Palese, P., Henklein, P., Bennink, J. R., & Yewdell, J. W. (2001). A novel influenza A virus mitochondrial protein that induces cell death. *Nature Medicine*, *7*(12), 1306–1312. https://doi.org/10.1038/nm1201-1306

Chen, Z., Li, Y., & Krug, R. M. (1999). Influenza A virus NS1 protein targets poly(A)-binding protein II of the cellular 3'-end processing machinery. *The EMBO Journal*, *18*(8), 2273–2283. https://doi.org/10.1093/emboj/18.8.2273

Chien, C., Xu, Y., Xiao, R., Aramini, J. M., Sahasrabudhe, P. V., Krug, R. M., & Montelione, G. T. (2004). Biophysical characterization of the complex between double-stranded RNA and the N-terminal domain of the NS1 protein from influenza A virus: Evidence for a novel RNA-binding mode. *Biochemistry*, *43*(7), 1950–1962. https://doi.org/10.1021/bi030176o

Ciampor, F., Thompson, C. A., Grambas, S., & Hay, A. J. (1992). Regulation of pH by the M2 protein of influenza A viruses. *Virus Research*, *22*(3), 247–258. https://doi.org/10.1016/0168-1702(92)90056-f

Compans, R. W. (1973). Influenza virus proteins: II. Association with components of the cytoplasm. *Virology*, *51*(1), 56–70. https://doi.org/10.1016/0042-6822(73)90365-6

Cros, J. F., García-Sastre, A., & Palese, P. (2005). An unconventional NLS is critical for the nuclear import of the Influenza A Virus nucleoprotein and ribonucleoprotein. *Traffic*, *6*(3), 205–213. https://doi.org/10.1111/j.1600-0854.2005.00263.x

Das, K., Ma, L.-C., Xiao, R., Radvansky, B., Aramini, J., Zhao, L., Marklund, J., Kuo, R.-L., Twu, K. Y., Arnold, E., Krug, R. M., & Montelione, G. T. (2008). Structural basis for suppression of a host antiviral response by influenza A virus. *Proceedings of the National Academy of Sciences of the United States of America*, *105*(35), 13093–13098. https://doi.org/10.1073/pnas.0805213105

de la Luna, S., Fortes, P., Beloso, A., & Ortín, J. (1995). Influenza virus NS1 protein enhances the rate of translation initiation of viral mRNAs. *Journal of Virology*, *69*(4), 2427–2433. https://doi.org/10.1128/jvi.69.4.2427-2433.1995

Desmet, E. A., Bussey, K. A., Stone, R., & Takimoto, T. (2013). Identification of the N-terminal domain of the influenza virus PA responsible for the suppression of host protein synthesis. *Journal of Virology*, *87*(6), 3108–3118. https://doi.org/10.1128/JVI.02826-12

Dey, M., Cao, C., Dar, A. C., Tamura, T., Ozato, K., Sicheri, F., & Dever, T. E. (2005). Mechanistic link between PKR dimerization, autophosphorylation, and eIF2α substrate recognition. *Cell*, *122*(6), 901–913. https://doi.org/10.1016/j.cell.2005.06.041

Dias, A., Bouvier, D., Crépin, T., McCarthy, A. A., Hart, D. J., Baudin, F., Cusack, S., & Ruigrok, R. W. H. (2009). The cap-snatching endonuclease of influenza virus polymerase resides in the PA subunit. *Nature*, *458*(7240), 914–918. https://doi.org/10.1038/nature07745

Dong, B., Xu, L., Zhou, A., Hassel, B. A., Lee, X., Torrence, P. F., & Silverman, R. H. (1994). Intrinsic molecular activities of the interferon-induced 2-5A-dependent RNase. *The Journal of Biological Chemistry*, *269*(19), 14153–14158.

Dou, D., Revol, R., Östbye, H., Wang, H., & Daniels, R. (2018). Influenza A Virus cell entry, replication, virion assembly and movement. *Frontiers in Immunology*, *9*. https://www.frontiersin.org/articles/10.3389/fimmu.2018.01581

Dubois, J., Terrier, O., & Rosa-Calatrava, M. (2014). Influenza viruses and mRNA splicing: doing more with less. *MBio*, *5*(3), e00070-14. https://doi.org/10.1128/mBio.00070-14

Egorov, A., Brandt, S., Sereinig, S., Romanova, J., Ferko, B., Katinger, D., Grassauer, A., Alexandrova, G., Katinger, H., & Muster, T. (1998). Transfectant Influenza A Viruses with long deletions in the NS1 protein grow efficiently in vero cells. *Journal of Virology*, *72*(8), 6437–6441.

Ehrhardt, C., Wolff, T., Pleschka, S., Planz, O., Beermann, W., Bode, J. G., Schmolke, M., & Ludwig, S. (2007). Influenza A Virus NS1 protein activates the PI3K/Akt pathway to mediate antiapoptotic signaling responses. *Journal of Virology*, *81*(7), 3058–3067. https://doi.org/10.1128/JVI.02082-06

Eisfeld, A. J., Kawakami, E., Watanabe, T., Neumann, G., & Kawaoka, Y. (2011). RAB11A is essential for transport of the Influenza Virus genome to the plasma membrane. *Journal of Virology*, *85*(13), 6117–6126. https://doi.org/10.1128/JVI.00378-11

Engel, S., Scolari, S., Thaa, B., Krebs, N., Korte, T., Herrmann, A., & Veit, M. (2010). FLIM-FRET and FRAP reveal association of influenza virus haemagglutinin with membrane rafts. *Biochemical Journal*, *425*(3), 567–573. https://doi.org/10.1042/BJ20091388

Fang, R., Jiang, Q., Zhou, X., Wang, C., Guan, Y., Tao, J., Xi, J., Feng, J.-M., & Jiang, Z. (2017). MAVS activates TBK1 and IKKε through TRAFs in NEMO dependent and independent manner. *PLOS Pathogens*, *13*(11), e1006720. https://doi.org/10.1371/journal.ppat.1006720

Fitzgerald, K. A., McWhirter, S. M., Faia, K. L., Rowe, D. C., Latz, E., Golenbock, D. T., Coyle, A. J., Liao, S.-M., & Maniatis, T. (2003). IKKε and TBK1 are essential components of the IRF3 signaling pathway. *Nature Immunology*, *4*(5), Article 5. https://doi.org/10.1038/ni921

Fournier, E., Moules, V., Essere, B., Paillart, J.-C., Sirbat, J.-D., Isel, C., Cavalier, A., Rolland, J.-P., Thomas, D., Lina, B., & Marquet, R. (2012). A supramolecular assembly formed by influenza A virus genomic RNA segments. *Nucleic Acids Research*, *40*(5), 2197–2209. https://doi.org/10.1093/nar/gkr985

Furusawa, Y., Yamada, S., & Kawaoka, Y. (2018). Host factor nucleoporin 93 is involved in the nuclear export of influenza virus RNA. *Frontiers in Microbiology*, *9*. https://www.frontiersin.org/articles/10.3389/fmicb.2018.01675

Gack, M. U., Albrecht, R. A., Urano, T., Inn, K.-S., Huang, I.-C., Carnero, E., Farzan, M., Inoue, S., Jung, J. U., & García-Sastre, A. (2009). Influenza A virus NS1 targets the ubiquitin ligase TRIM25 to evade recognition by RIG-I. *Cell Host & Microbe*, *5*(5), 439–449. https://doi.org/10.1016/j.chom.2009.04.006

Gack, M. U., Shin, Y. C., Joo, C.-H., Urano, T., Liang, C., Sun, L., Takeuchi, O., Akira, S., Chen, Z., Inoue, S., & Jung, J. U. (2007). TRIM25 RING-finger E3 ubiquitin ligase is essential for RIG-I-mediated antiviral activity. *Nature*, *446*(7138), 916–920. https://doi.org/10.1038/nature05732

Gaglia, M. M., Covarrubias, S., Wong, W., & Glaunsinger, B. A. (2012). A common strategy for host RNA degradation by divergent viruses. *Journal of Virology*, *86*(17), 9527–9530. https://doi.org/10.1128/JVI.01230-12

Gale, M., & Katze, M. G. (1998). Molecular mechanisms of interferon resistance mediated by viral-directed inhibition of PKR, the interferon-induced protein kinase. *Pharmacology & Therapeutics*, *78*(1), 29–46. https://doi.org/10.1016/S0163-7258(97)00165-4

García-Sastre, A., Egorov, A., Matassov, D., Brandt, S., Levy, D. E., Durbin, J. E., Palese, P., & Muster, T. (1998). Influenza A virus lacking the NS1 gene replicates in interferon-deficient systems. *Virology*, *252*(2), 324–330. https://doi.org/10.1006/viro.1998.9508

Gaucherand, L., Porter, B. K., Levene, R. E., Price, E. L., Schmaling, S. K., Rycroft, C. H., Kevorkian, Y., McCormick, C., Khaperskyy, D. A., & Gaglia, M. M. (2019). The Influenza A Virus endoribonuclease PA-X usurps host mRNA processing machinery to limit host gene expression. *Cell Reports*, *27*(3), 776-792.e7. https://doi.org/10.1016/j.celrep.2019.03.063

Gavazzi, C., Isel, C., Fournier, E., Moules, V., Cavalier, A., Thomas, D., Lina, B., & Marquet, R. (2013). An in vitro network of intermolecular interactions between viral RNA segments of an avian H5N2 influenza A virus: Comparison with a human H3N2 virus. *Nucleic Acids Research*, *41*(2), 1241–1254. https://doi.org/10.1093/nar/gks1181

Glaunsinger, B., Chavez, L., & Ganem, D. (2005). The exonuclease and host shutoff functions of the SOX protein of Kaposi's Sarcoma-Associated Herpesvirus are genetically separable. *Journal of Virology*, *79*(12), 7396–7401. https://doi.org/10.1128/JVI.79.12.7396-7401.2005

Glaunsinger, B., & Ganem, D. (2004). Lytic KSHV infection inhibits host gene expression by accelerating global mRNA turnover. *Molecular Cell*, *13*(5), 713–723. https://doi.org/10.1016/S1097-2765(04)00091-7

Gong, D., Kim, Y. H., Xiao, Y., Du, Y., Xie, Y., Lee, K. K., Feng, J., Farhat, N., Zhao, D., Shu, S., Dai, X., Chanda, S. K., Rana, T. M., Krogan, N. J., Sun, R., & Wu, T.-T. (2016). A herpesvirus protein selectively inhibits cellular mRNA nuclear export. *Cell Host & Microbe*, *20*(5), 642–653. https://doi.org/10.1016/j.chom.2016.10.004

Gray, N. K., Hrabálková, L., Scanlon, J. P., & Smith, R. W. P. (2015). Poly(A)-binding proteins and mRNA localization: Who rules the roost? *Biochemical Society Transactions*, *43*(6), 1277–1284. https://doi.org/10.1042/BST20150171

Guillot, L., Goffic, R. L., Bloch, S., Escriou, N., Akira, S., Chignard, M., & Si-Tahar, M. (2005). Involvement of Toll-like Receptor 3 in the immune response of lung epithelial cells to double-stranded RNA and Influenza A Virus *. *Journal of Biological Chemistry*, *280*(7), 5571–5580. https://doi.org/10.1074/jbc.M410592200

Häcker, H., Redecke, V., Blagoev, B., Kratchmarova, I., Hsu, L.-C., Wang, G. G., Kamps, M. P., Raz, E., Wagner, H., Häcker, G., Mann, M., & Karin, M. (2006). Specificity in Toll-like receptor signalling through distinct effector functions of TRAF3 and TRAF6. *Nature*, *439*(7073), Article 7073. https://doi.org/10.1038/nature04369

Hale, B. G. (2014). Conformational plasticity of the influenza A virus NS1 protein. *The Journal of General Virology*, *95*(Pt 10), 2099–2105. https://doi.org/10.1099/vir.0.066282-0

Hale, B. G., Randall, R. E., Ortín, J., & Jackson, D. (2008). The multifunctional NS1 protein of influenza A viruses. *The Journal of General Virology*, *89*(Pt 10), 2359–2376. https://doi.org/10.1099/vir.0.2008/004606-0

Hale, B. G., Steel, J., Medina, R. A., Manicassamy, B., Ye, J., Hickman, D., Hai, R., Schmolke, M., Lowen, A. C., Perez, D. R., & García-Sastre, A. (2010). Inefficient control of host gene expression by the 2009 pandemic H1N1 Influenza A Virus NS1 protein. *Journal of Virology*, *84*(14), 6909–6922. https://doi.org/10.1128/JVI.00081-10

Hara, K., Schmidt, F. I., Crow, M., & Brownlee, G. G. (2006). amino acid residues in the N-Terminal region of the PA subunit of Influenza A Virus RNA polymerase play a critical role in protein stability, endonuclease activity, cap binding, and virion RNA promoter binding. *Journal of Virology*, *80*(16), 7789–7798. https://doi.org/10.1128/JVI.00600-06

Hatada, E., & Fukuda, R. (1992). Binding of influenza A virus NS1 protein to dsRNA in vitro. *The Journal of General Virology*, *73 (Pt 12)*, 3325–3329. https://doi.org/10.1099/0022-1317-73-12-3325

Hayashi, T., Chaimayo, C., McGuinness, J., & Takimoto, T. (2016). Critical role of the PA-X C-terminal domain of Influenza A Virus in Its subcellular localization and shutoff activity. *Journal of Virology*, *90*(16), 7131–7141. https://doi.org/10.1128/JVI.00954-16

Hayashi, T., Chaimayo, C., & Takimoto, T. (2015). Impact of influenza PA-X on host response. *Oncotarget*, *6*(23), 19364–19365.

Hemmings, B. A., & Restuccia, D. F. (2012). PI3K-PKB/Akt pathway. *Cold Spring Harbor Perspectives in Biology*, *4*(9), a011189. https://doi.org/10.1101/cshperspect.a011189

Hett, A., & West, S. (2014). Inhibition of U4 snRNA in human cells causes the stable retention of polyadenylated pre-mRNA in the nucleus. *PLOS ONE*, *9*(5), e96174. https://doi.org/10.1371/journal.pone.0096174

Hom, N., Gentles, L., Bloom, J. D., & Lee, K. K. (2019). deep mutational scan of the highly conserved Influenza A Virus M1 matrix protein reveals substantial intrinsic mutational tolerance. *Journal of Virology*, *93*(13), e00161-19. https://doi.org/10.1128/JVI.00161-19

Hosoda, N., Lejeune, F., & Maquat, L. E. (2006). Evidence that poly(A) binding protein C1 binds nuclear pre-mrna poly(A) tails. *Molecular and Cellular Biology*, *26*(8), 3085–3097. https://doi.org/10.1128/MCB.26.8.3085-3097.2006

Hou, F., Sun, L., Zheng, H., Skaug, B., Jiang, Q.-X., & Chen, Z. J. (2011). MAVS forms functional prion-like aggregates to activate and propagate antiviral innate immune response. *Cell*, *146*(3), 448–461. https://doi.org/10.1016/j.cell.2011.06.041

Hrincius, E. R., Hennecke, A.-K., Gensler, L., Nordhoff, C., Anhlan, D., Vogel, P., McCullers, J. A., Ludwig, S., & Ehrhardt, C. (2012). A single point mutation (Y89F) within the non-structural protein 1 of Influenza A Viruses limits epithelial cell tropism and virulence in mice. *The American Journal of Pathology*, *180*(6), 2361–2374. https://doi.org/10.1016/j.ajpath.2012.02.029

Hussain, S., Turnbull, M. L., Wise, H. M., Jagger, B. W., Beard, P. M., Kovacikova, K., Taubenberger, J. K., Vervelde, L., Engelhardt, O. G., & Digard, P. (2019). mutation of Influenza A Virus PA-X decreases pathogenicity in chicken embryos and can increase the yield of reassortant candidate vaccine viruses. *Journal of Virology*, *93*(2), e01551-18. https://doi.org/10.1128/JVI.01551-18

Jagger, B. W., Wise, H. M., Kash, J. C., Walters, K.-A., Wills, N. M., Xiao, Y.-L., Dunfee, R. L., Schwartzman, L. M., Ozinsky, A., Bell, G. L., Dalton, R. M., Lo, A., Efstathiou, S., Atkins, J. F., Firth, A. E., Taubenberger, J. K., & Digard, P. (2012). An overlapping protein-coding region in Influenza A Virus segment 3 modulates the host response. *Science (New York, N.Y.)*, *337*(6091), 199–204. https://doi.org/10.1126/science.1222213

Jänicke, A., Vancuylenberg, J., Boag, P. R., Traven, A., & Beilharz, T. H. (2012). ePAT: A simple method to tag adenylated RNA to measure poly(A)-tail length and other 3′ RACE applications. *RNA*, *18*(6), 1289–1295. https://doi.org/10.1261/rna.031898.111

Jiang, F., Ramanathan, A., Miller, M. T., Tang, G.-Q., Gale, M., Patel, S. S., & Marcotrigiano, J. (2011). Structural basis of RNA recognition and activation by innate immune receptor RIG-I. *Nature*, *479*(7373), 423–427. https://doi.org/10.1038/nature10537

Jureka, A. S., Kleinpeter, A. B., Tipper, J. L., Harrod, K. S., & Petit, C. M. (2020). The influenza NS1 protein modulates RIG-I activation via a strain-specific direct interaction with the second CARD of RIG-I. *Journal of Biological Chemistry*, *295*(4), 1153–1164. https://doi.org/10.1016/S0021-9258(17)49923-6

Karasik, A., Jones, G. D., DePass, A. V., & Guydosh, N. R. (2021). Activation of the antiviral factor RNase L triggers translation of non-coding mRNA sequences. *Nucleic Acids Research*, *49*(11), 6007–6026. https://doi.org/10.1093/nar/gkab036

Kathum, O. A., Schräder, T., Anhlan, D., Nordhoff, C., Liedmann, S., Pande, A., Mellmann, A., Ehrhardt, C., Wixler, V., & Ludwig, S. (2016). Phosphorylation of influenza A virus NS1 protein at threonine 49 suppresses its interferon antagonistic activity. *Cellular Microbiology*, *18*(6), 784–791. https://doi.org/10.1111/cmi.12559

Kato, H., Takeuchi, O., Sato, S., Yoneyama, M., Yamamoto, M., Matsui, K., Uematsu, S., Jung, A., Kawai, T., Ishii, K. J., Yamaguchi, O., Otsu, K., Tsujimura, T., Koh, C.-S., Reis e Sousa, C., Matsuura, Y., Fujita, T., & Akira, S. (2006). Differential roles of MDA5 and RIG-I helicases in the recognition of RNA viruses. *Nature*, *441*(7089), 101–105. https://doi.org/10.1038/nature04734

Kerry, P., Ayllon, J., Taylor, M., Hass, C., Lewis, A., García-Sastre, A., Randall, R., Hale, B., & Russell, R. (2011). A transient homotypic interaction model for the Influenza A Virus NS1 protein effector domain. *PloS One*, *6*, e17946. https://doi.org/10.1371/journal.pone.0017946

Khaperskyy, D. A., Emara, M. M., Johnston, B. P., Anderson, P., Hatchette, T. F., & McCormick, C. (2014). Influenza A Virus host shutoff disables antiviral stress-induced translation arrest. *PLoS Pathogens*, *10*(7), e1004217. https://doi.org/10.1371/journal.ppat.1004217

Khaperskyy, D. A., Hatchette, T. F., & McCormick, C. (2012). Influenza A virus inhibits cytoplasmic stress granule formation. *The FASEB Journal*, *26*(4), 1629–1639. https://doi.org/10.1096/fj.11-196915

Khaperskyy, D. A., Schmaling, S., Larkins-Ford, J., McCormick, C., & Gaglia, M. M. (2016). Selective degradation of host RNA Polymerase II transcripts by Influenza A Virus PA-X host shutoff protein. *PLOS Pathogens*, *12*(2), e1005427. https://doi.org/10.1371/journal.ppat.1005427

Kida, H., Ito, T., Yasuda, J., Shimizu, Y., Itakura, C., Shortridge, K. F., Kawaoka, Y., & Webster, R. G. Y. 1994. (1994). Potential for transmission of avian influenza viruses to pigs. *Journal of General Virology*, *75*(9), 2183–2188. https://doi.org/10.1099/0022-1317-75-9-2183

Kim, H. J., Jeong, M. S., & Jang, S. B. (2021). Structure and activities of the NS1 influenza protein and progress in the development of small-molecule drugs. *International Journal of Molecular Sciences*, *22*(8), 4242. https://doi.org/10.3390/ijms22084242

Kim, S. J., Fernandez-Martinez, J., Nudelman, I., Shi, Y., Zhang, W., Raveh, B., Herricks, T., Slaughter, B. D., Hogan, J., Upla, P., Chemmama, I. E., Pellarin, R., Echeverria, I., Shivaraju, M., Chaudhury, A. S., Wang, J., Williams, R., Unruh, J. R., Greenberg, C. H., … Rout, M. P. (2018). Integrative structure and functional anatomy of a nuclear pore complex. *Nature*, *555*(7697), 475–482. https://doi.org/10.1038/nature26003

Klemm, C., Boergeling, Y., Ludwig, S., & Ehrhardt, C. (2018). Immunomodulatory nonstructural proteins of Influenza A Viruses. *Trends in Microbiology*, *26*(7), 624–636. https://doi.org/10.1016/j.tim.2017.12.006

Kowalinski, E., Lunardi, T., McCarthy, A. A., Louber, J., Brunel, J., Grigorov, B., Gerlier, D., & Cusack, S. (2011). Structural basis for the activation of innate immune pattern-recognition receptor RIG-I by viral RNA. *Cell*, *147*(2), 423–435. https://doi.org/10.1016/j.cell.2011.09.039

Krug, R. M. (2015). Functions of the Influenza A Virus NS1 protein in antiviral defense. *Current Opinion in Virology*, *12*, 1–6. https://doi.org/10.1016/j.coviro.2015.01.007

Krug, R. M., & Etkind, P. R. (1973). Cytoplasmic and nuclear virus-specific proteins in influenza virus-infected MDCK cells. *Virology*, *56*(1), 334–348. https://doi.org/10.1016/0042-6822(73)90310-3

Kühn, U., Gündel, M., Knoth, A., Kerwitz, Y., Rüdel, S., & Wahle, E. (2009). Poly(A) tail length is controlled by the nuclear poly(A)-binding protein regulating the interaction between poly(A) polymerase and the cleavage and polyadenylation specificity factor. *Journal of Biological Chemistry*, *284*(34), 22803–22814. https://doi.org/10.1074/jbc.M109.018226

Kumar, G. R., & Glaunsinger, B. A. (2010). Nuclear import of cytoplasmic poly(A) binding protein restricts gene expression via hyperadenylation and nuclear retention of mRNA. *Molecular and Cellular Biology*, *30*(21), 4996–5008. https://doi.org/10.1128/MCB.00600-10

Kumar, G. R., Shum, L., & Glaunsinger, B. A. (2011). Importin α-mediated nuclear import of cytoplasmic poly(A) binding protein occurs as a direct consequence of cytoplasmic mRNA depletion. *Molecular and Cellular Biology*, *31*(15), 3113–3125. https://doi.org/10.1128/MCB.05402-11

LaCava, J., Houseley, J., Saveanu, C., Petfalski, E., Thompson, E., Jacquier, A., & Tollervey, D. (2005). RNA degradation by the exosome is promoted by a nuclear polyadenylation complex. *Cell*, *121*(5), 713–724. https://doi.org/10.1016/j.cell.2005.04.029

Lamb, R. A., & Lai, C. J. (1980). Sequence of interrupted and uninterrupted mRNAs and cloned DNA coding for the two overlapping nonstructural proteins of influenza virus. *Cell*, *21*(2), 475–485. https://doi.org/10.1016/0092-8674(80)90484-5

Lamotte, L.-A., & Tafforeau, L. (2021). How Influenza A Virus NS1 deals with the ubiquitin system to evade innate immunity. *Viruses*, *13*(11), Article 11. https://doi.org/10.3390/v13112309

Le Goffic, R., Pothlichet, J., Vitour, D., Fujita, T., Meurs, E., Chignard, M., & Si-Tahar, M. (2007). Cutting edge: Influenza A Virus activates TLR3-dependent inflammatory and RIG-I-dependent antiviral responses in human lung epithelial cells. *The Journal of Immunology*, *178*(6), 3368–3372. https://doi.org/10.4049/jimmunol.178.6.3368

Le Sage, V., Kanarek, J. P., Snyder, D. J., Cooper, V. S., Lakdawala, S. S., & Lee, N. (2020). Mapping of influenza virus RNA-rna interactions reveals a flexible network. *Cell Reports*, *31*(13), 107823. https://doi.org/10.1016/j.celrep.2020.107823

Le Sage, V., Nanni, A. V., Bhagwat, A. R., Snyder, D. J., Cooper, V. S., Lakdawala, S. S., & Lee, N. (2018). Non-uniform and non-random binding of nucleoprotein to Influenza A and B viral RNA. *Viruses*, *10*(10), 522. https://doi.org/10.3390/v10100522

Lee, M.-C., Yu, C.-P., Chen, X.-H., Liu, M.-T., Yang, J.-R., Chen, A.-Y., & Huang, C.-H. (2022). Influenza A virus NS1 protein represses antiviral immune response by hijacking NF-κB to mediate transcription of type III IFN. *Frontiers in Cellular and Infection Microbiology*, *12*. https://www.frontiersin.org/articles/10.3389/fcimb.2022.998584

Lee, N., Le Sage, V., Nanni, A. V., Snyder, D. J., Cooper, V. S., & Lakdawala, S. S. (2017). Genome-wide analysis of influenza viral RNA and nucleoprotein association. *Nucleic Acids Research*, *45*(15), 8968–8977. https://doi.org/10.1093/nar/gkx584

Lee, Y. J., & Glaunsinger, B. A. (2009). Aberrant herpesvirus-induced polyadenylation correlates with cellular messenger RNA destruction. *PLoS Biology*, *7*(5), e1000107. https://doi.org/10.1371/journal.pbio.1000107

Leser, G. P., & Lamb, R. A. (2005). Influenza virus assembly and budding in raft-derived microdomains: A quantitative analysis of the surface distribution of HA, NA and M2 proteins. *Virology*, *342*(2), 215–227. https://doi.org/10.1016/j.virol.2005.09.049

Li, S., Min, J.-Y., Krug, R. M., & Sen, G. C. (2006). Binding of the influenza A virus NS1 protein to PKR mediates the inhibition of its activation by either PACT or double-stranded RNA. *Virology*, *349*(1), 13–21. https://doi.org/10.1016/j.virol.2006.01.005

Li, W., Wang, G., Zhang, H., Shen, Y., Dai, J., Wu, L., Zhou, J., Jiang, Z., & Li, K. (2012). Inability of NS1 protein from an H5N1 influenza virus to activate PI3K/Akt signaling pathway correlates to the enhanced virus replication upon PI3K inhibition. *Veterinary Research*, *43*(1), 36. https://doi.org/10.1186/1297-9716-43-36

Li, Y., Banerjee, S., Wang, Y., Goldstein, S. A., Dong, B., Gaughan, C., Silverman, R. H., & Weiss, S. R. (2016). Activation of RNase L is dependent on OAS3 expression during infection with diverse human viruses. *Proceedings of the National Academy of Sciences*, *113*(8), 2241–2246. https://doi.org/10.1073/pnas.1519657113

Ling, Y.-H., Wang, H., Han, M.-Q., Wang, D., Hu, Y.-X., Zhou, K., & Li, Y. (2022). Nucleoporin 85 interacts with influenza A virus PB1 and PB2 to promote its replication by facilitating nuclear import of ribonucleoprotein. *Frontiers in Microbiology*, *13*. https://www.frontiersin.org/articles/10.3389/fmicb.2022.895779

Liu, S., Chen, J., Cai, X., Wu, J., Chen, X., Wu, Y.-T., Sun, L., & Chen, Z. J. (2013). MAVS recruits multiple ubiquitin E3 ligases to activate antiviral signaling cascades. *ELife*, *2*, e00785. https://doi.org/10.7554/eLife.00785

Loo, Y.-M., Fornek, J., Crochet, N., Bajwa, G., Perwitasari, O., Martinez-Sobrido, L., Akira, S., Gill, M. A., García-Sastre, A., Katze, M. G., & Gale, M. (2008). Distinct RIG-I and MDA5 signaling by RNA viruses in innate immunity. *Journal of Virology*, *82*(1), 335–345. https://doi.org/10.1128/JVI.01080-07

Lu, Y., Qian, X. Y., & Krug, R. M. (1994). The influenza virus NS1 protein: A novel inhibitor of pre-mRNA splicing. *Genes & Development*, *8*(15), 1817–1828. https://doi.org/10.1101/gad.8.15.1817

Lund, J. M., Alexopoulou, L., Sato, A., Karow, M., Adams, N. C., Gale, N. W., Iwasaki, A., & Flavell, R. A. (2004). Recognition of single-stranded RNA viruses by Toll-like receptor 7. *Proceedings of the National Academy of Sciences*, *101*(15), 5598–5603. https://doi.org/10.1073/pnas.0400937101

Luo, G. X., Luytjes, W., Enami, M., & Palese, P. (1991). The polyadenylation signal of influenza virus RNA involves a stretch of uridines followed by the RNA duplex of the panhandle structure. *Journal of Virology*, *65*(6), 2861. https://doi.org/10.1128/jvi.65.6.2861-2867.1991

Ma, J., Wu, R., Xu, G., Cheng, Y., Wang, Z., Wang, H., Yan, Y., Li, J., & Sun, J. (2020). Acetylation at K108 of the NS1 protein is important for the replication and virulence of influenza virus. *Veterinary Research*, *51*(1), 20. https://doi.org/10.1186/s13567-020-00747-3

Matrosovich, M., Tuzikov, A., Bovin, N., Gambaryan, A., Klimov, A., Castrucci, M. R., Donatelli, I., & Kawaoka, Y. (2000). early alterations of the receptor-binding properties of H1, H2, and H3 avian influenza virus hemagglutinins after their introduction into mammals. *Journal of Virology*, *74*(18), 8502–8512. https://doi.org/10.1128/JVI.74.18.8502-8512.2000

Mazewski, C., Perez, R. E., Fish, E. N., & Platanias, L. C. (2020). Type I Interferon (IFN)-regulated activation of canonical and non-canonical signaling pathways. *Frontiers in Immunology*, *11*. https://www.frontiersin.org/articles/10.3389/fimmu.2020.606456

Meyerson, N. R., Zhou, L., Guo, Y. R., Zhao, C., Tao, Y. J., Krug, R. M., & Sawyer, S. L. (2017). Nuclear TRIM25 specifically targets influenza virus ribonucleoproteins to block the onset of RNA chain elongation. *Cell Host & Microbe*, *22*(5), 627-638.e7. https://doi.org/10.1016/j.chom.2017.10.003

Mifsud, E. J., Kuba, M., & Barr, I. G. (2021). innate immune responses to influenza virus infections in the upper respiratory tract. *Viruses*, *13*(10), 2090. https://doi.org/10.3390/v13102090

Min, J.-Y., Li, S., Sen, G. C., & Krug, R. M. (2007). A site on the influenza A virus NS1 protein mediates both inhibition of PKR activation and temporal regulation of viral RNA synthesis. *Virology*, *363*(1), 236–243. https://doi.org/10.1016/j.virol.2007.01.038

Nacken, W., Schreiber, A., Masemann, D., & Ludwig, S. (2021). the effector domain of the Influenza A Virus nonstructural protein NS1 triggers host shutoff by mediating inhibition and global deregulation of host transcription when associated with specific structures in the nucleus. *MBio*, *12*(5), e02196-21. https://doi.org/10.1128/mBio.02196-21

Nakajima, K., Desselberger, U., & Palese, P. (1978). Recent human influenza A (H1N1) viruses are closely related genetically to strains isolated in 1950. *Nature*, *274*(5669), Article 5669. https://doi.org/10.1038/274334a0

Nemeroff, M. E., Barabino, S. M. L., Li, Y., Keller, W., & Krug, R. M. (1998). Influenza virus NS1 protein interacts with the cellular 30 kda subunit of CPSF and inhibits 3′ end formation of cellular pre-mRNAs. *Molecular Cell*, *1*(7), 991–1000. https://doi.org/10.1016/S1097-2765(00)80099-4

Neumann, G., Noda, T., & Kawaoka, Y. (2009). Emergence and pandemic potential of swine-origin H1N1 influenza virus. *Nature*, *459*(7249), 931–939. https://doi.org/10.1038/nature08157

Newcomb, L. L., Kuo, R.-L., Ye, Q., Jiang, Y., Tao, Y. J., & Krug, R. M. (2009). Interaction of the Influenza A Virus nucleocapsid protein with the viral RNA polymerase potentiates unprimed viral RNA replication. *Journal of Virology*, *83*(1), 29–36. https://doi.org/10.1128/JVI.02293-07

Nunes-Correia, I., Eulálio, A., Nir, S., & Pedroso de Lima, M. (2004). Caveolae as an additional route for influenza virus endocytosis in MDCK cells. *Cellular & Molecular Biology Letters*, *9*(1). https://pubmed.ncbi.nlm.nih.gov/15048150/?dopt=Abstract

Oishi, K., Yamayoshi, S., Kozuka-Hata, H., Oyama, M., & Kawaoka, Y. (2018). N-terminal acetylation by NatB is required for the shutoff activity of influenza A virus PA-X. *Cell Reports*, *24*(4), 851–860. https://doi.org/10.1016/j.celrep.2018.06.078

O'Neill, R. E., Jaskunas, R., Blobel, G., Palese, P., & Moroianu, J. (1995). Nuclear import of influenza virus RNA can be mediated by viral nucleoprotein and transport factors required for protein import. *Journal of Biological Chemistry*, *270*(39), 22701–22704. https://doi.org/10.1074/jbc.270.39.22701

Oshiumi, H., Miyashita, M., Inoue, N., Okabe, M., Matsumoto, M., & Seya, T. (2010). The ubiquitin ligase Riplet is essential for RIG-I-dependent innate immune responses to RNA virus infection. *Cell Host & Microbe*, *8*(6), 496–509. https://doi.org/10.1016/j.chom.2010.11.008

Oshiumi, H., Miyashita, M., Matsumoto, M., & Seya, T. (2013). A distinct role of Riplet-Mediated K63-linked polyubiquitination of the RIG-I repressor domain in human antiviral innate immune responses. *PLOS Pathogens*, *9*(8), e1003533. https://doi.org/10.1371/journal.ppat.1003533

Pal, S., Santos, A., Rosas, J. M., Ortiz-Guzman, J., & Rosas-Acosta, G. (2011). Influenza A virus interacts extensively with the cellular SUMOylation system during infection. *Virus Research*, *158*(1–2), 12–27. https://doi.org/10.1016/j.virusres.2011.02.017

Park, E.-H., Walker, S. E., Lee, J. M., Rothenburg, S., Lorsch, J. R., & Hinnebusch, A. G. (2011). Multiple elements in the eIF4G1 N-terminus promote assembly of eIF4G1•PABP mRNPs in vivo. *The EMBO Journal*, *30*(2), 302–316. https://doi.org/10.1038/emboj.2010.312

Parry, J. (2013). H7N9 avian flu infects humans for the first time. *BMJ (Clinical Research Ed.)*, *346*, f2151. https://doi.org/10.1136/bmj.f2151

Patel, R. C., & Sen, G. C. (1998). PACT, a protein activator of the interferon-induced protein kinase, PKR. *The EMBO Journal*, *17*(15), 4379–4390. https://doi.org/10.1093/emboj/17.15.4379

Paterson, D., & Fodor, E. (2012). Emerging roles for the Influenza A Virus nuclear export protein (NEP). *PLoS Pathogens*, *8*(12), e1003019. https://doi.org/10.1371/journal.ppat.1003019

Pemberton, L. F., & Paschal, B. M. (2005). Mechanisms of receptor-mediated nuclear import and nuclear export. *Traffic*, *6*(3), 187–198. https://doi.org/10.1111/j.1600-0854.2005.00270.x

Pflug, A., Guilligay, D., Reich, S., & Cusack, S. (2014). Structure of influenza A polymerase bound to the viral RNA promoter. *Nature*, *516*(7531), 355–360. https://doi.org/10.1038/nature14008

Platanias, L. C. (2005). Mechanisms of type-I- and type-II-interferon-mediated signalling. *Nature Reviews Immunology*, *5*(5), Article 5. https://doi.org/10.1038/nri1604

Qiu, Y., & Krug, R. M. (1994). The influenza virus NS1 protein is a poly(A)-binding protein that inhibits nuclear export of mRNAs containing poly(A). *Journal of Virology*, *68*(4), 2425–2432. https://doi.org/10.1128/JVI.68.4.2425-2432.1994

Qiu, Y., Nemeroff, M., & Krug, R. M. (1995). The influenza virus NS1 protein binds to a specific region in human U6 snRNA and inhibits U6-U2 and U6-U4 snRNA interactions during splicing. *RNA (New York, N.Y.)*, *1*(3), 304–316.

Rahim, M. M. A., Parsons, B. D., Price, E. L., Slaine, P. D., Chilvers, B. L., Seaton, G. S., Wight, A., Medina-Luna, D., Dey, S., Grandy, S. L., Anderson, L. E., Zamorano Cuervo, N., Grandvaux, N., Gaglia, M. M., Kelvin, A. A., Khaperskyy, D. A., McCormick, C., & Makrigiannis, A. P. (2020). Defective Influenza A Virus RNA products mediate MAVS-dependent upregulation of human leukocyte antigen class I proteins. *Journal of Virology*, *94*(13), e00165-20. https://doi.org/10.1128/JVI.00165-20

Rahim, M. N., Selman, M., Sauder, P. J., Forbes, N. E., Stecho, W., Xu, W., Lebar, M., Brown, E. G., & Coombs, K. M. Y. (2013). Generation and characterization of a new panel of broadly reactive anti-NS1 mAbs for detection of influenza A virus. *Journal of General Virology*, *94*(3), 593–605. https://doi.org/10.1099/vir.0.046649-0

Rajsbaum, R., Albrecht, R. A., Wang, M. K., Maharaj, N. P., Versteeg, G. A., Nistal-Villán, E., García-Sastre, A., & Gack, M. U. (2012). Species-specific inhibition of RIG-I ubiquitination and IFN induction by the influenza A virus NS1 protein. *PLoS Pathogens*, *8*(11), e1003059. https://doi.org/10.1371/journal.ppat.1003059

Rehwinkel, J., & Gack, M. U. (2020). RIG-I-like receptors: Their regulation and roles in RNA sensing. *Nature Reviews Immunology*, *20*(9), Article 9. https://doi.org/10.1038/s41577-020-0288-3

Ren, Z., Ding, T., Zuo, Z., Xu, Z., Deng, J., & Wei, Z. (2020). Regulation of MAVS expression and signaling function in the antiviral innate immune response. *Frontiers in Immunology*, *11*. https://www.frontiersin.org/articles/10.3389/fimmu.2020.01030

Rigby, R. E., Wise, H. M., Smith, N., Digard, P., & Rehwinkel, J. (2019). PA-X antagonises MAVS-dependent accumulation of early type I interferon messenger RNAs during influenza A virus infection. *Scientific Reports*, *9*(1), Article 1. https://doi.org/10.1038/s41598-019-43632-6

Rogers, G. N., & Paulson, J. C. (1983). Receptor determinants of human and animal influenza virus isolates: Differences in receptor specificity of the H3 hemagglutinin based on species of origin. *Virology*, *127*(2), 361–373. https://doi.org/10.1016/0042-6822(83)90150-2

Santos, A., Pal, S., Chacón, J., Meraz, K., Gonzalez, J., Prieto, K., & Rosas-Acosta, G. (2013). SUMOylation affects the interferon blocking activity of the Influenza A Nonstructural Protein NS1 without affecting its stability or cellular localization. *Journal of Virology*, *87*(10), 5602–5620. https://doi.org/10.1128/JVI.02063-12

Sarkar, D. P., Morris, S. J., Eidelman, O., Zimmerberg, J., & Blumenthal, R. (1989). Initial stages of influenza hemagglutinin-induced cell fusion monitored simultaneously by two fluorescent events: Cytoplasmic continuity and lipid mixing. *The Journal of Cell Biology*, *109*(1), 113–122. https://doi.org/10.1083/jcb.109.1.113

Satoh, T., Kato, H., Kumagai, Y., Yoneyama, M., Sato, S., Matsushita, K., Tsujimura, T., Fujita, T., Akira, S., & Takeuchi, O. (2010). LGP2 is a positive regulator of RIG-I- and MDA5-mediated antiviral responses. *Proceedings of the National Academy of Sciences of the United States of America*, *107*(4), 1512–1517. https://doi.org/10.1073/pnas.0912986107

Scheiffele, P., Roth, M. G., & Simons, K. (1997). Interaction of influenza virus haemagglutinin with sphingolipid-cholesterol membrane domains via its transmembrane domain. *The EMBO Journal*, *16*(18), 5501–5508. https://doi.org/10.1093/emboj/16.18.5501

Seng, L.-G., Daly, J., Chang, K.-C., & Kuchipudi, S. V. (2014). High basal expression of interferon-stimulated genes in human bronchial epithelial (BEAS-2B) cells contributes to Influenza A Virus resistance. *PLoS ONE*, *9*(10), e109023. https://doi.org/10.1371/journal.pone.0109023

Seth, R. B., Sun, L., Ea, C.-K., & Chen, Z. J. (2005). Identification and characterization of MAVS, a mitochondrial antiviral signaling protein that activates NF-κB and IRF3. *Cell*, *122*(5), 669–682. https://doi.org/10.1016/j.cell.2005.08.012

Shi, M., Jagger, B. W., Wise, H. M., Digard, P., Holmes, E. C., & Taubenberger, J. K. (2012). Evolutionary conservation of the PA-X open reading frame in segment 3 of Influenza A Virus. *Journal of Virology*, *86*(22), 12411–12413. https://doi.org/10.1128/JVI.01677-12

Shih, S. R., Nemeroff, M. E., & Krug, R. M. (1995). The choice of alternative 5' splice sites in influenza virus M1 mRNA is regulated by the viral polymerase complex. *Proceedings of the National Academy of Sciences of the United States of America*, *92*(14), 6324–6328.

Shu, M., Taddeo, B., Zhang, W., & Roizman, B. (2013). Selective degradation of mRNAs by the HSV host shutoff RNase is regulated by the UL47 tegument protein. *Proceedings of the National Academy of Sciences*, *110*(18), E1669–E1675. https://doi.org/10.1073/pnas.1305475110

Sonnberg, S., Webby, R. J., & Webster, R. G. (2013). 2.1 Natural history of highly pathogenic avian influenza H5N1. *Virus Research*, *178*(1), 10.1016/j.virusres.2013.05.009. https://doi.org/10.1016/j.virusres.2013.05.009

Sorokin, A. V., Kim, E. R., & Ovchinnikov, L. P. (2007). Nucleocytoplasmic transport of proteins. *Biochemistry*, *72*(13), 1439–1457. https://doi.org/10.1134/S0006297907130032

Stewart, M. (2010). Nuclear export of mRNA. *Trends in Biochemical Sciences*, *35*(11), 609–617. https://doi.org/10.1016/j.tibs.2010.07.001

Talon, J., Horvath, C. M., Polley, R., Basler, C. F., Muster, T., Palese, P., & García-Sastre, A. (2000). Activation of Interferon Regulatory Factor 3 Is inhibited by the Influenza A Virus NS1 protein. *Journal of Virology*, *74*(17), 7989–7996. https://doi.org/10.1128/JVI.74.17.7989-7996.2000

Tang, Y., Zhong, G., Zhu, L., Liu, X., Shan, Y., Feng, H., Bu, Z., Chen, H., & Wang, C. (2010). Herc5 attenuates influenza A virus by catalyzing ISGylation of viral NS1 protein. *Journal of Immunology (Baltimore, Md.: 1950)*, *184*(10), 5777–5790. https://doi.org/10.4049/jimmunol.0903588

Tristan, C., Shahani, N., Sedlak, T. W., & Sawa, A. (2011). The diverse functions of GAPDH: Views from different subcellular compartments. *Cellular Signalling*, *23*(2), 317–323. https://doi.org/10.1016/j.cellsig.2010.08.003

Tynell, J., Melén, K., & Julkunen, I. (2014). Mutations within the conserved NS1 nuclear export signal lead to inhibition of influenza A virus replication. *Virology Journal*, *11*(1), 128. https://doi.org/10.1186/1743-422X-11-128

Wahle, E. (1991). A novel poly(A)-binding protein acts as a specificity factor in the second phase of messenger RNA polyadenylation. *Cell*, *66*(4), 759–768. https://doi.org/10.1016/0092-8674(91)90119-j

Wang, W., Riedel, K., Lynch, P., Chien, C. Y., Montelione, G. T., & Krug, R. M. (1999). RNA binding by the novel helical domain of the influenza virus NS1 protein requires its dimer structure and a small number of specific basic amino acids. *RNA*, *5*(2), 195–205.

Webster, R. G., Bean, W. J., Gorman, O. T., Chambers, T. M., & Kawaoka, Y. (1992). Evolution and ecology of influenza A viruses. *Microbiological Reviews*, *56*(1), 152–179.

Wegener, M., & Müller-McNicoll, M. (2018). Nuclear retention of mRNAs – quality control, gene regulation and human disease. *Seminars in Cell & Developmental Biology*, *79*, 131–142. https://doi.org/10.1016/j.semcdb.2017.11.001

Wells, S. E., Hillner, P. E., Vale, R. D., & Sachs, A. B. (1998). Circularization of mRNA by eukaryotic translation initiation factors. *Molecular Cell*, *2*(1), 135–140. https://doi.org/10.1016/s1097-2765(00)80122-7

Williams, B. R. (1999). PKR; a sentinel kinase for cellular stress. *Oncogene*, *18*(45), Article 45. https://doi.org/10.1038/sj.onc.1203127

Williams, G. D., Townsend, D., Wylie, K. M., Kim, P. J., Amarasinghe, G. K., Kutluay, S. B., & Boon, A. C. M. (2018). Nucleotide resolution mapping of influenza A virus nucleoprotein-RNA interactions reveals RNA features required for replication. *Nature Communications*, *9*, 465. https://doi.org/10.1038/s41467-018-02886-w

Wilusz, J. E., Freier, S. M., & Spector, D. L. (2008). 3' end processing of a long nuclear-retained non-coding RNA yields a tRNA-like cytoplasmic RNA. *Cell*, *135*(5), 919–932. https://doi.org/10.1016/j.cell.2008.10.012

Wu, B., & Hur, S. (2015). How RIG-I like receptors activate MAVS. *Current Opinion in Virology*, *12*, 91–98. https://doi.org/10.1016/j.coviro.2015.04.004

Wu, W. W., Sun, Y.-H. B., & Panté, N. (2007). Nuclear import of Influenza A viral ribonucleoprotein complexes is mediated by two nuclear localization sequences on viral nucleoprotein. *Virology Journal*, *4*(1), 49. https://doi.org/10.1186/1743-422X-4-49

Xu, K., Klenk, C., Liu, B., Keiner, B., Cheng, J., Zheng, B.-J., Li, L., Han, Q., Wang, C., Li, T., Chen, Z., Shu, Y., Liu, J., Klenk, H.-D., & Sun, B. (2011). Modification of Nonstructural protein 1 of Influenza A Virus by SUMO1. *Journal of Virology*, *85*(2), 1086–1098. https://doi.org/10.1128/JVI.00877-10

Yamamoto, M., Sato, S., Hemmi, H., Hoshino, K., Kaisho, T., Sanjo, H., Takeuchi, O., Sugiyama, M., Okabe, M., Takeda, K., & Akira, S. (2003). Role of adaptor TRIF in the MyD88-Independent toll-like receptor signaling pathway. *Science*, *301*(5633), 640–643. https://doi.org/10.1126/science.1087262

Yángüez, E., & Nieto, A. (2011). So similar, yet so different: Selective translation of capped and polyadenylated viral mRNAs in the influenza virus infected cell. *Virus Research*, *156*(1), 1–12. https://doi.org/10.1016/j.virusres.2010.12.016

Yoneyama, M., Kikuchi, M., Natsukawa, T., Shinobu, N., Imaizumi, T., Miyagishi, M., Taira, K., Akira, S., & Fujita, T. (2004). The RNA helicase RIG-I has an essential function in double-stranded RNA-induced innate antiviral responses. *Nature Immunology*, *5*(7), Article 7. https://doi.org/10.1038/ni1087

York, A., & Fodor, E. (2013). Biogenesis, assembly, and export of viral messenger ribonucleoproteins in the influenza A virus infected cell. *RNA Biology*, *10*(8), 1274–1282. https://doi.org/10.4161/rna.25356

York, A., Hengrung, N., Vreede, F. T., Huiskonen, J. T., & Fodor, E. (2013). Isolation and characterization of the positive-sense replicative intermediate of a negative-strand RNA virus. *Proceedings of the National Academy of Sciences of the United States of America*, *110*(45), E4238–E4245. https://doi.org/10.1073/pnas.1315068110

Yuan, S., Balaji, S., Lomakin, I. B., & Xiong, Y. (2021). Coronavirus Nsp1: immune response suppression and protein expression inhibition. *Frontiers in Microbiology*, *12*. https://www.frontiersin.org/articles/10.3389/fmicb.2021.752214

Zenner, H. L., Mauricio, R., Banting, G., & Crump, C. M. (2013). Herpes Simplex Virus 1 counteracts tetherin restriction via its virion host shutoff activity. *Journal of Virology*, *87*(24), 13115–13123. https://doi.org/10.1128/JVI.02167-13

Zhang, K., Miorin, L., Makio, T., Dehghan, I., Gao, S., Xie, Y., Zhong, H., Esparza, M., Kehrer, T., Kumar, A., Hobman, T. C., Ptak, C., Gao, B., Minna, J. D., Chen, Z., García-Sastre, A., Ren, Y., Wozniak, R. W., & Fontoura, B. M. A. (2021a). Nsp1 protein of SARS-CoV-2 disrupts the mRNA export machinery to inhibit host gene expression. *Science Advances*, *7*(6), eabe7386. https://doi.org/10.1126/sciadv.abe7386

Zhang, K., Xie, Y., Muñoz-Moreno, R., Wang, J., Zhang, L., Esparza, M., García-Sastre, A., Fontoura, B. M. A., & Ren, Y. (2019). Structural basis for influenza virus NS1 protein block of mRNA nuclear export. *Nature Microbiology*, *4*(10), 1671–1679. https://doi.org/10.1038/s41564-019-0482-x

Zhang, M., Li, J., Yan, H., Huang, J., Wang, F., Liu, T., Zeng, L., & Zhou, F. (2021b). ISGylation in innate antiviral immunity and pathogen defense responses: a review. *Frontiers in Cell and Developmental Biology*, *9*. https://www.frontiersin.org/articles/10.3389/fcell.2021.788410

Zhang, X., Hamblin, M. H., & Yin, K.-J. (2017). The long noncoding RNA MALAT1: Its physiological and pathophysiological functions. *RNA Biology*, *14*(12), 1705–1714. https://doi.org/10.1080/15476286.2017.1358347

Zhao, C., Hsiang, T.-Y., Kuo, R.-L., & Krug, R. M. (2010). ISG15 conjugation system targets the viral NS1 protein in influenza A virus–infected cells. *Proceedings of the National Academy of Sciences*, *107*(5), 2253–2258. https://doi.org/10.1073/pnas.0909144107

Zheng, H., Lee, H. A., Palese, P., & García-Sastre, A. (1999). Influenza A virus RNA polymerase has the ability to stutter at the polyadenylation site of a viral RNA template during RNA replication. *Journal of Virology*, *73*(6), 5240. https://doi.org/10.1128/jvi.73.6.5240-5243.1999